Experimental Studies Specific to Chemical Kinetic Model Validations

Charles Westbrook

Tsinghua-Princeton
2014 Summer School on Combustion
July 20-25, 2014

Experimental Studies: Engine Relevant

Rapid Compression Machine

Shock Tube

Jet Stirred Reactor

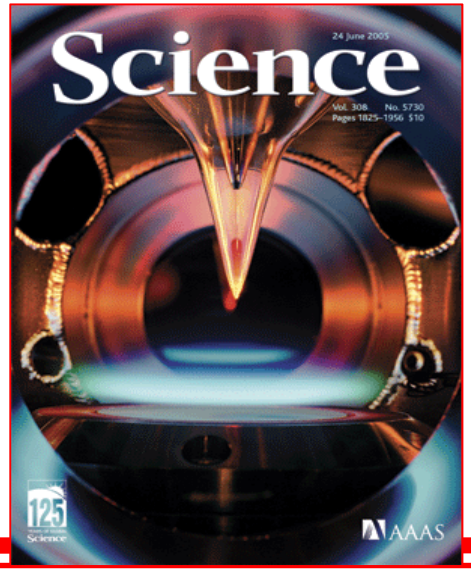

Flat Flame Burner

Fuel component and surrogate models validated by comparison to fundamental experimental data

Jet Stirred Reactors

Premixed Laminar Flames

Twin premixed flames

Shock tube

Combustion Parameters
Temperature
Pressure
Mixture fraction (air-fuel ratio)
Mixing of fuel and air

Non Premixed Flames

Rapid Compression Machine

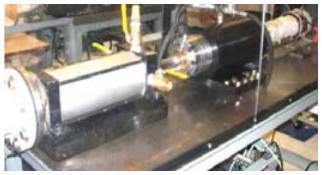

Engine Combustion

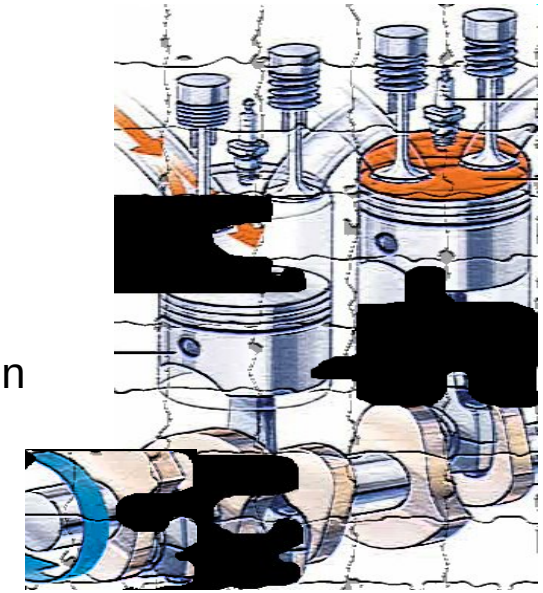

High pressure flow reactors:

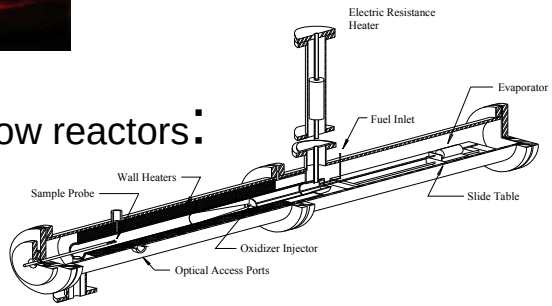

JSRs and Flow Reactors

Proper rate of reaction

- Define as: $(1/\nu_i)(dn_i/dt)$ mol s^{-1}

where ν_i is a stoichiometric coefficient

+ve for products, – ve for reactants

Example: $2H_2 + O_2 = 2H_2O$

- $\nu(H_2) = -2$, $\nu(O_2) = -1$ and $\nu(H_2O) = +2$
- At constant volume: [A] = n /V *or* n = V × [A]

So: (dn/dt) = V. (d[A]/dt)

Old rate of reaction (*was* rxn rate per unit volume)

- (d[A]/dt) = (1 / V) (dn_A/dt)

Flow versus batch reactors $[A]=[A]_0 \exp\{-kt\}$

Stirred flow; perfect mixing

- *spherical* shape of volume **V**

$$\mathbf{[A]_{outlet} = [A]_{inlet} / \{ 1 + k (V/\nu)\}}$$

'Plug' flow; no mixing at all at all

- *cylindrical* shape of volume **V**

$$\mathbf{[A]_{outlet} = [A]_{inlet} \exp\{ - k (V/\nu)\}}$$

NB $\mathbf{(V/\nu)}$ has dimensions $\mathbf{(m^3 / m^3 s^{-1}) = s}$

A 'residence' or 'contact' time

Stirred flow; 1st order

$-(dn_A/dt) = k\, n_A = k\, V\, [A]$

- inflow = outflow + reaction

  Assume system at constant volume so that inlet flow rate is equal to outlet flow rate

- $\nu[A]_i = \nu[A]_o - (dn_A/dt)$
- $\nu[A]_i = \nu[A]_o + k\, V\, [A]_o$
- $[A]_o = [A]_i / \{1 + k(V/\nu)\}$
- **Test?** vary ν, measure $[A]_o$ & $[A]_i$, is k the same?

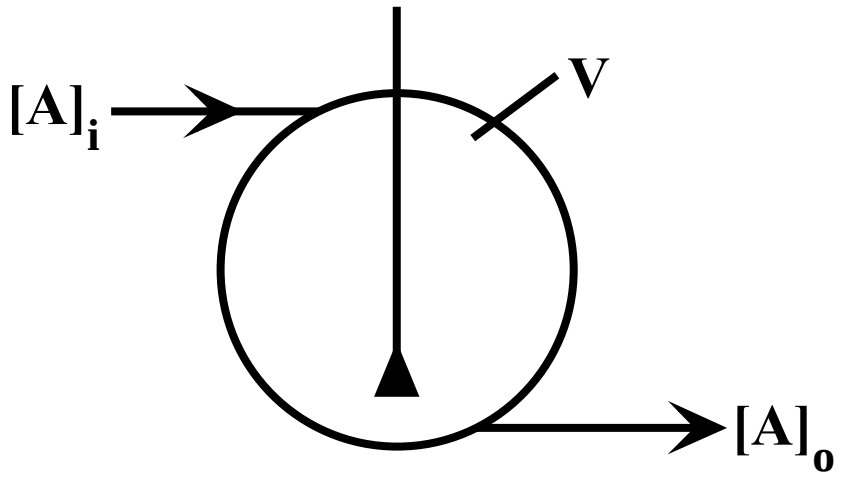

Jet Stirred Reactor (JSR)

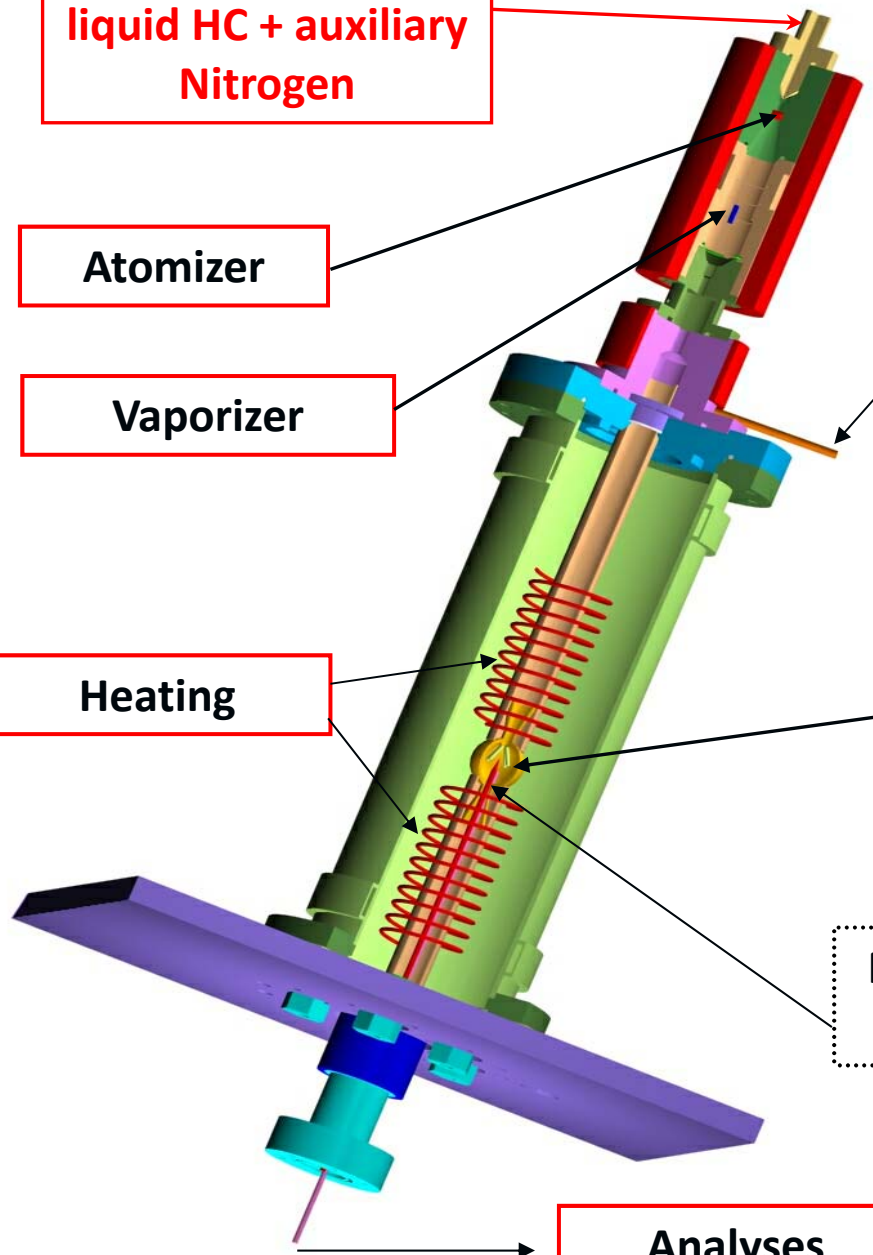

Premixed Well Stirred Reactor (JSR)

CNRS Orleans, P. Dagaut

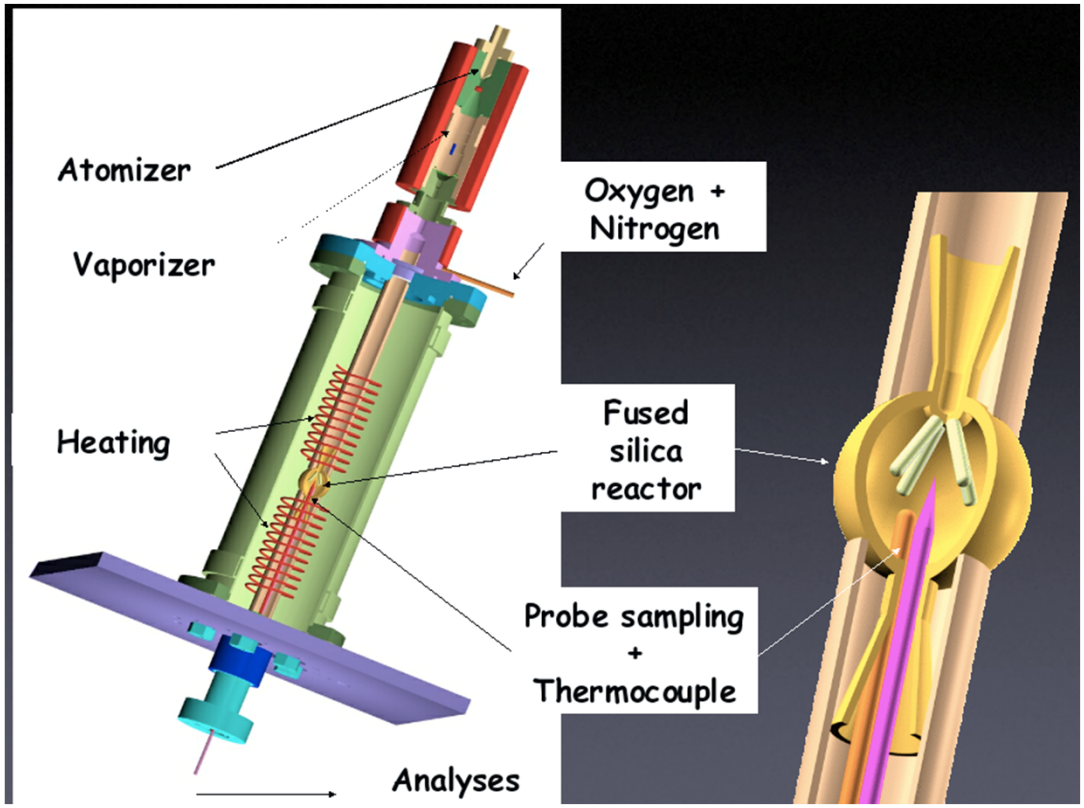

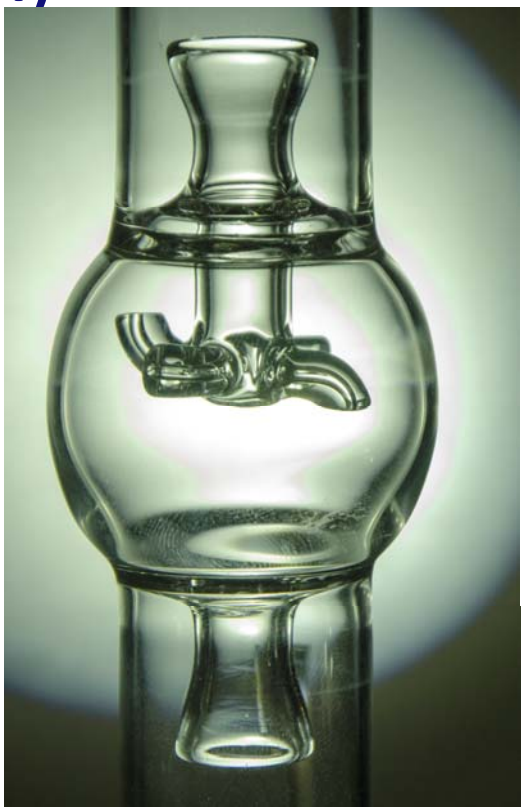

- The zero dimensional perfectly system is ideal for modeling.
- The products species profiles are dependent on chemical kinetics due to the perfectly mixed homogeneous environment.

JSR Results

CNRS Orleans, P. Dagaut

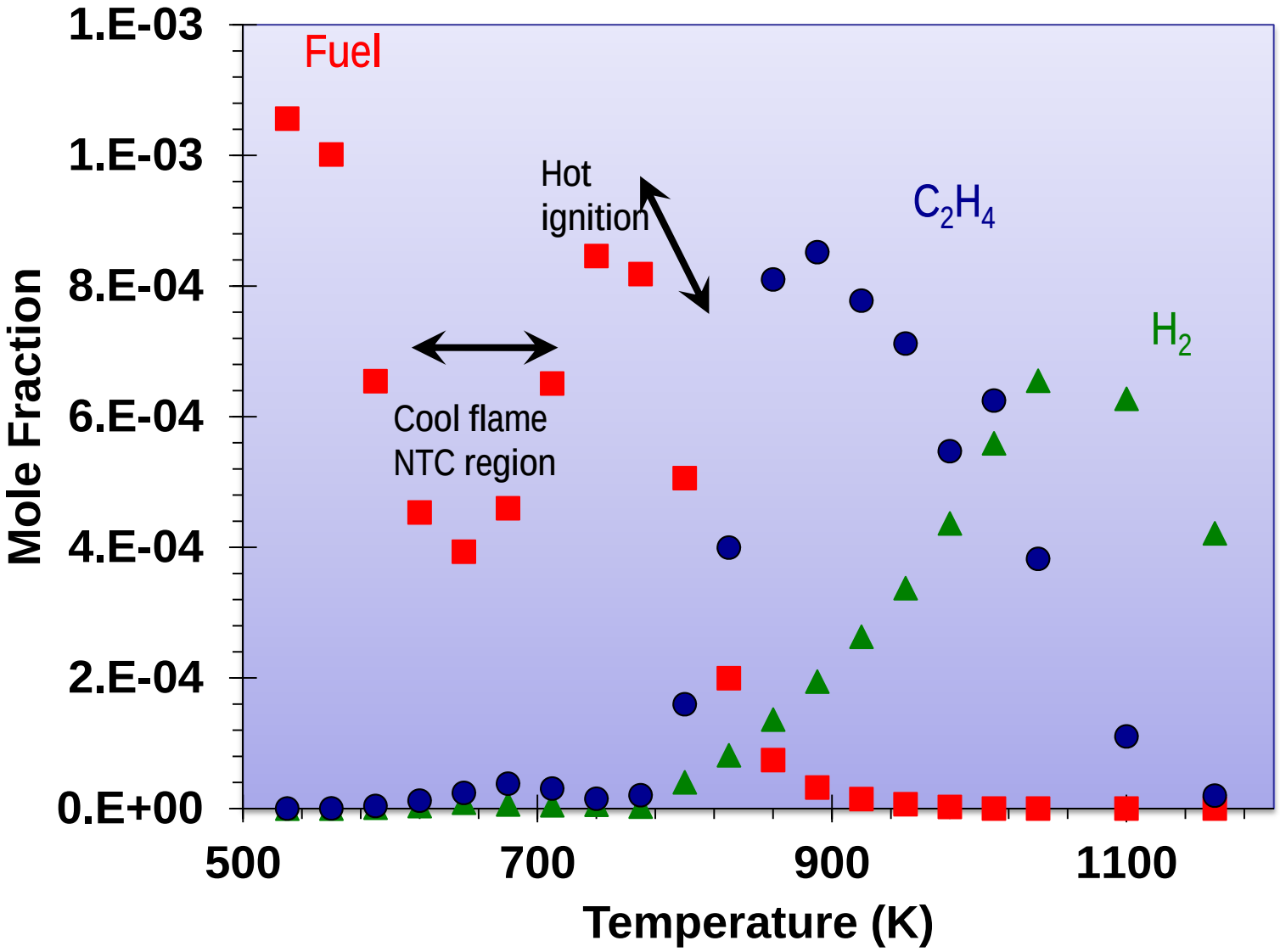

JSR Results

CNRS Orleans, P. Dagaut

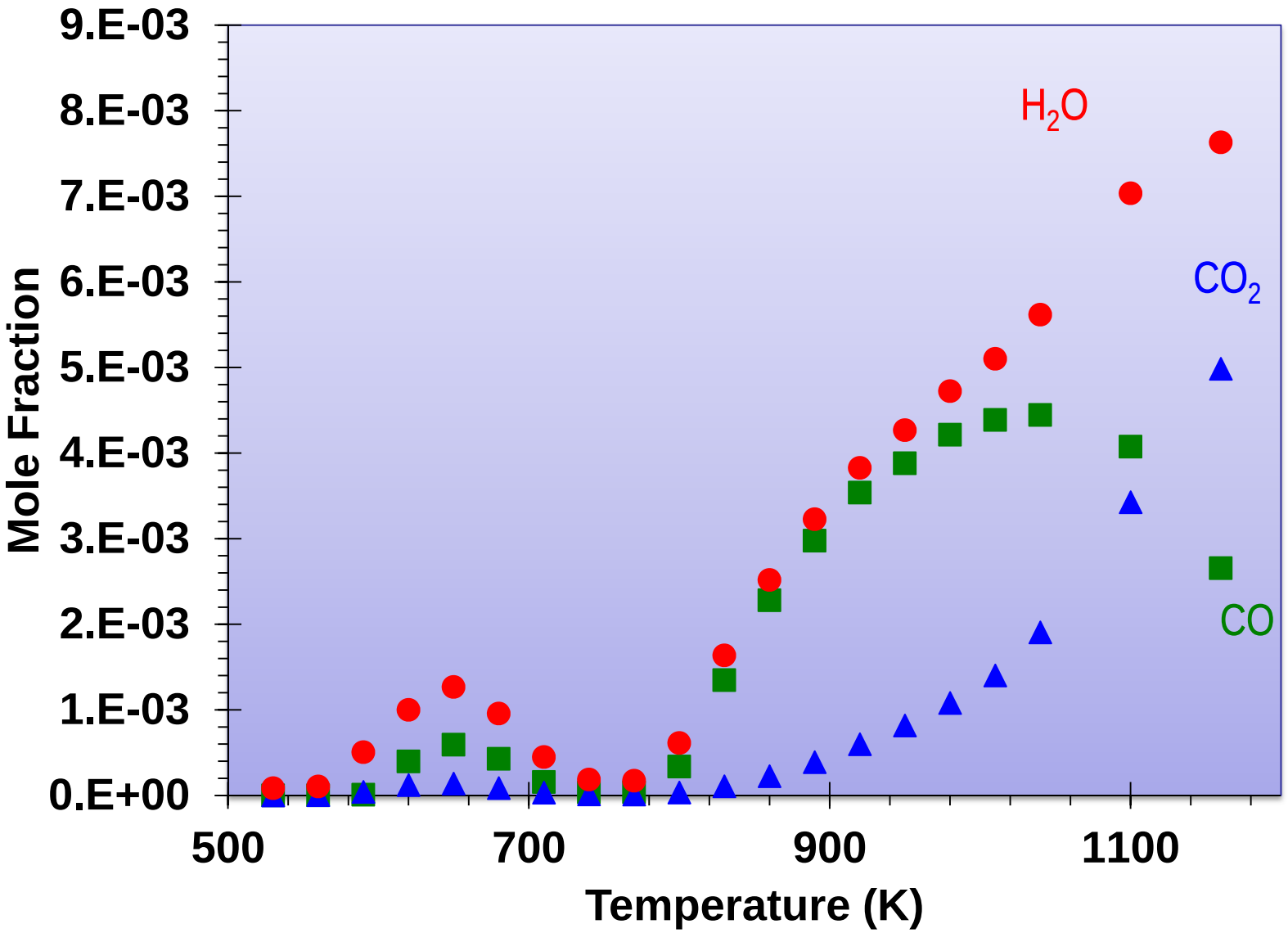

Biodiesel components ignite in order of number of double bonds

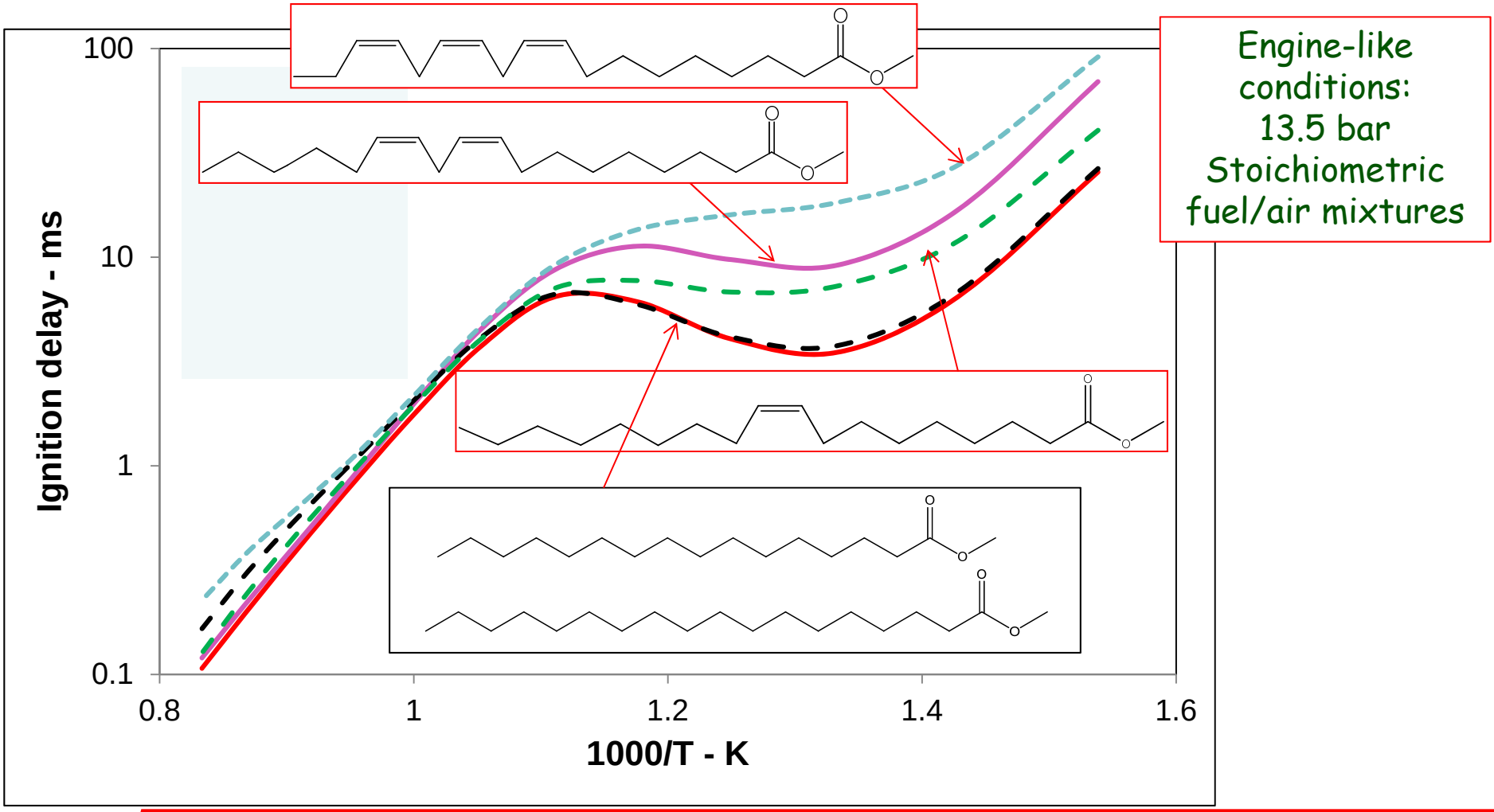

Biodiesel component reactivities in JSR

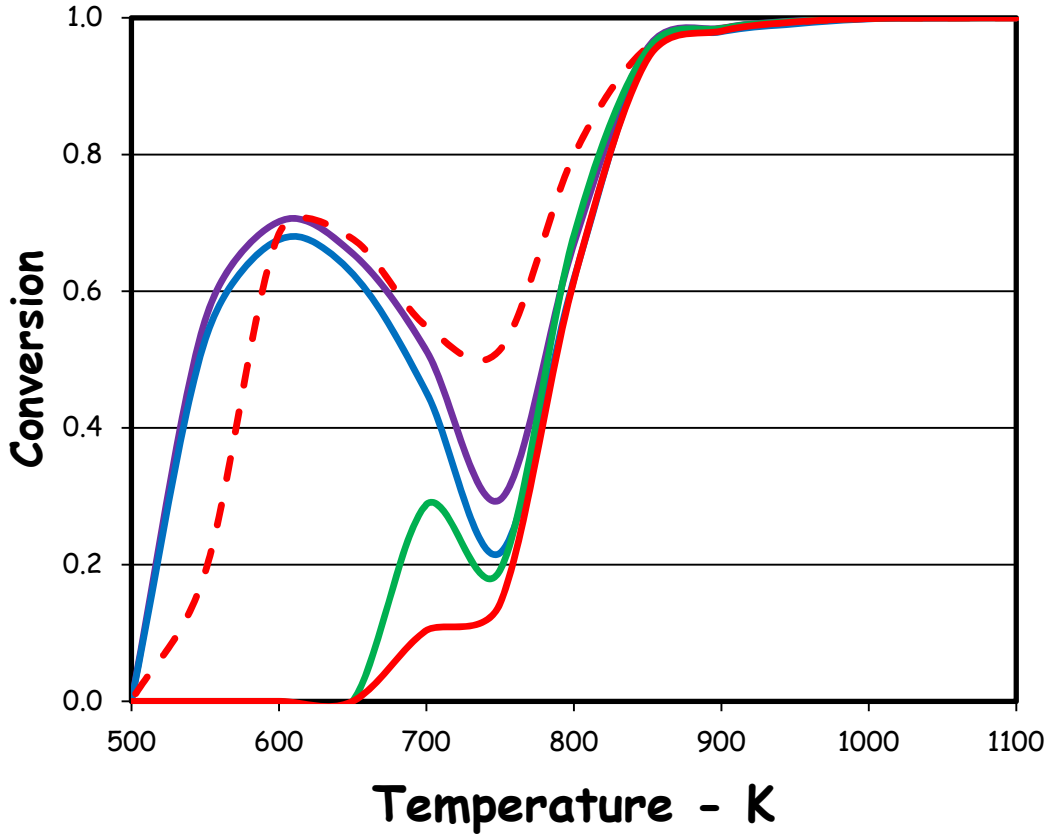

Stoichiometric
Single-component fuels
Atmospheric pressure
Very dilute in He

stearate
palmitate
oleate
linoleate
linolenate

JSR might be a better CN or ON test than customary shock tubes

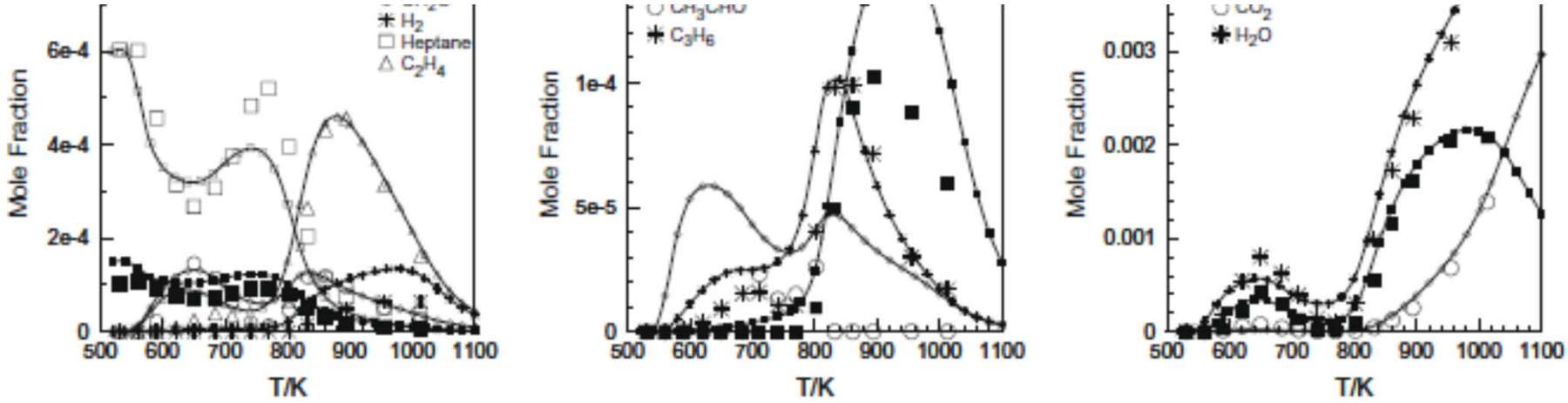

Fig. 7. The oxidation of an ethanol/heptane 20/80 mol% fuel mixture in a JSR at 10 atm, 700 ms, and $\varphi = 0.5$. Comparison between experimental results (symbols) and detailed modeling (lines and small symbols).

Fuel 89 (2010) 280–286

Contents lists available at ScienceDirect

Fuel

journal homepage: www.elsevier.com/locate/fuel

Experimental and modeling study of the kinetics of oxidation of ethanol-*n*-heptane mixtures in a jet-stirred reactor

Philippe Dagaut *, Casimir Togbé

CNRS, 1c, Avenue de la Recherche, Scientifique, 45071 Orléans, cedex 2, France

Variable Pressure Flow reactor

(Princeton U.)

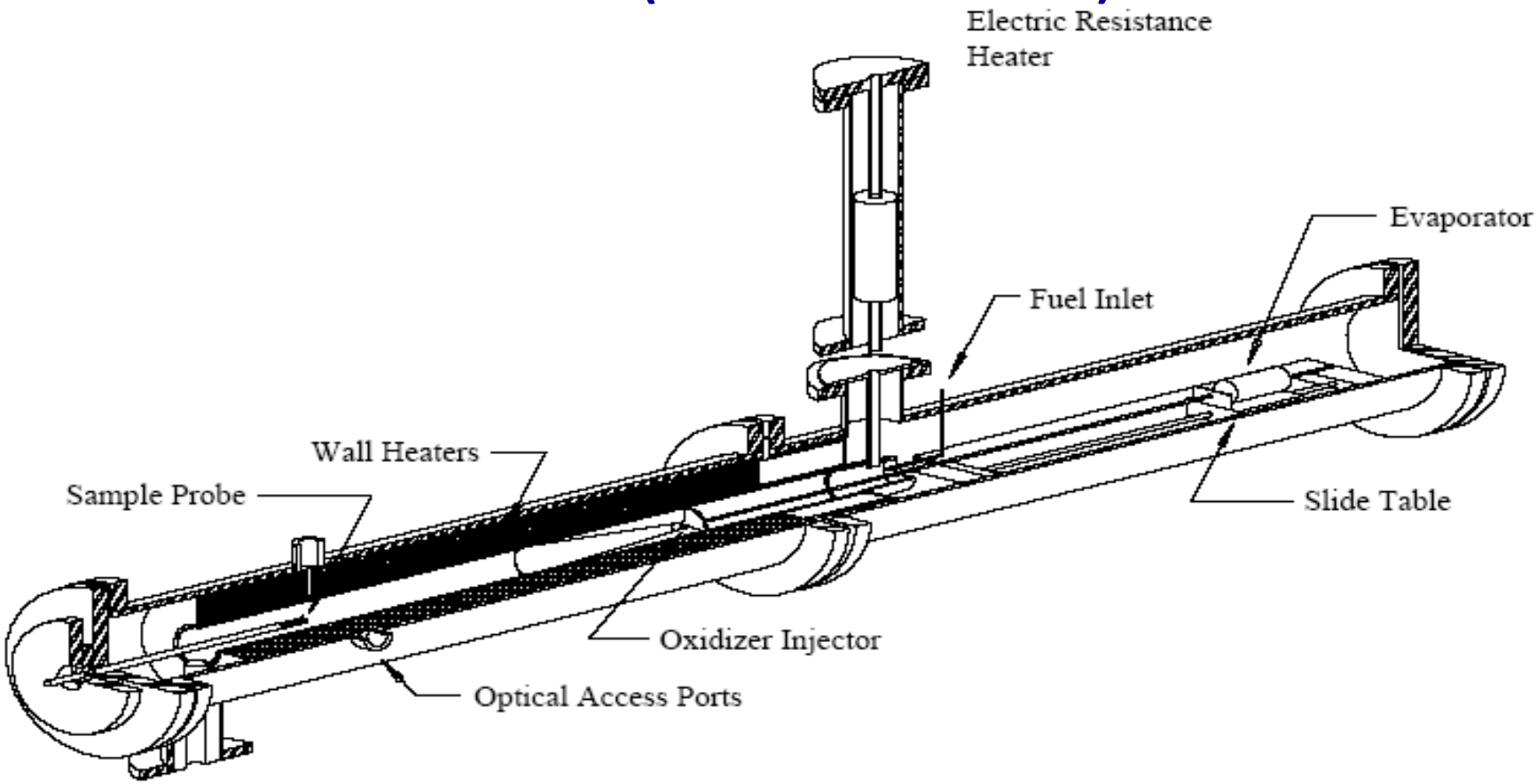

Combustion Science and Technology, 1979, Vol. 20, pp. 125–140
0010-2202/79/2003-0125$04.50/0

A Comprehensive Mechanism for Methanol Oxidation

CHARLES K. WESTBROOK *Lawrence Livermore Laboratory, University of California, Livermore, California 94550*

FREDERICK L. DRYER *Department of Mechanical and Aerospace Engineering, Princeton University, Princeton, N.J. 08540*

(*Received August 15, 1978; in final form January 2, 1979*)

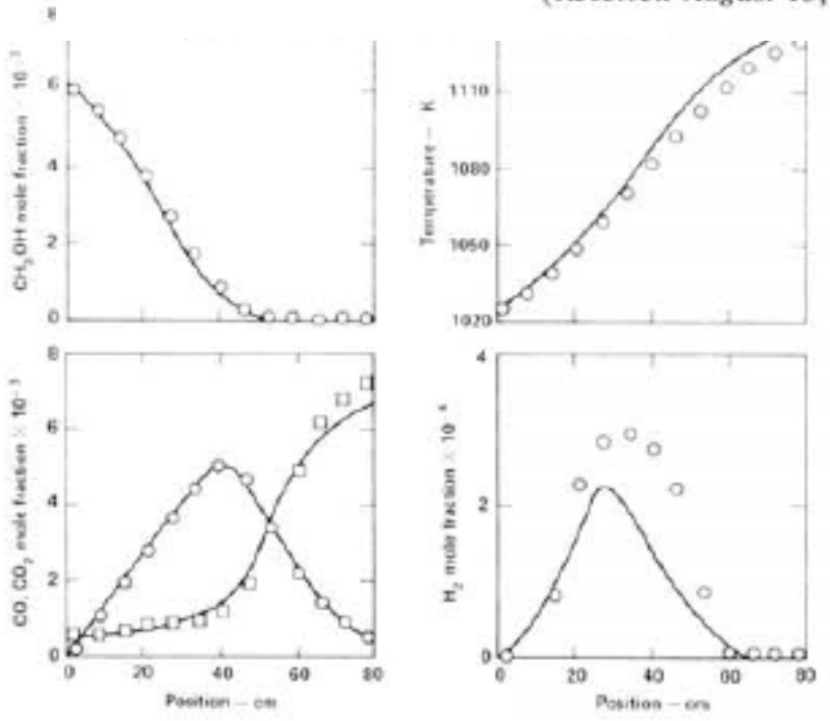

FIGURE 3 Lean flow reactor results using the detailed mechanism from Table I.

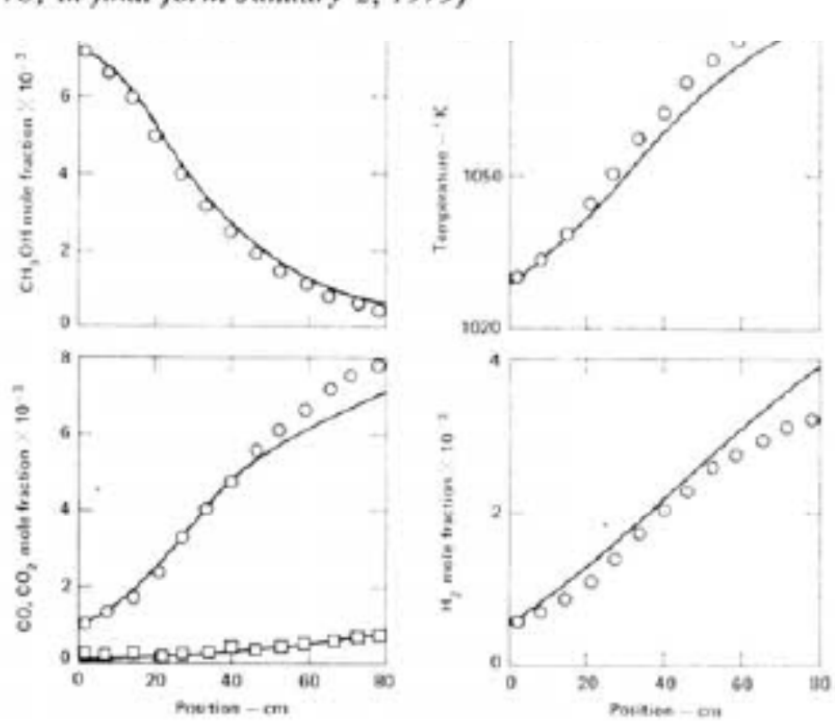

FIGURE 4 Rich flow reactor results using the detailed mechanism from Table I.

Fall Technical Meeting
of the Eastern States Section of the Combustion Institute
Hosted by the University of Connecticut, Storrs, CT Oct 9-12, 2011

Experimental and Modeling Study of 2-Methylheptane Oxidation in a Flow Reactor, Shock Tube, and Rapid Compression Machine

S. Jahangirian[1], D. Healy[2], S.M. Sarathy[3], S. Dooley[1], M. Mehl[3], W.J. Pitz[3], F.L. Dryer[1], H.J. Curran[3], C.K. Westbrook[3]

[1] *Princeton University, New Jersey, USA*

[2] *National University of Ireland, Galway, Ireland*

[3] *Lawrence Livermore National Laboratory, Livermore, California, USA*

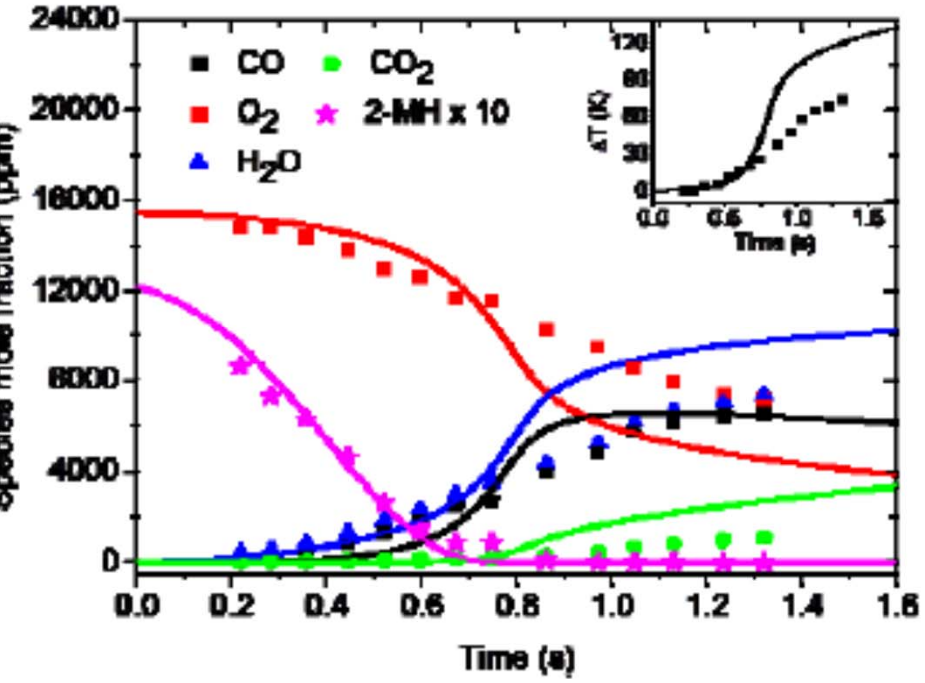

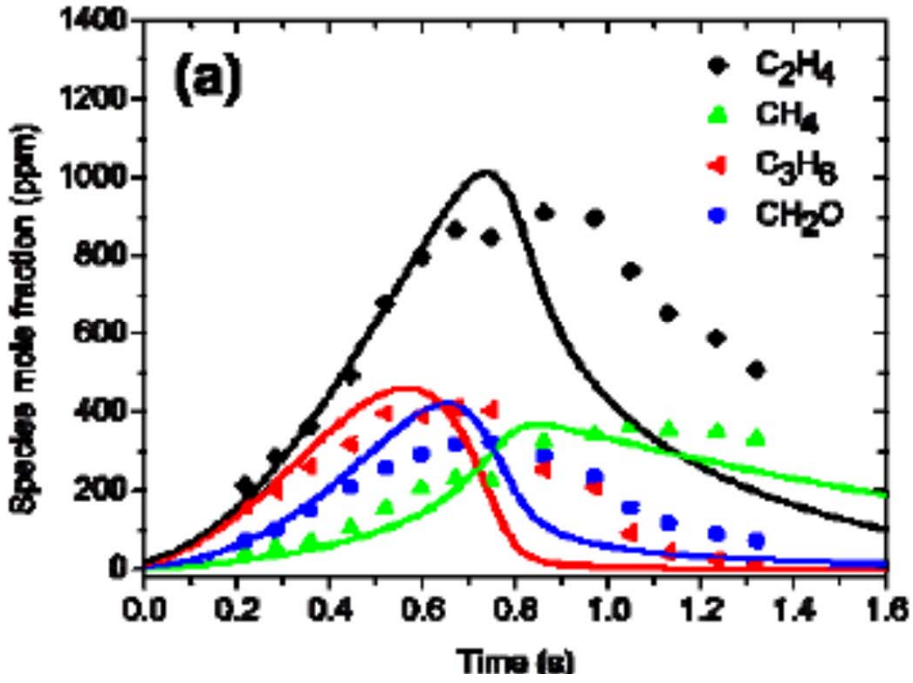

Available online at www.sciencedirect.com
SCIENCE DIRECT®
Experimental Thermal and Fluid Science 28 (2004) 701–708
Experimental Thermal and Fluid Science
www.elsevier.com/locate/etfs

Reference components of jet fuels: kinetic modeling and experimental results

A. Agosta [a], N.P. Cernansky [a], D.L. Miller [a], T. Faravelli [b], E. Ranzi [b,*]

[a] *Department of Mechanical Engineering and Mechanics, Drexel University, USA*
[b] *CMIC Department, Politecnico di Milano, Piazza Leonardo da Vinci 32, Milan 20133, Italy*

Received 20 June 2003; received in revised form 15 November 2003; accepted 1 December 2003

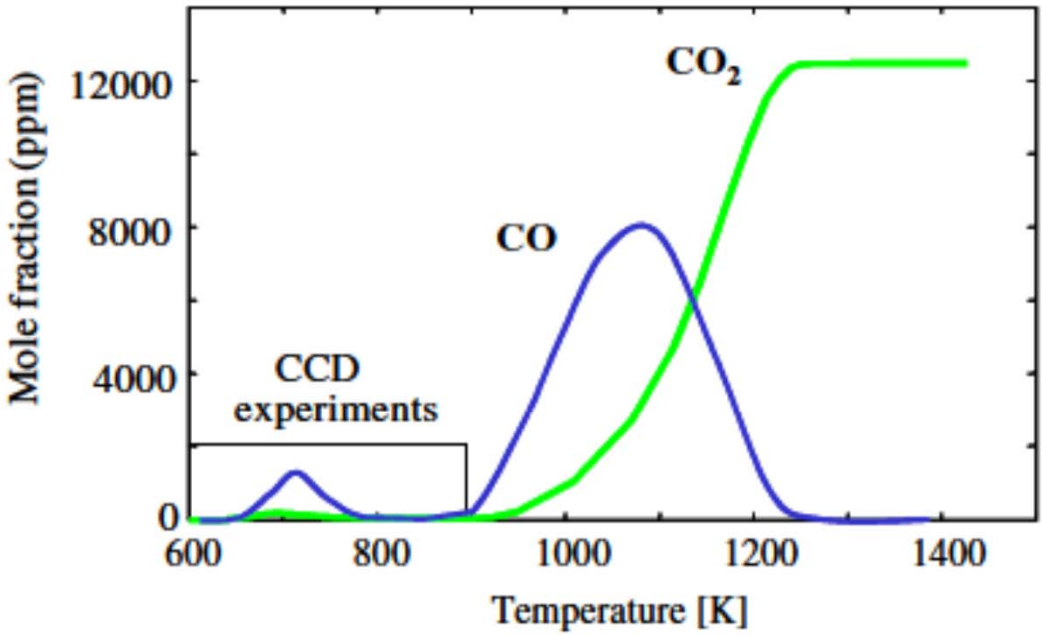

Fig. 2. CO and CO_2 production vs. reactor temperature for *n*-dodecane oxidation (ND1), showing the typical extent of a CCD experiment.

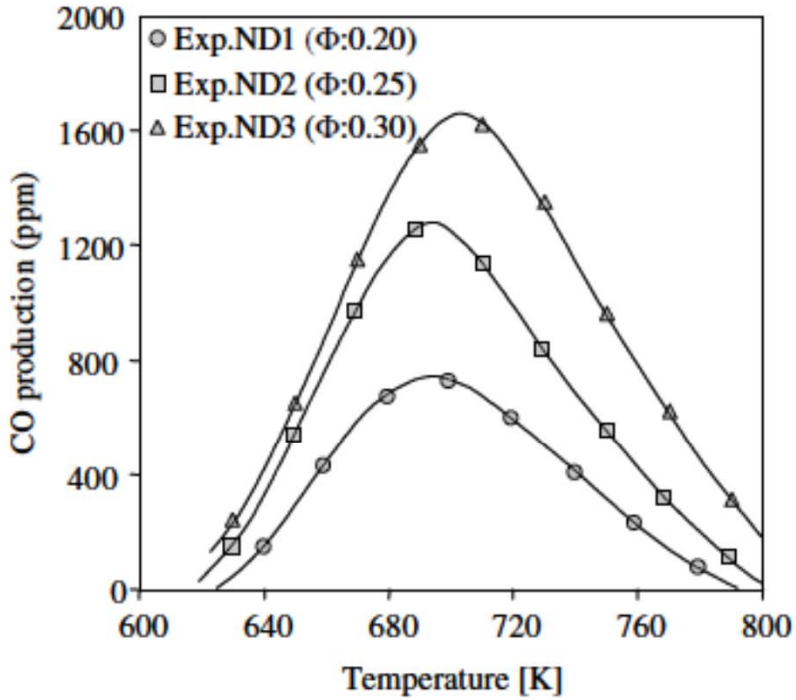

Fig. 3. *n*-Dodecane reactivity maps: effect of temperature and equivalence ratio on CO formation.

ST and RCM contribution to mechanism generation and validation

4-Stroke Engine

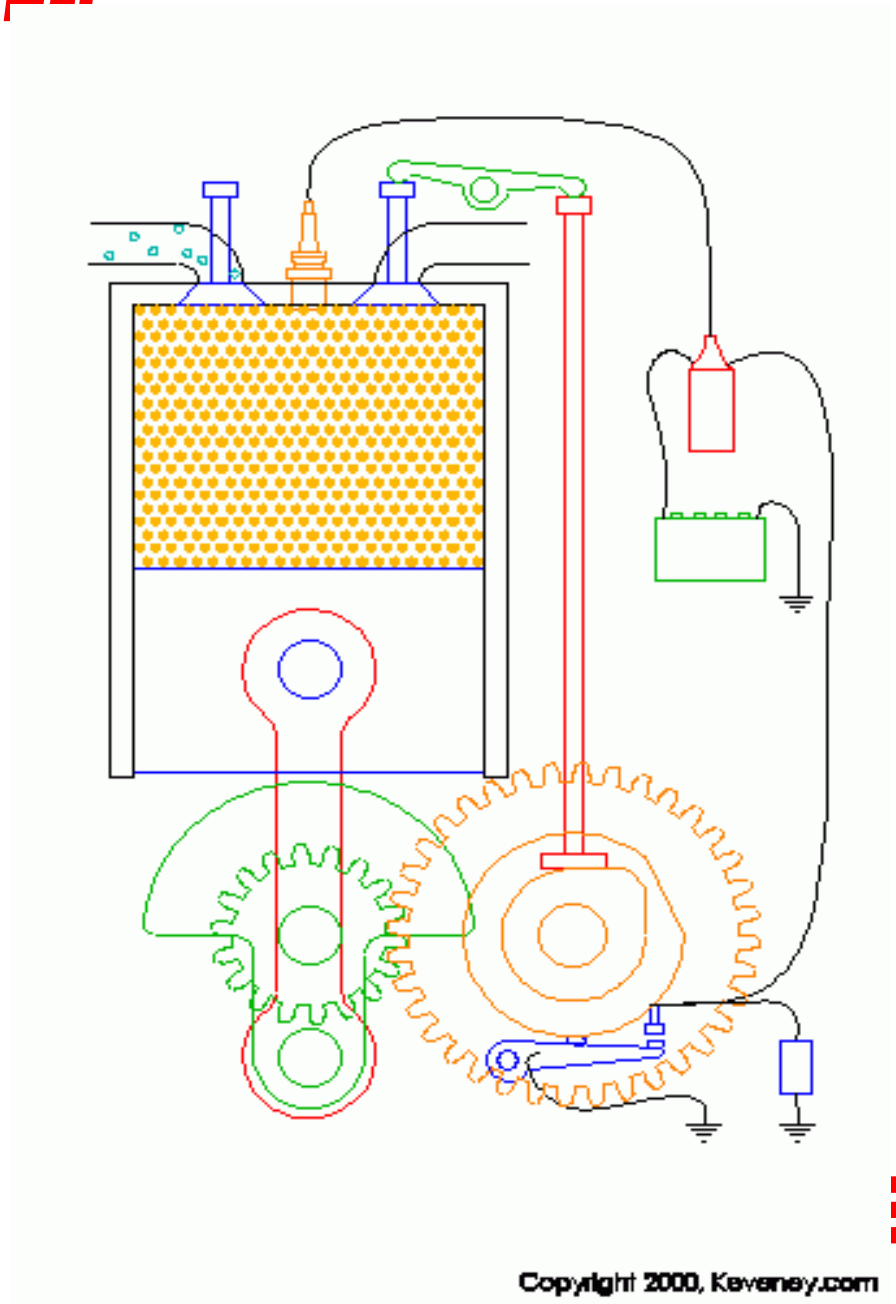

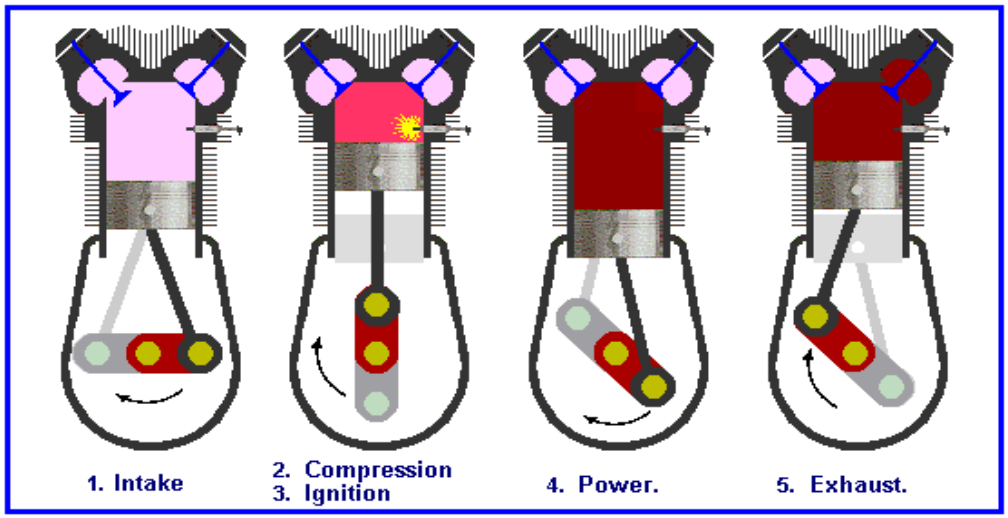

Figure 6-3 Four-stroke five-event cycle.

Pressure vs CAD in an engine

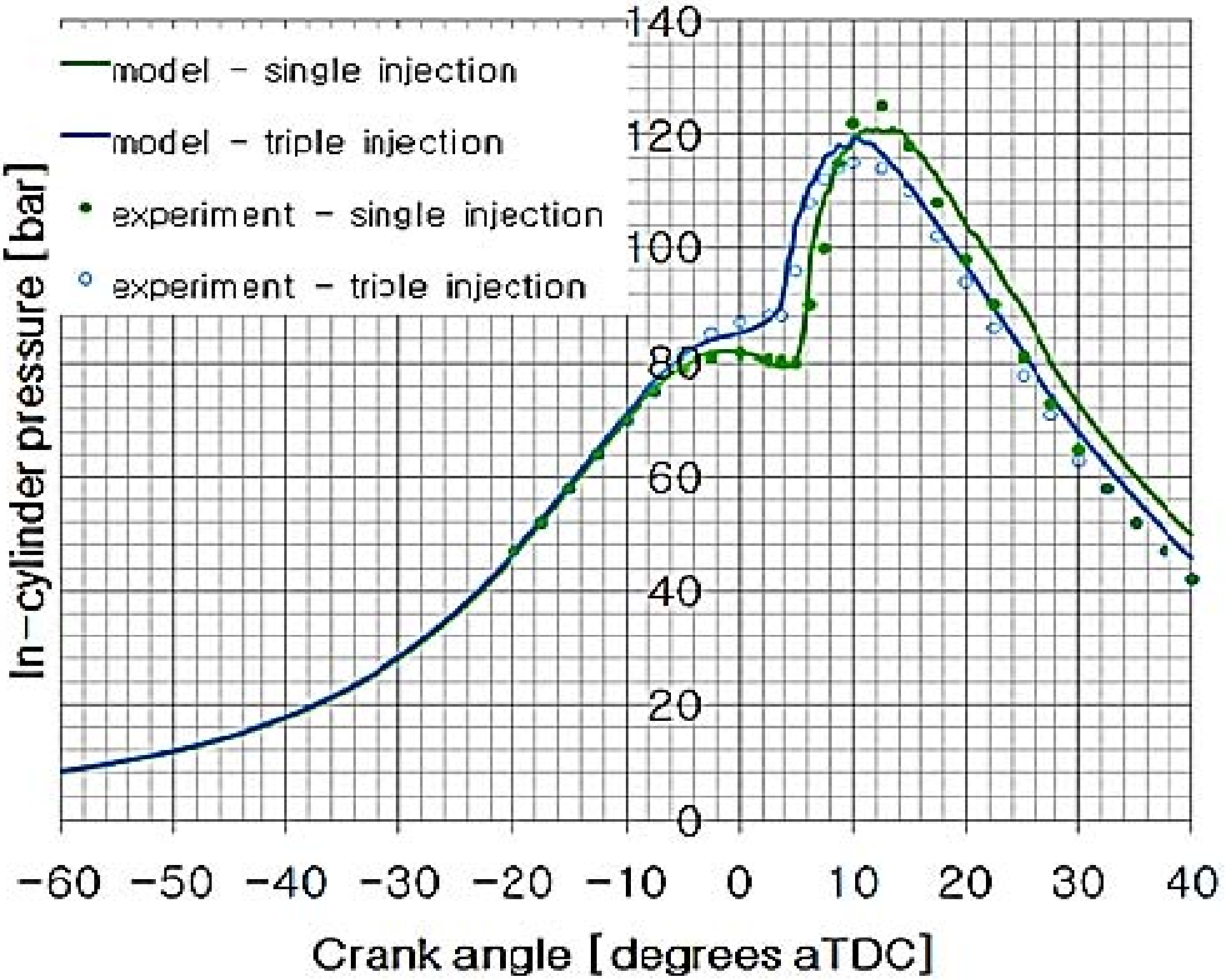

Experimental Studies: Engine Relevant

Rapid Compression Machine

Shock Tube

Jet Stirred Reactor

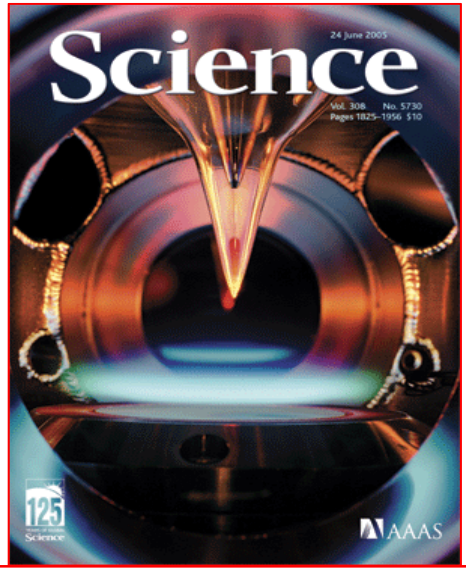

Flat Flame Burner

Rapid Compression Machine

Galway, Ireland, Curran group

Rapid Compression Machine

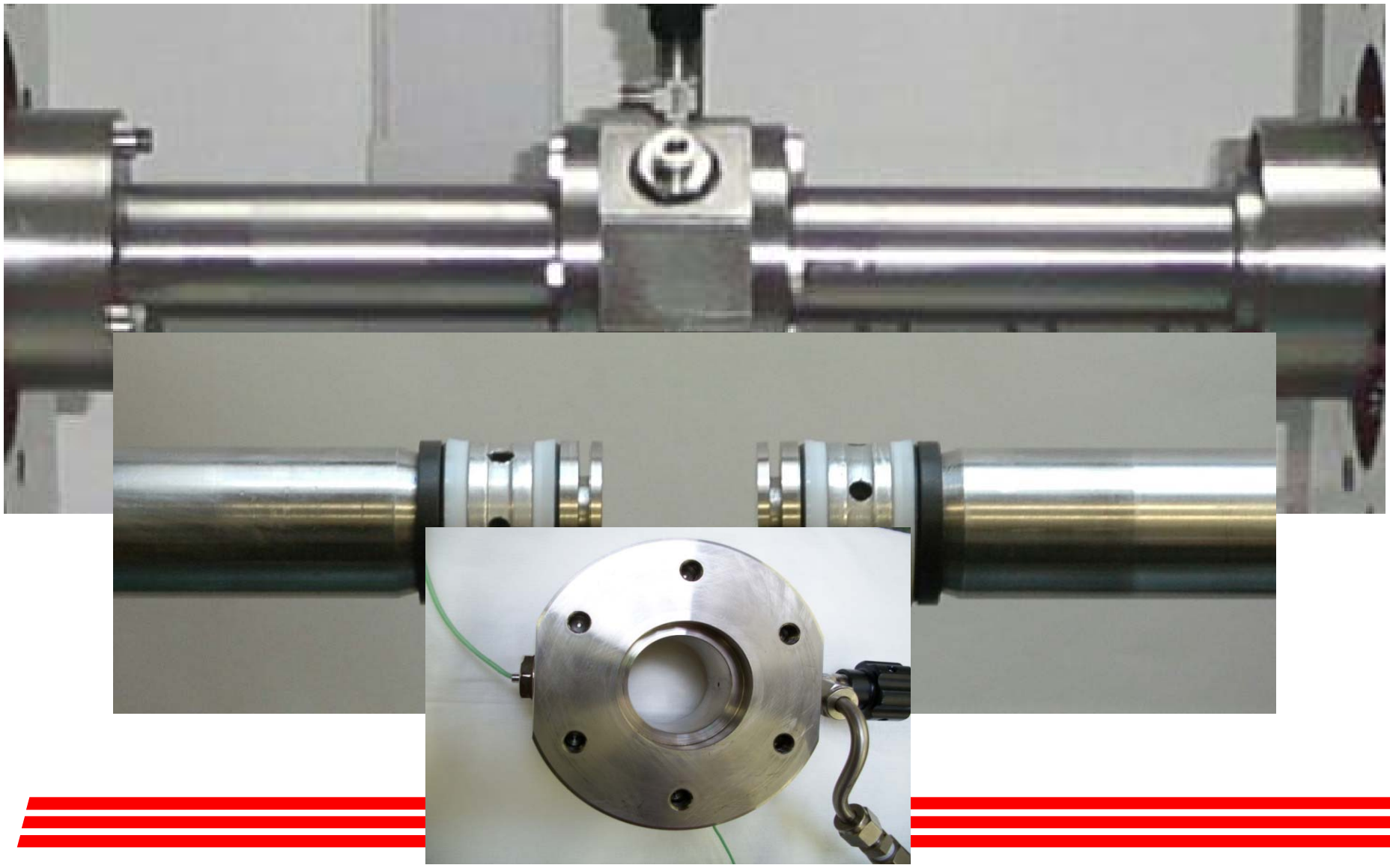

Rapid Compression Machine

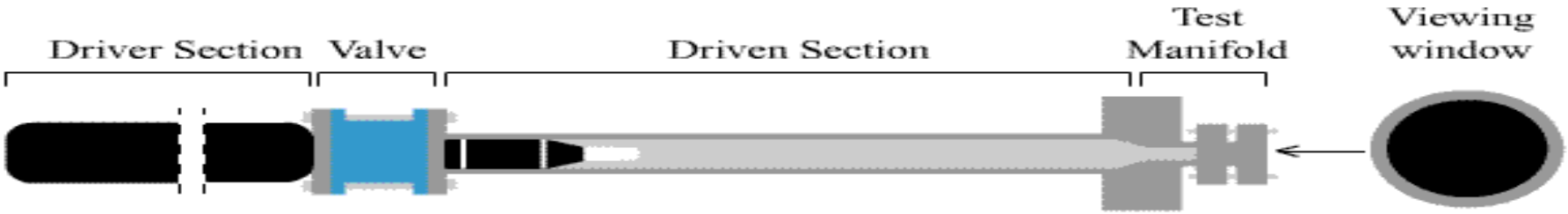

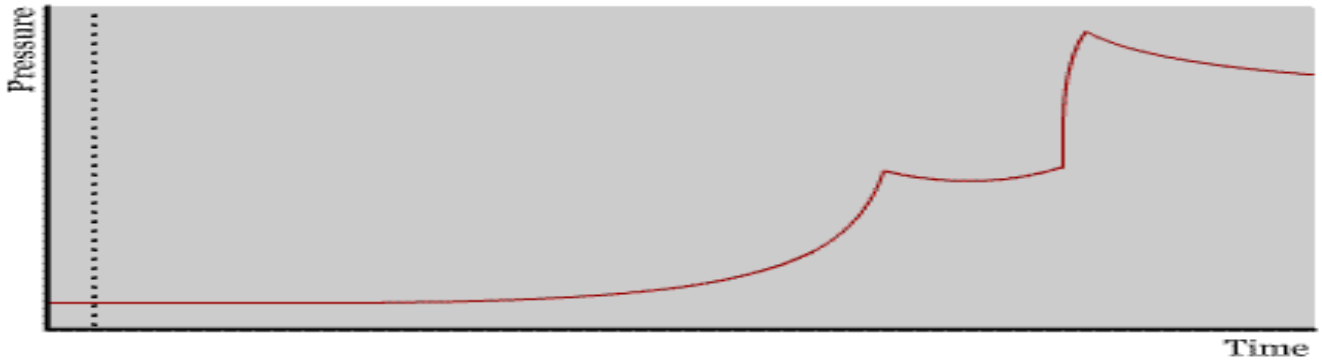

Roll up vortex

The formation of a vortex on the piston face inside the RCM disrupts the uniformity of the temperature field.

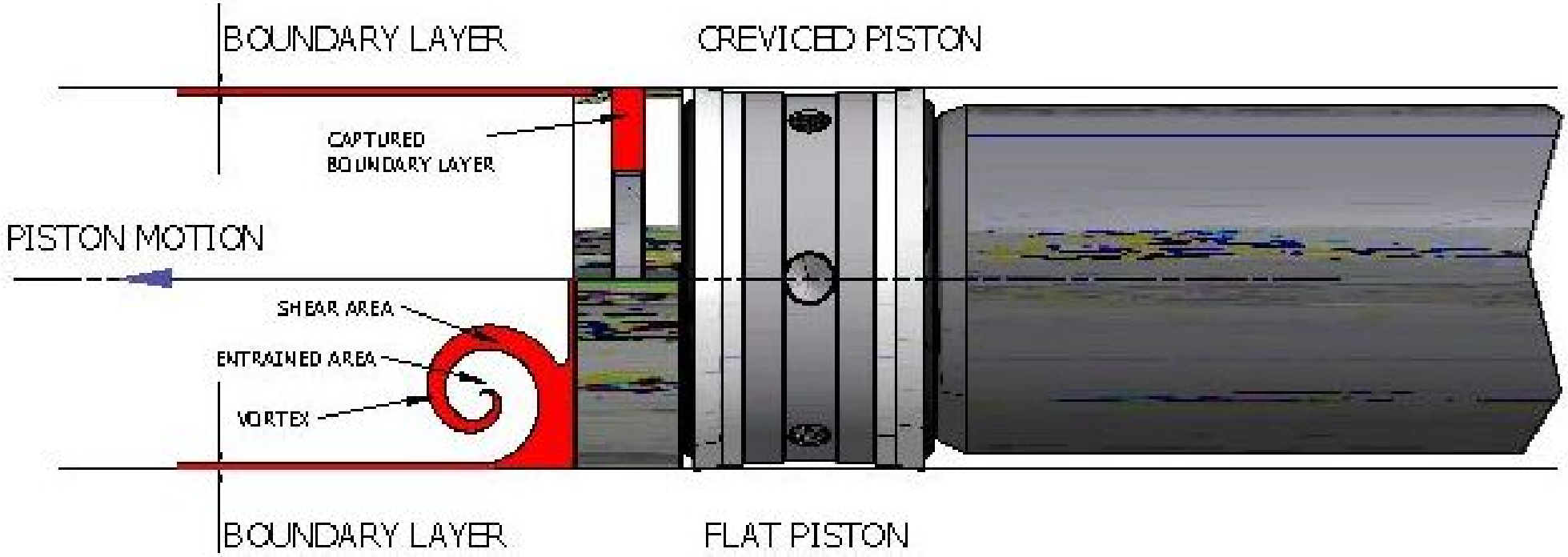

Piston heads: flat versus creviced

Flat piston

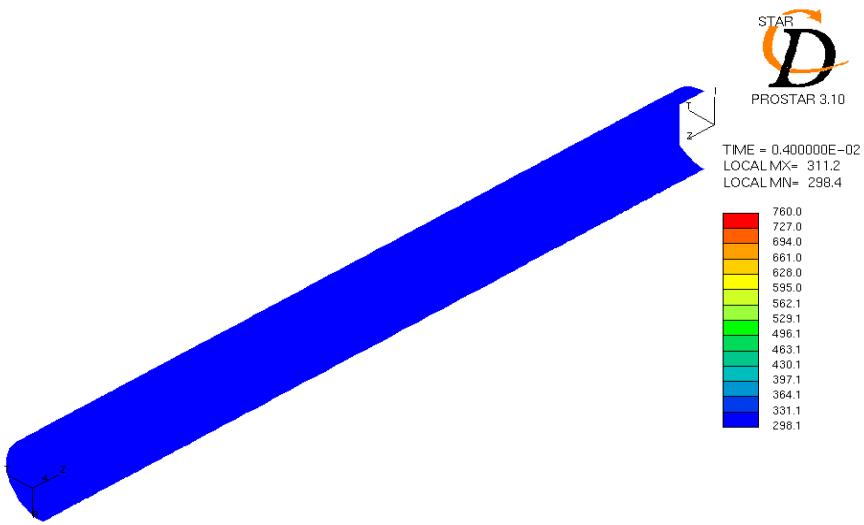

Creviced piston

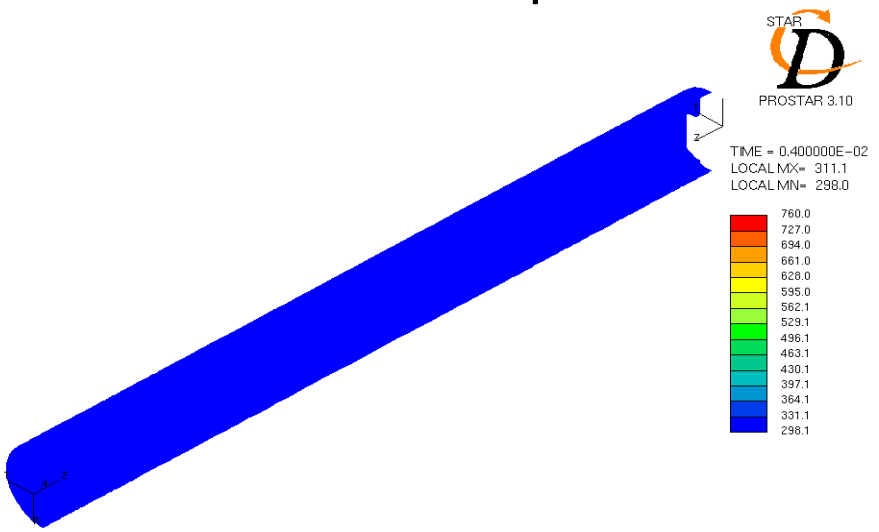

RCM Engine Relevant Studies

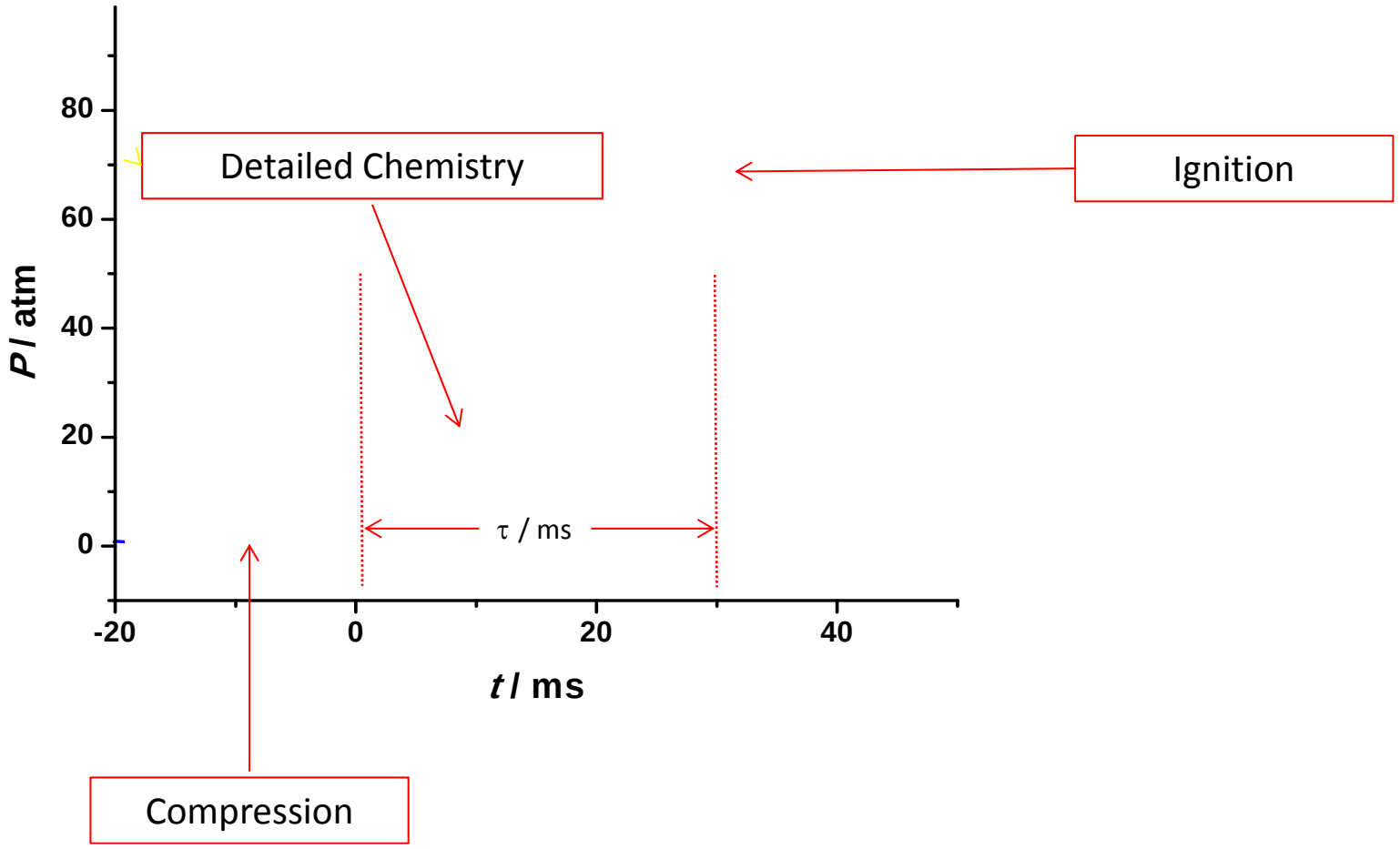

Data processing for RCM simulation

Step 1: Non-reactive experiment

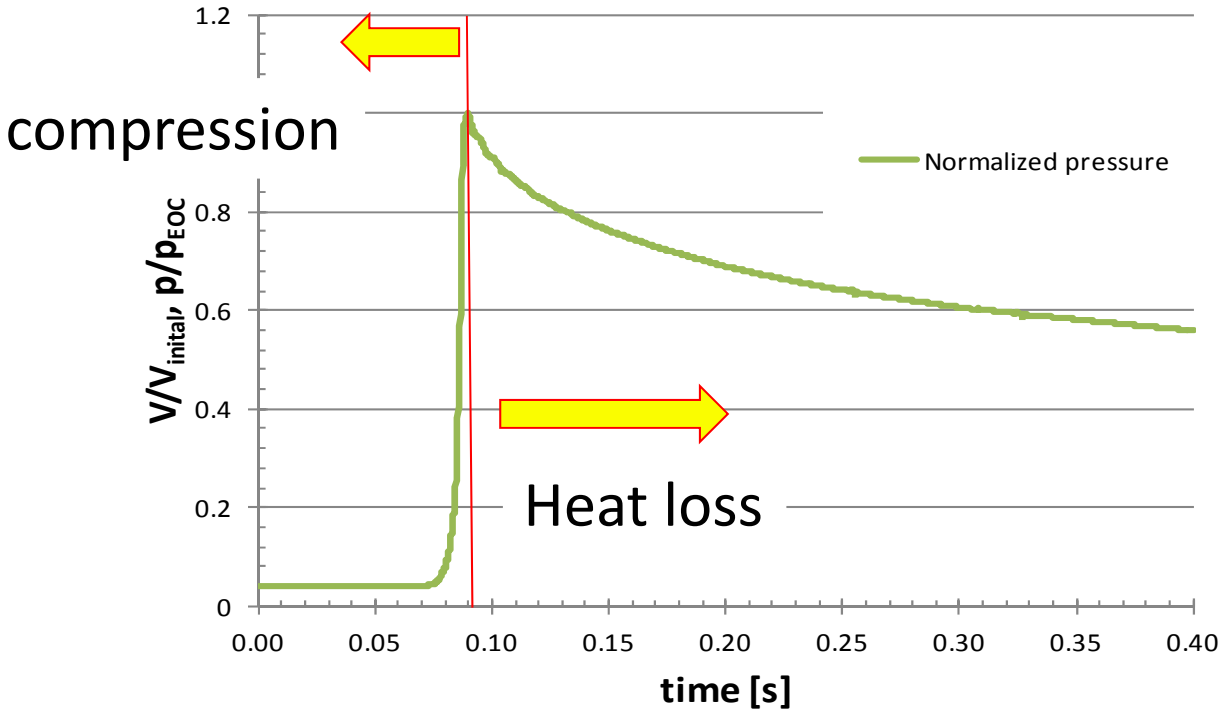

Experiment where O_2 is replaced by N_2 to characterize the compression and heat loss for a specific mixture

Data processing for RCM simulation

Step 2: Volume profile

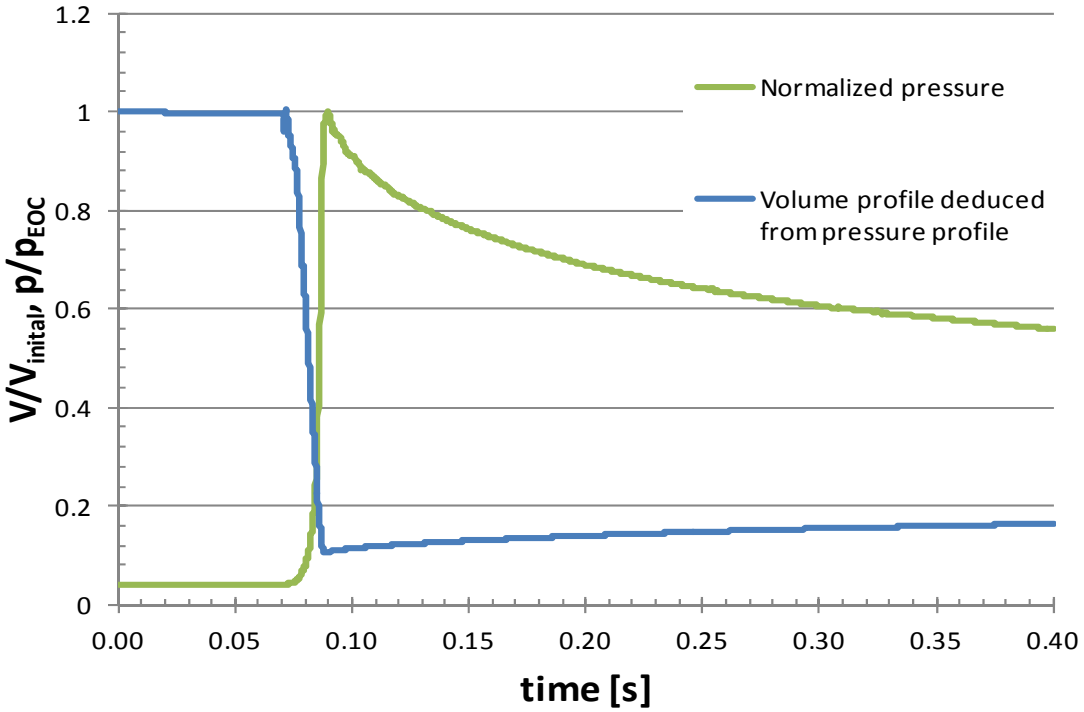

$$\frac{p_2}{p_1} = \left(\frac{V_1}{V_2}\right)^{\gamma}$$

- A volume profile is deduced from the pressure profile assuming isentropic behaviour (isentropic exponent not constant but temperature dependent).
- Heat loss effects are modelled as change in volume (Assumption of adiabatic core in RCM chamber).

Data processing for RCM simulation

Step 3: Reducing number of data points

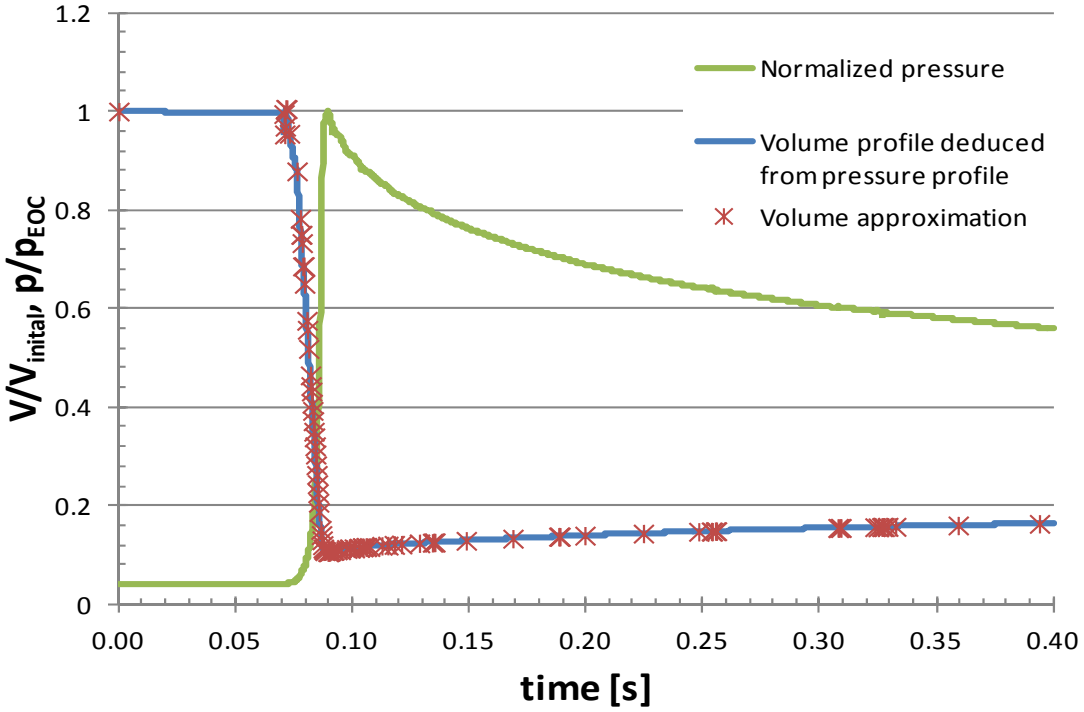

- Reduction in # of data points to reduce simulation time for reactive simulations.
- Non-uniform distribution of data points => accurate reproduction of volume profile.

Data processing for RCM simulation

- Rather than reporting polynomial fit parameters or providing subroutines for modelers to integrate into SENKIN, report the effective volume history in a tabular format
- Advantages:
  - Will not diverge if the maximum time is exceeded
  - Simpler to implement in CHEMKIN-Pro and CHEMKIN-II or III
  - Better agreement with experimental pressure profiles

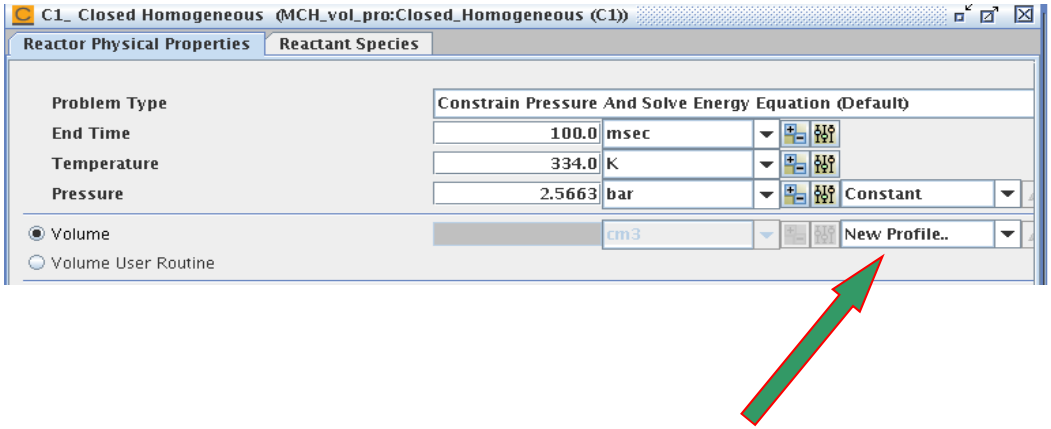

CHEMKIN-Pro Volume Profile Input

Data processing for RCM simulation

Step 4: Simulating reactive experiment

Input for simulation (CHEMKIN PRO): Volume profile, gas mixture, initial temperature and pressure.

Perturbation of the constant volume reactor by the given volume profile

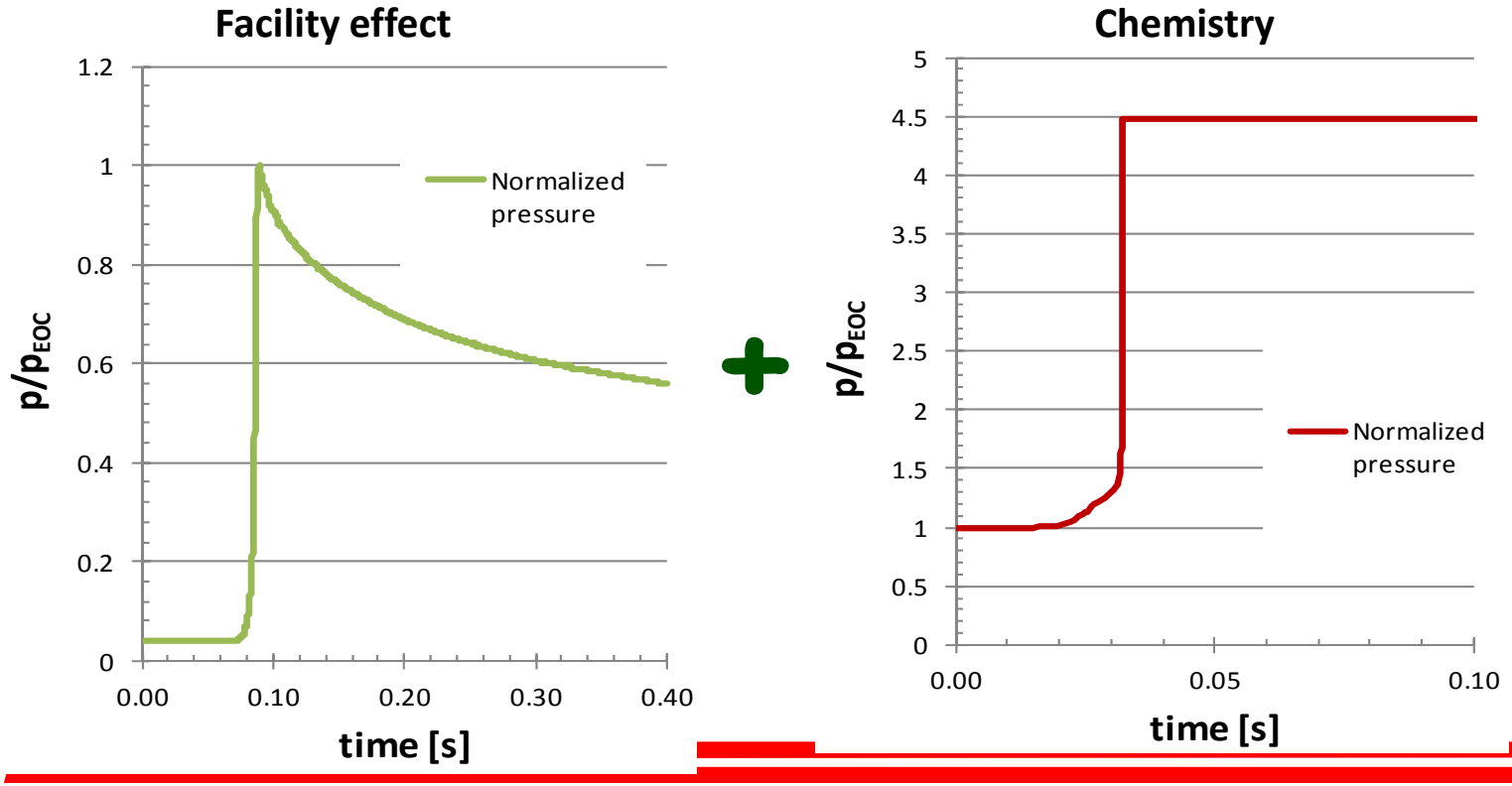

Early pressure rise used to estimate Temp rise

Assume Temperature and Pressure are Related by:

$$\frac{T}{T_i} = \left(\frac{P}{P_i}\right)^{\frac{\gamma-1}{\gamma}}$$

Two-Line Thermometry and H_2O Measurements in RCM

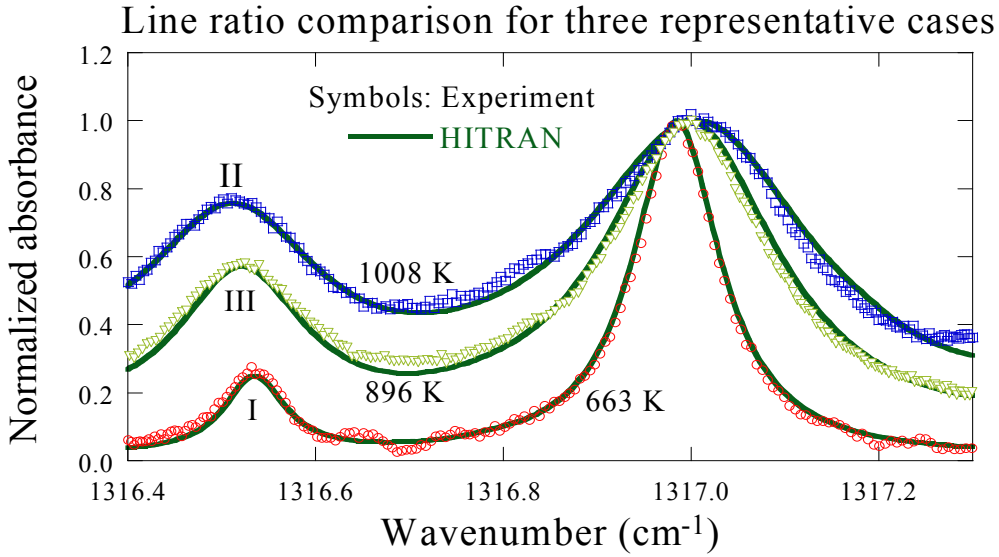

Non-Reactive Mixtures

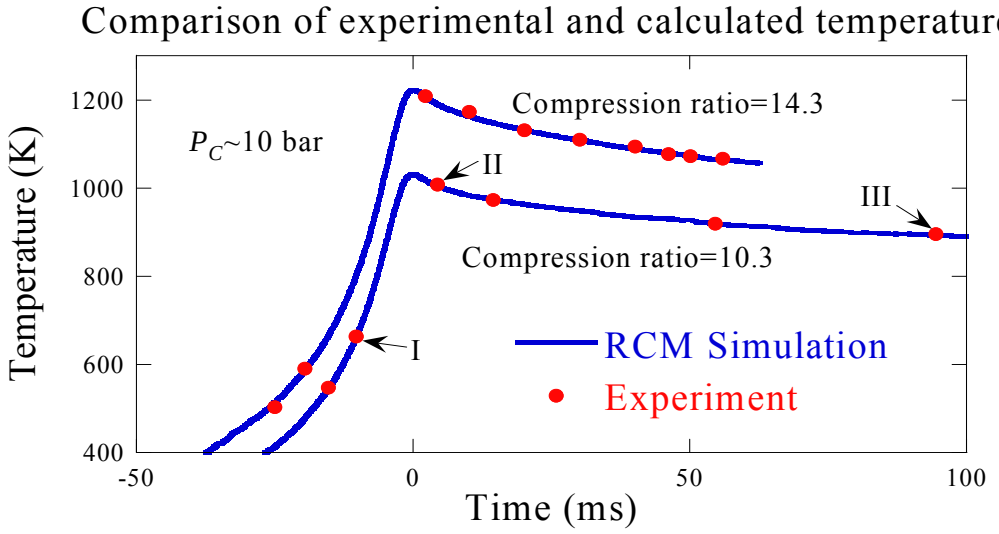

- Mixture of Ar with 2.87%H_2O used in a single pass RCM setup.
- Experiments at end of compression pressure P_C=10 bar.
  - Compression ratios of 10.3 and 14.3.
- Comparison of measured temperature was done with simulated temperature evolution (from RCM simulations).
- Good agreement within ±5 K.

Same non-reactive mixture used for higher pressure experiments for compression ratio 10.3 and P_C=15 and 20 bar.

- Good agreement of absorbance profiles for representative conditions (viz. points I, II and III).

A.K. Das, M. Uddi, C-J. Sung
Combust. Flame, 159 (2012) 3493–3501.

Rapid Sampling in Leeds RCM

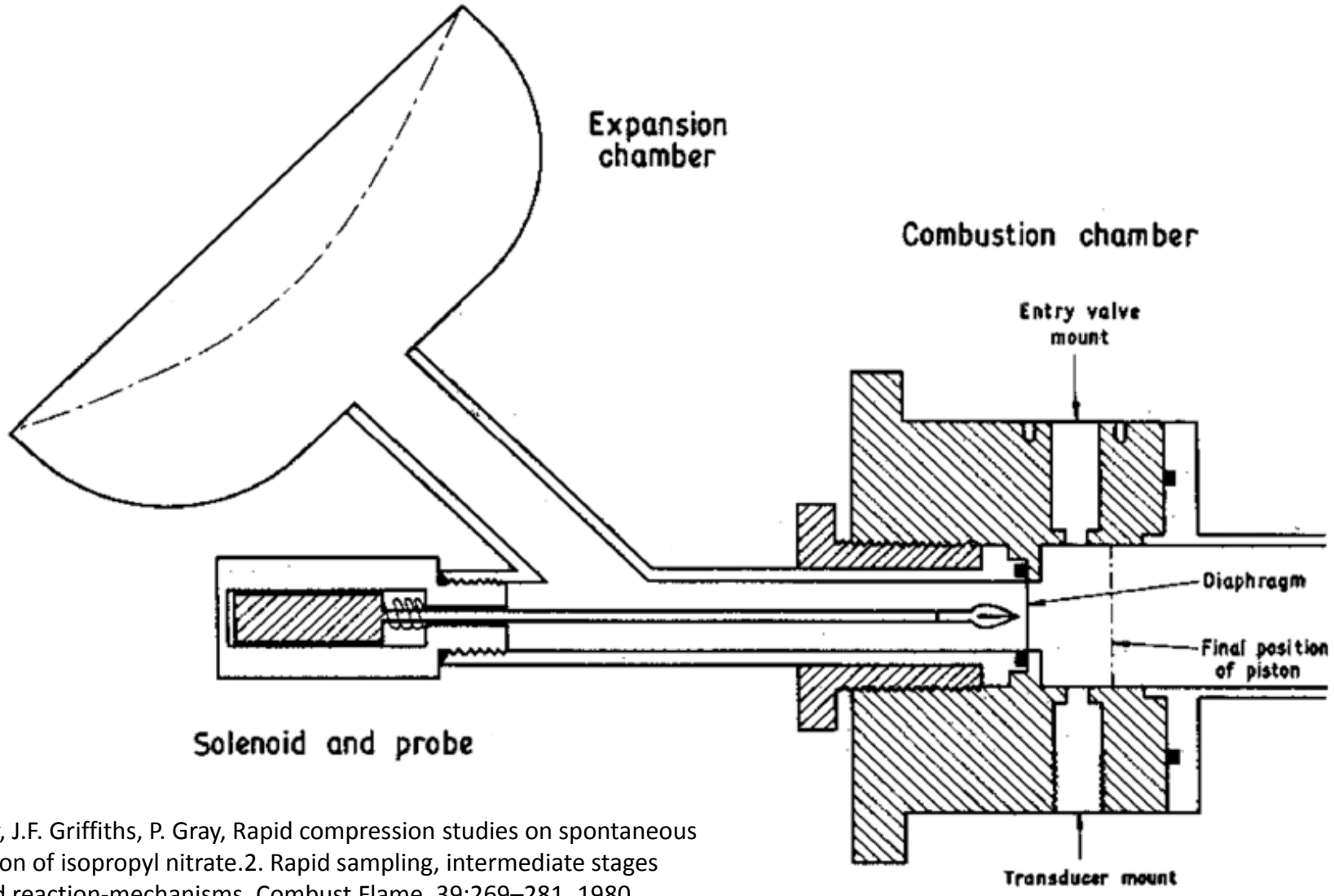

P. Beeley, J.F. Griffiths, P. Gray, Rapid compression studies on spontaneous ignition of isopropyl nitrate.2. Rapid sampling, intermediate stages and reaction-mechanisms, Combust Flame, 39:269–281, 1980.

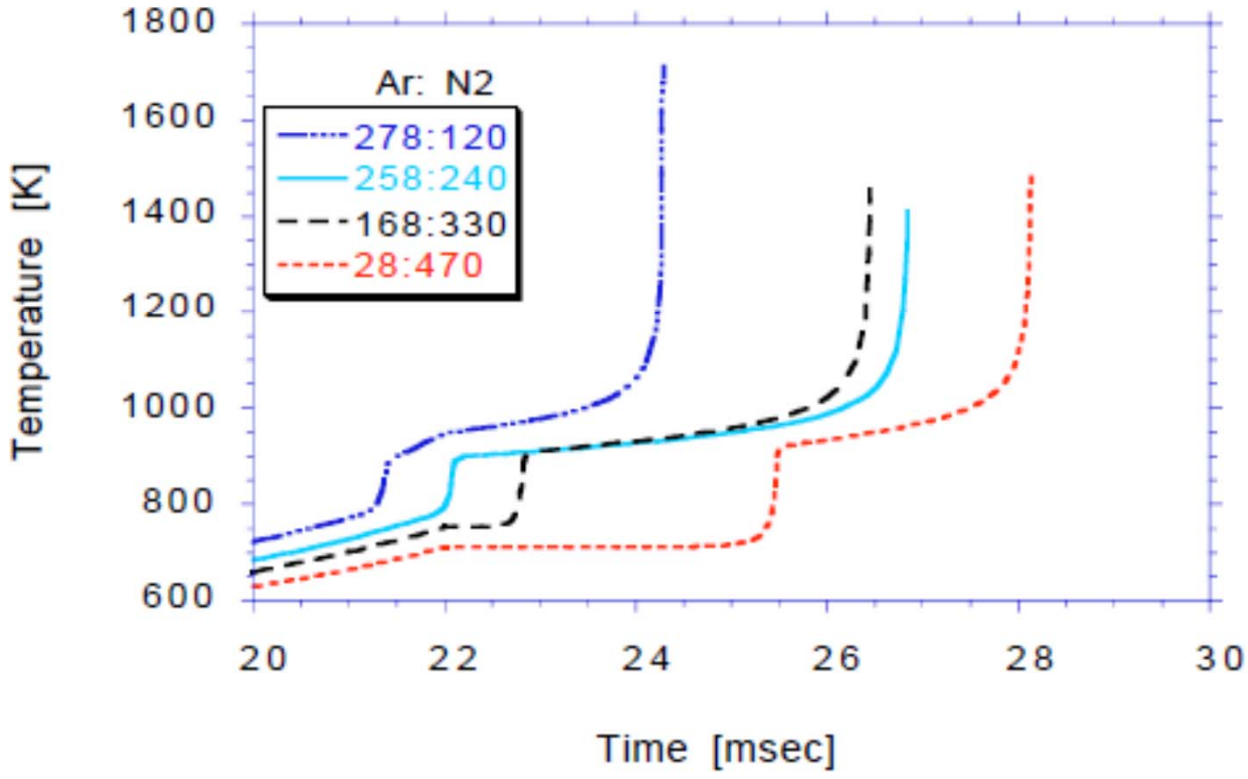

Figure 1. Computed temperature histories for four n-heptane/O_2/Ar/N_2 mixtures. Temperatures at end of compression are 711, 753, 798 and 949 K in order of increasing Ar concentration.

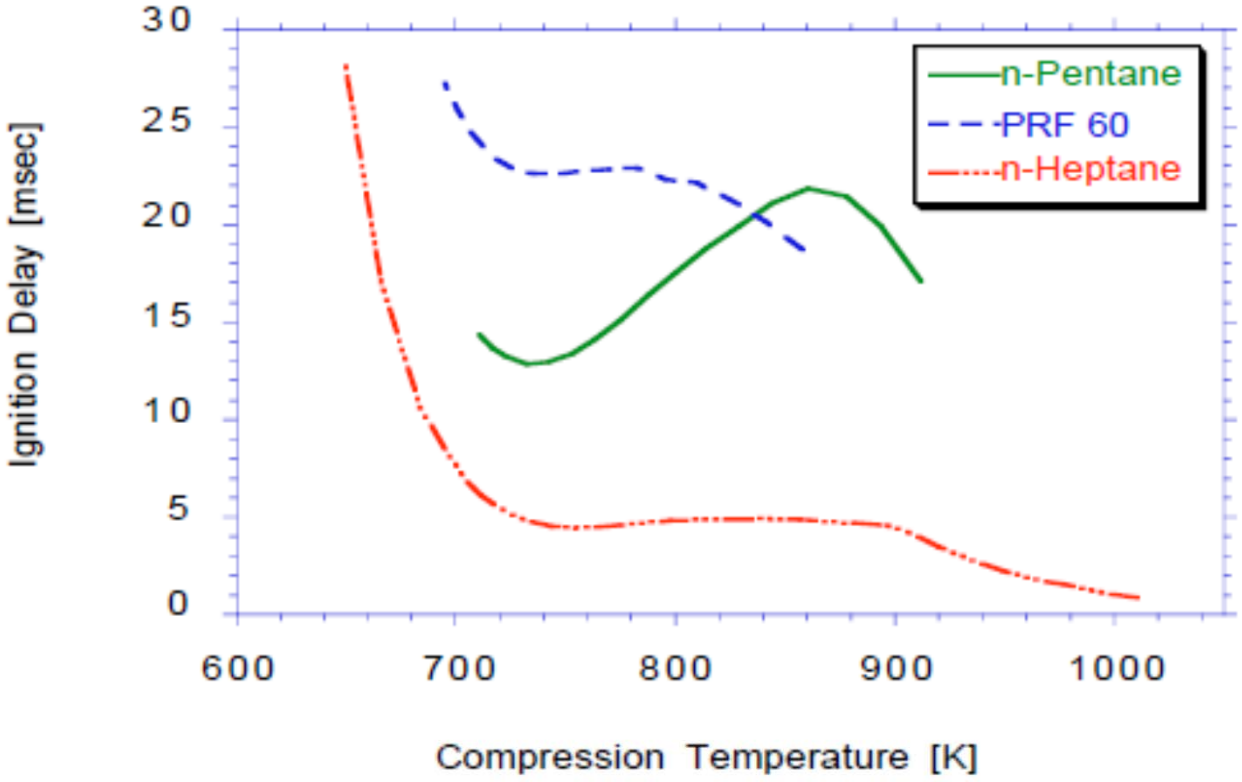

Figure 3. Computed ignition delay times, including reaction during compression stroke, for n-heptane, n-pentane, and PRF 60 mixture.

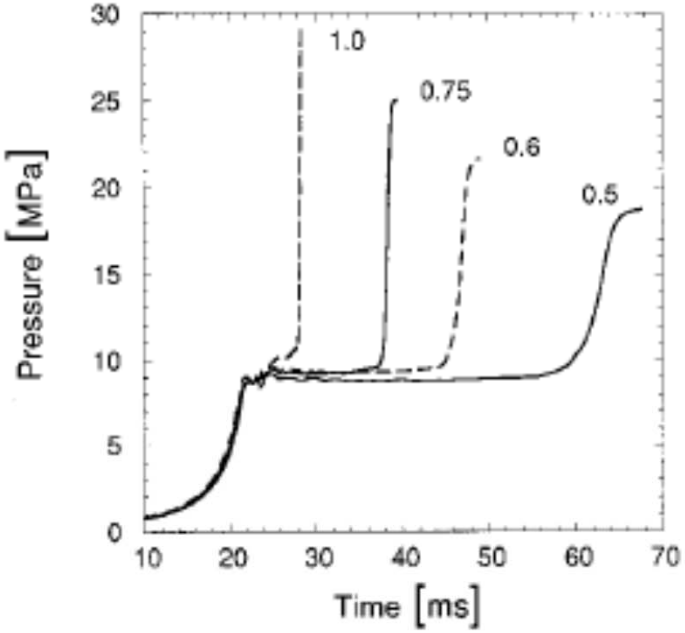

FIG. 2. Experimental pressure records for ignition following compression to 765 (±5 K) at indicated values of equivalence ratio. Initial pressures are all 0.33 bar.

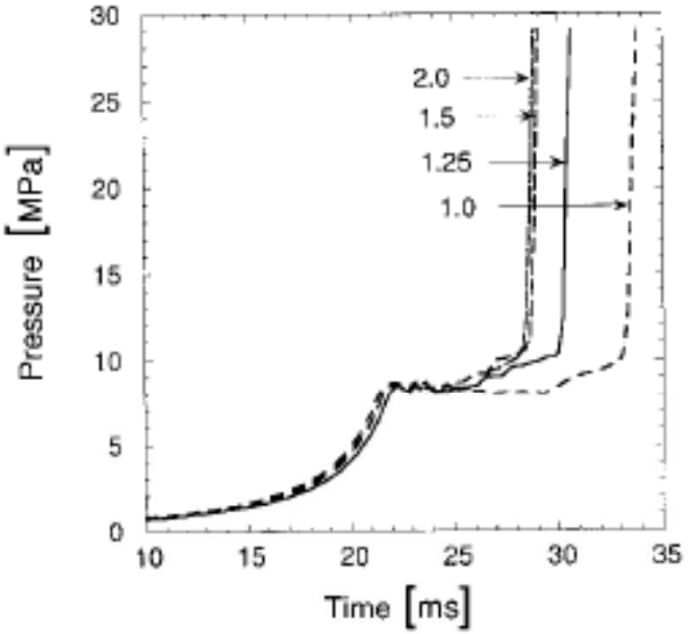

FIG. 3. Experimental pressure records for ignition following compression to 724 (±6 K) at indicated values of equivalence ratio. Initial pressures are all 0.33 bar.

Rich mixtures ignite faster than leaner mixtures at low temperatures

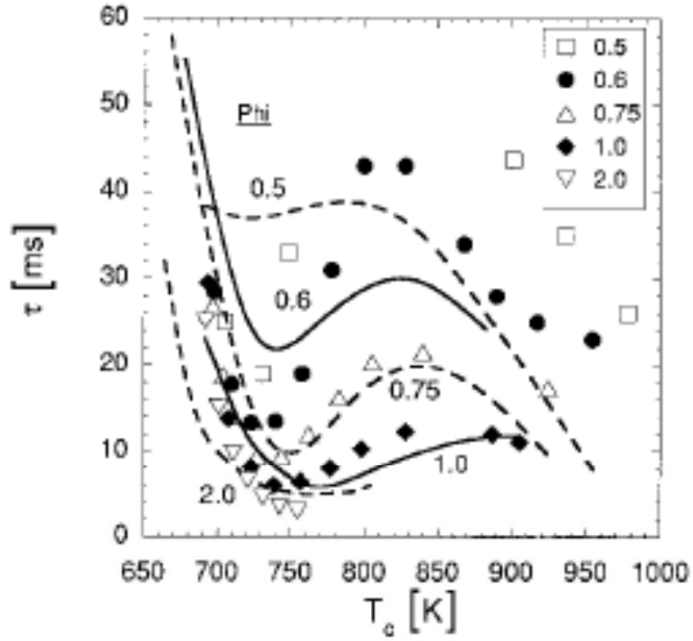

FIG. 4. Variations in total ignition delay time with compression temperature for selected values of equivalence ratio. Curves represent fits to experimental results and are labeled by the value of the equivalence ratio, symbols indicate computed results for values of ϕ shown in the legend. Initial pressures are all 0.33 bar.

"Crossover" temperature above 950K

Isomers of heptane – ignition delays

Some of these fuels were also studied in Galway RCM

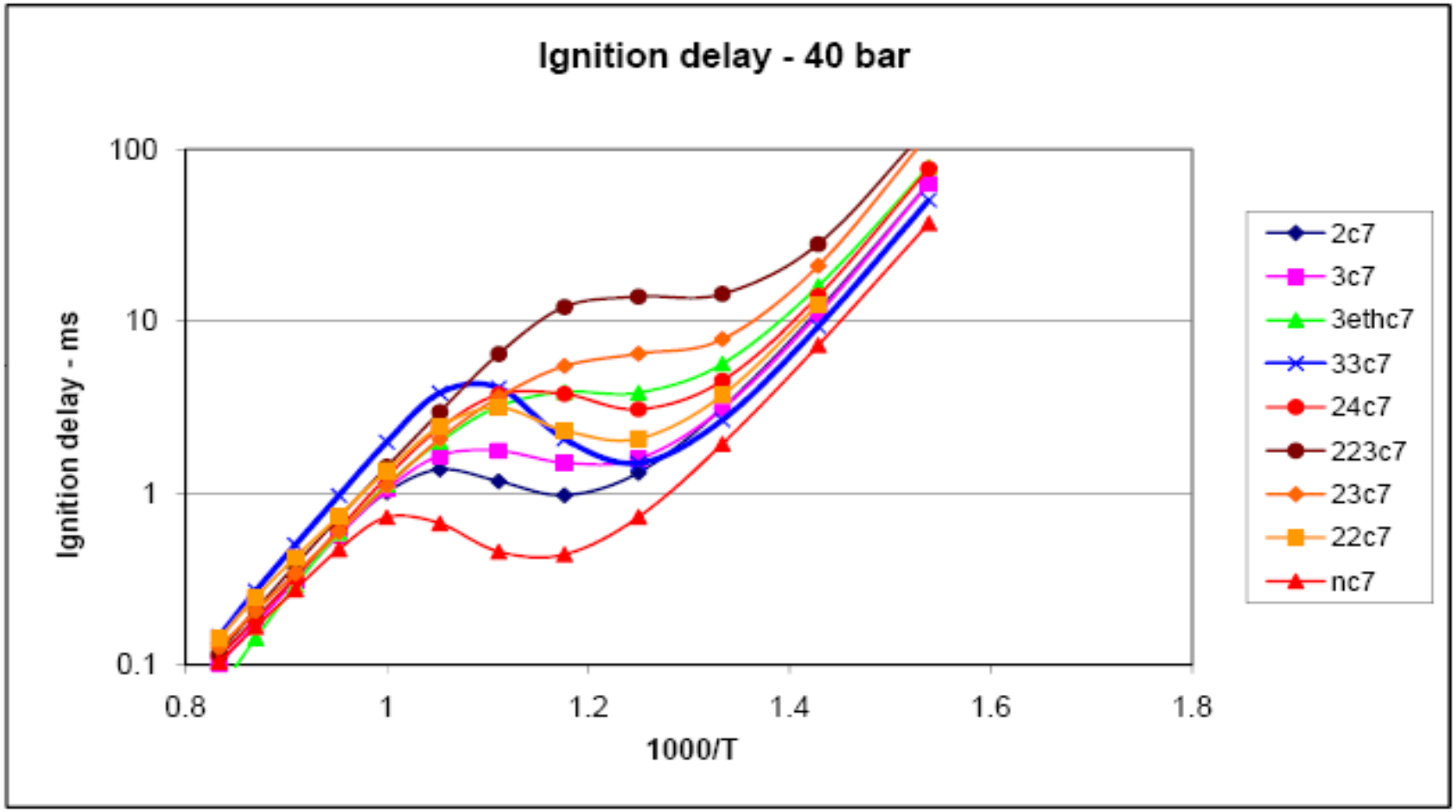

Simulated ignition under conditions in a rapid compression machine

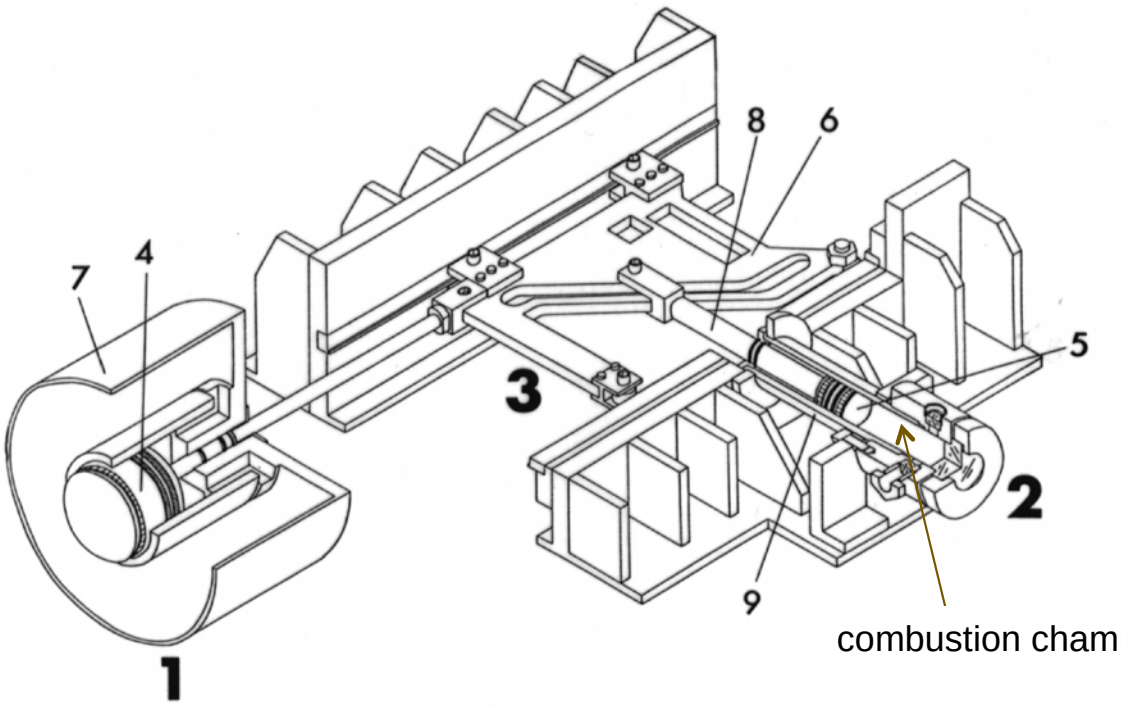

Vanhove, Minetti, Ribaucour, and coworkers, Lille, France

Rapid Sampling in Lille RCM

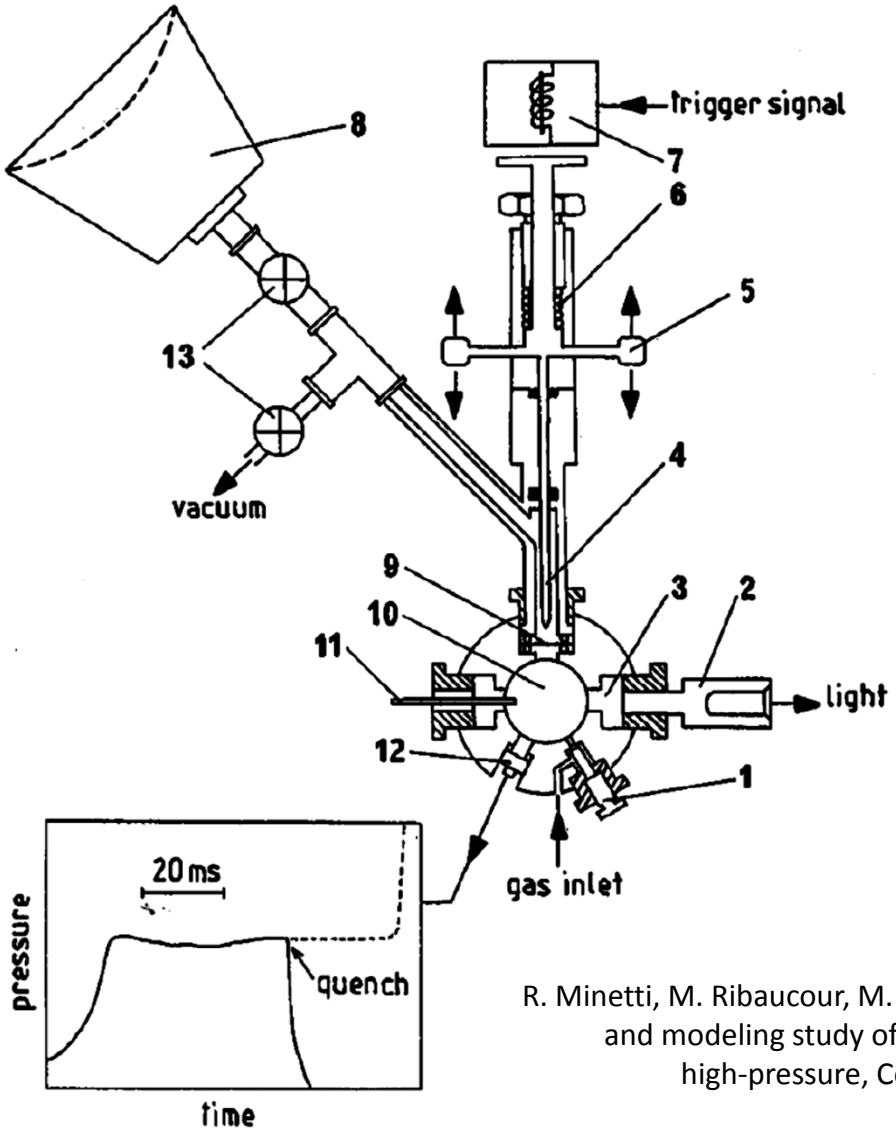

R. Minetti, M. Ribaucour, M. Carlier, C. Fittschen, L.R. Sochet, Experimental and modeling study of oxidation and autoignition of butane at high-pressure, Combust Flame, 96:201–211, 1994.

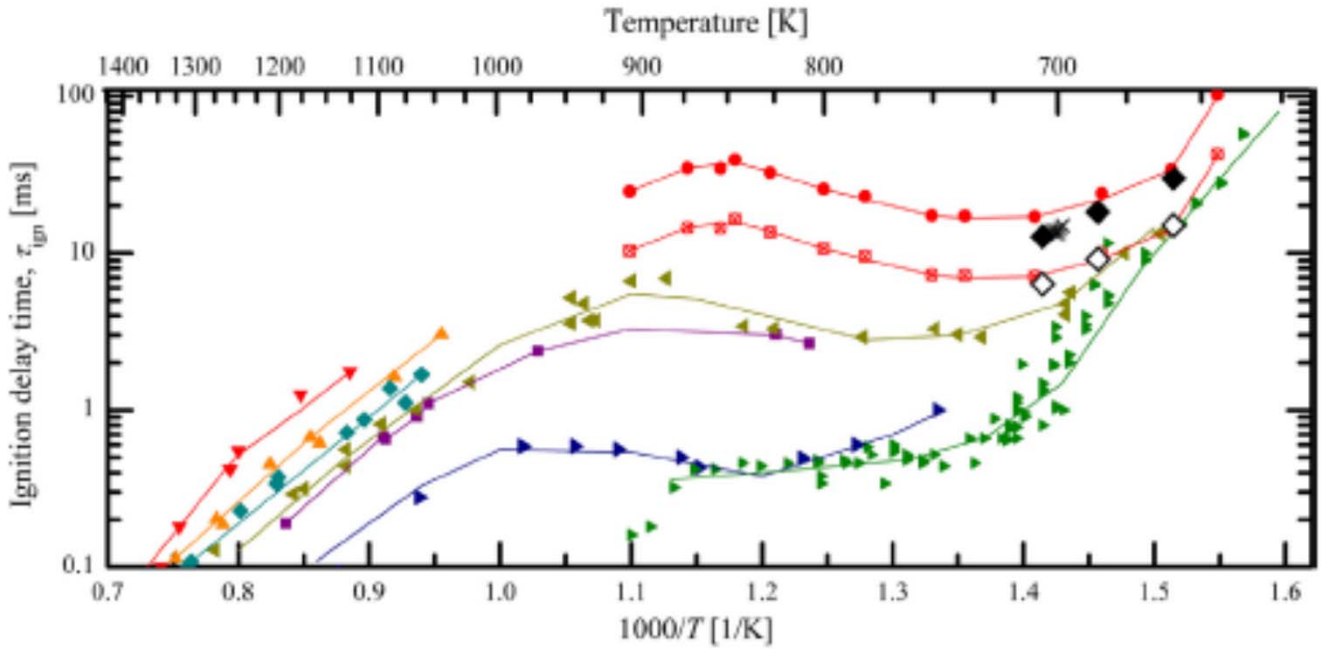
Temperature [K]
1400 1300 1200 1100 1000 900 800 700
100
10
1
0.1
Ignition delay time, τ_{ign} [ms]
0.7 0.8 0.9 1.0 1.1 1.2 1.3 1.4 1.5 1.6
1000/T [1/K]
Ciezki and Adomeit, P = 3.2 bar
Ciezki and Adomeit, P = 6.5 bar
Ciezki and Adomeit, P = 13.5 bar
Ciezki and Adomeit, P = 42 bar
Shen et al., P = 10-13 atm
Shen et al., P = 42 atm, ϕ = 0.25
Silke et al., P = 20 atm
Minetti et al., P = 3-4.5 bar
Minetti et al., P = 3-4.5 bar data scaled to 9 bar
UM RCF ignition data, P_{eff} = 9.3-9.5 atm
UM RCF ignition data scaled to inert/O_2 = 3.76
UM RCF sampling data, P_{eff} ~ 9 atm

Rapid Sampling in UM RCF

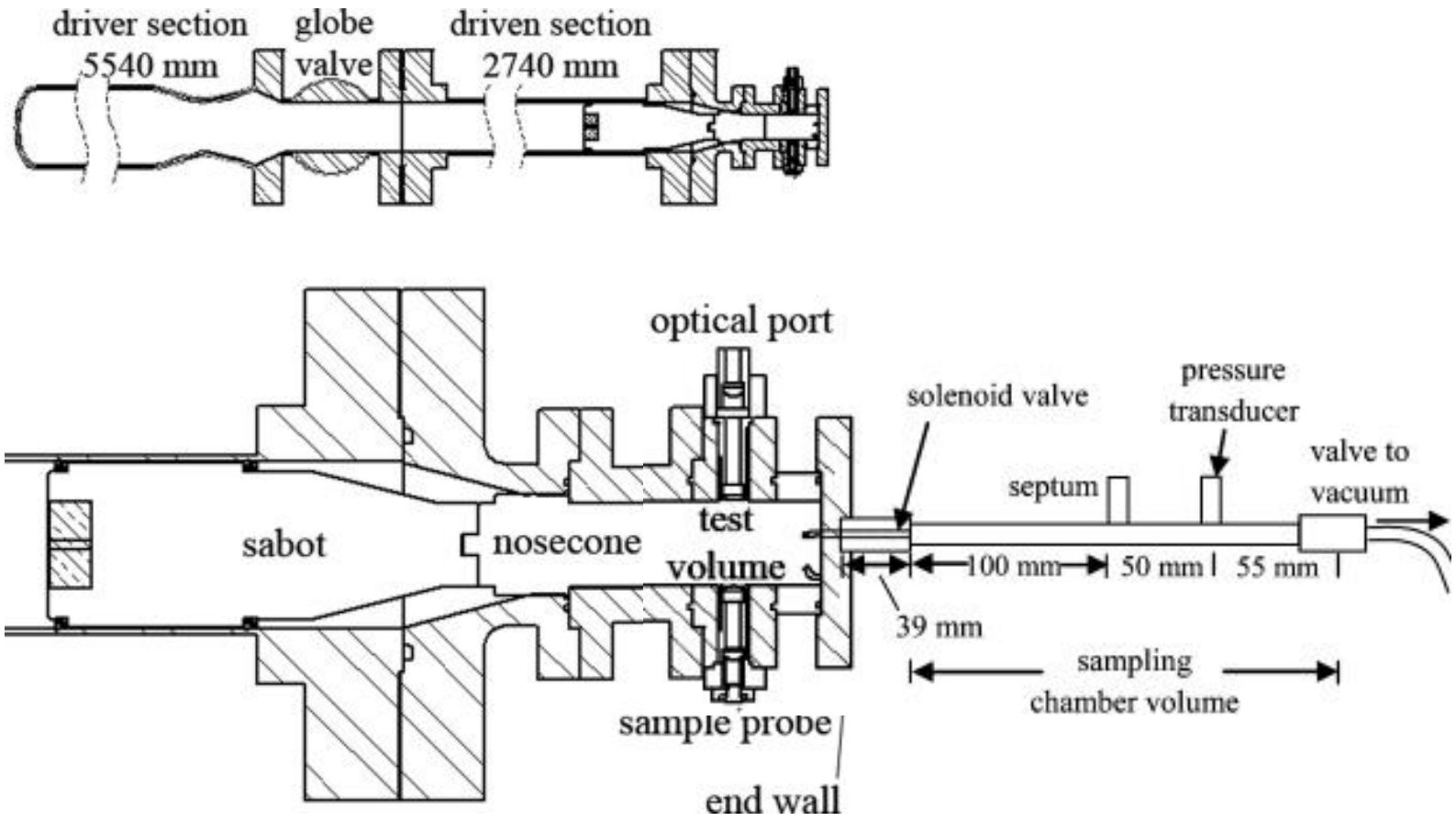

D.M.A. Karwat, S.W. Wagnon, P.D. Teini, M.S. Wooldridge
"On the Chemical Kinetics of n-Butanol: Ignition and Speciation Studies"
J. Phys. Chem. A, 115:4909–4921, 2011.

UM rapid compression facility

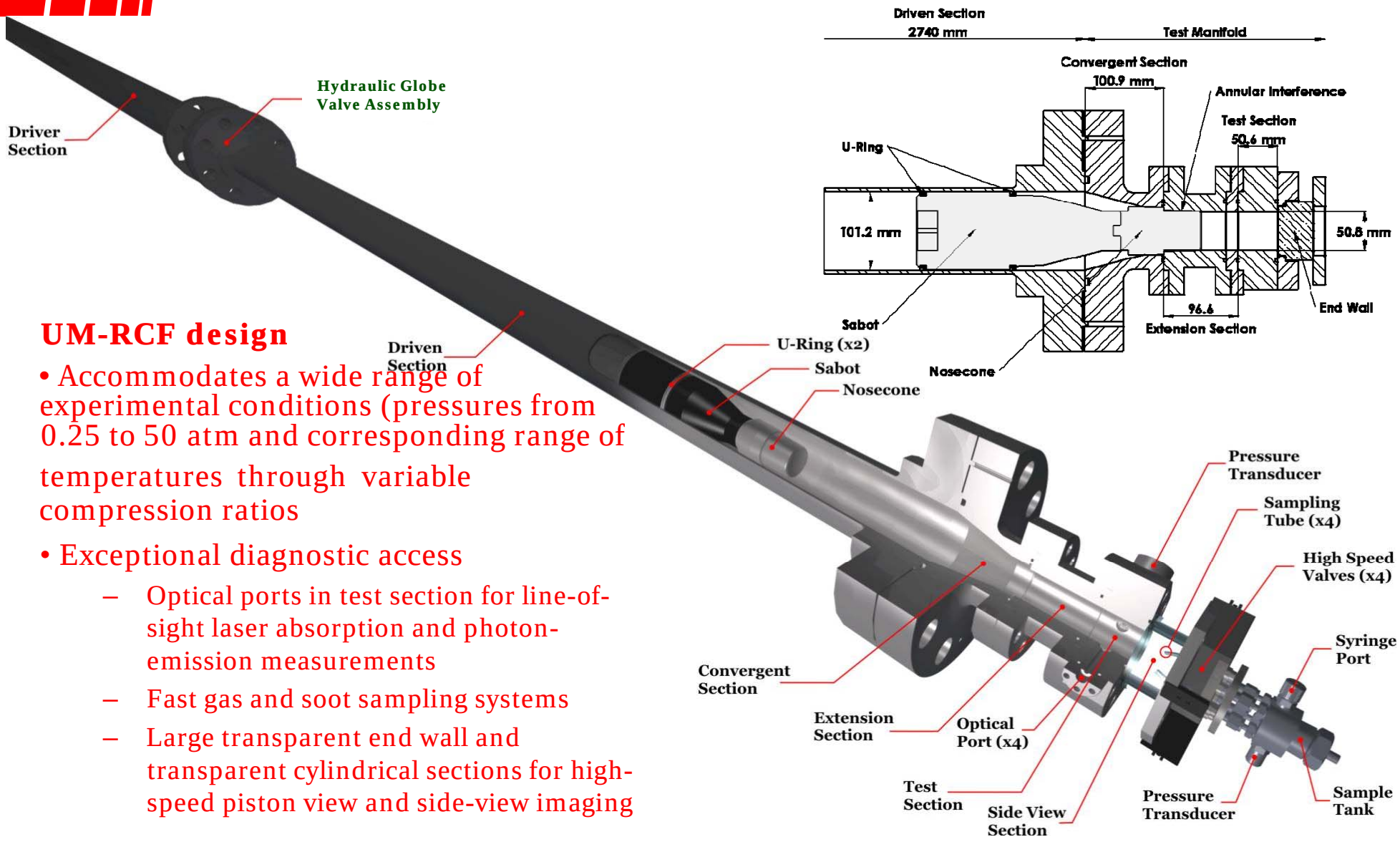

UM-RCF design

- Accommodates a wide range of experimental conditions (pressures from 0.25 to 50 atm and corresponding range of temperatures through variable compression ratios
- Exceptional diagnostic access
  - Optical ports in test section for line-of-sight laser absorption and photon-emission measurements
  - Fast gas and soot sampling systems
  - Large transparent end wall and transparent cylindrical sections for high-speed piston view and side-view imaging

Rapid Sampling in UM RCF

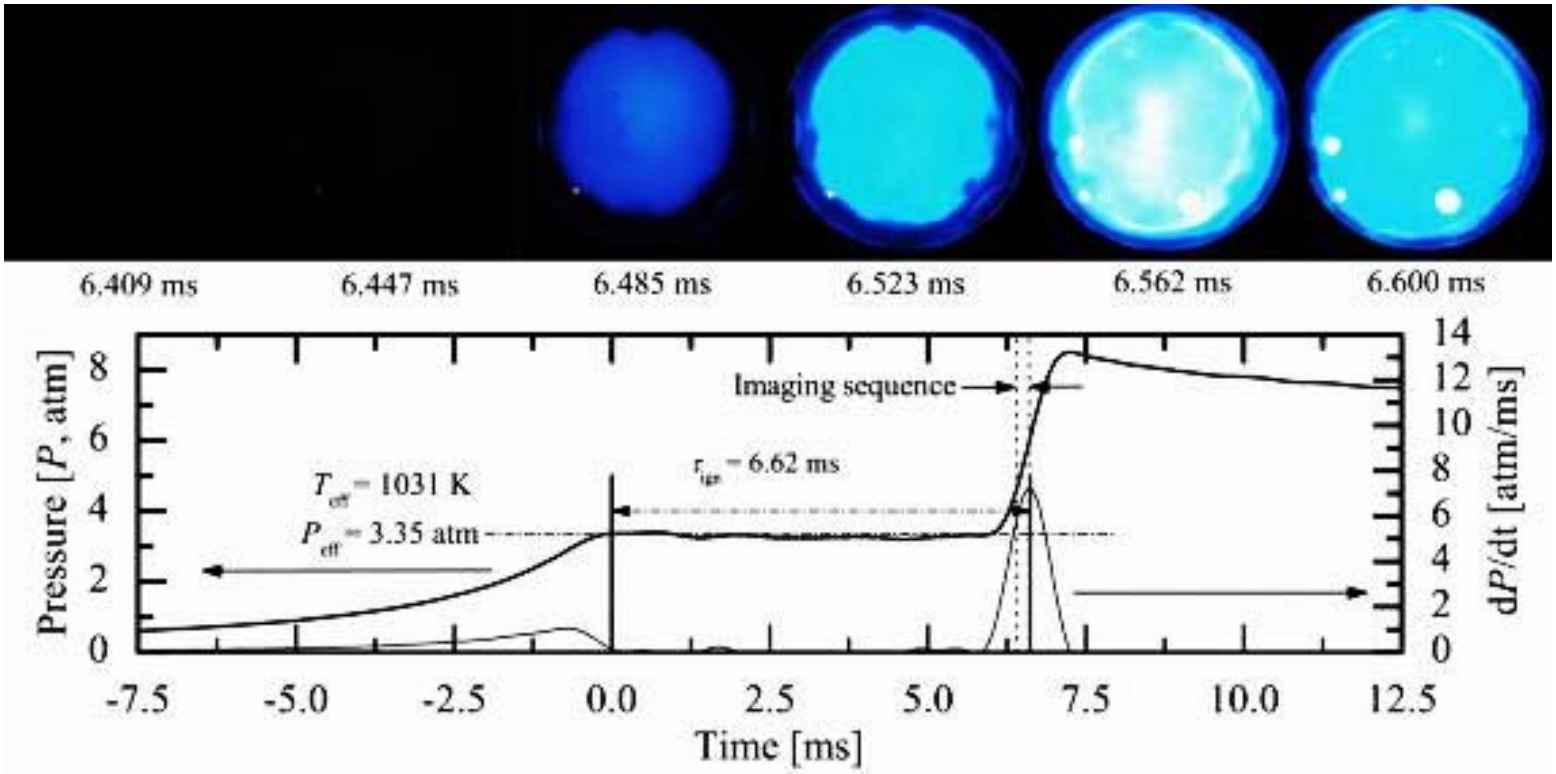

D.M.A. Karwat, S.W. Wagnon, P.D. Teini, M.S. Wooldridge
"On the Chemical Kinetics of n-Butanol: Ignition and Speciation Studies"
J. Phys. Chem. A, 115:4909–4921, 2011.

Progress in Energy and Combustion Science xxx (2014) 1–18

Contents lists available at ScienceDirect

Progress in Energy and Combustion Science

journal homepage: www.elsevier.com/locate/pecs

Review

Using rapid compression machines for chemical kinetics studies

Chih-Jen Sung [a,*], Henry J. Curran [b]

[a] Department of Mechanical Engineering, University of Connecticut, Storrs, CT 06269, USA
[b] Combustion Chemistry Centre, National University of Ireland, Galway, Ireland

Maruta microchannel reactor

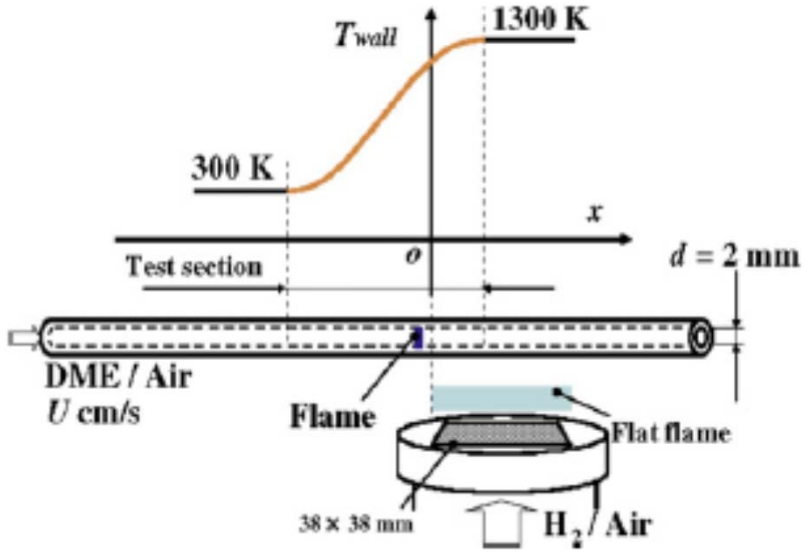

Fig. 13. A narrow channel with a prescribed wall temperature profile. Inner diameter of 2 mm, which is smaller than the ordinary quenching diameter, was chosen. Though hydrogen/air flat flame burner was shown as a heat source here, flat panel heaters were also used for earlier study.

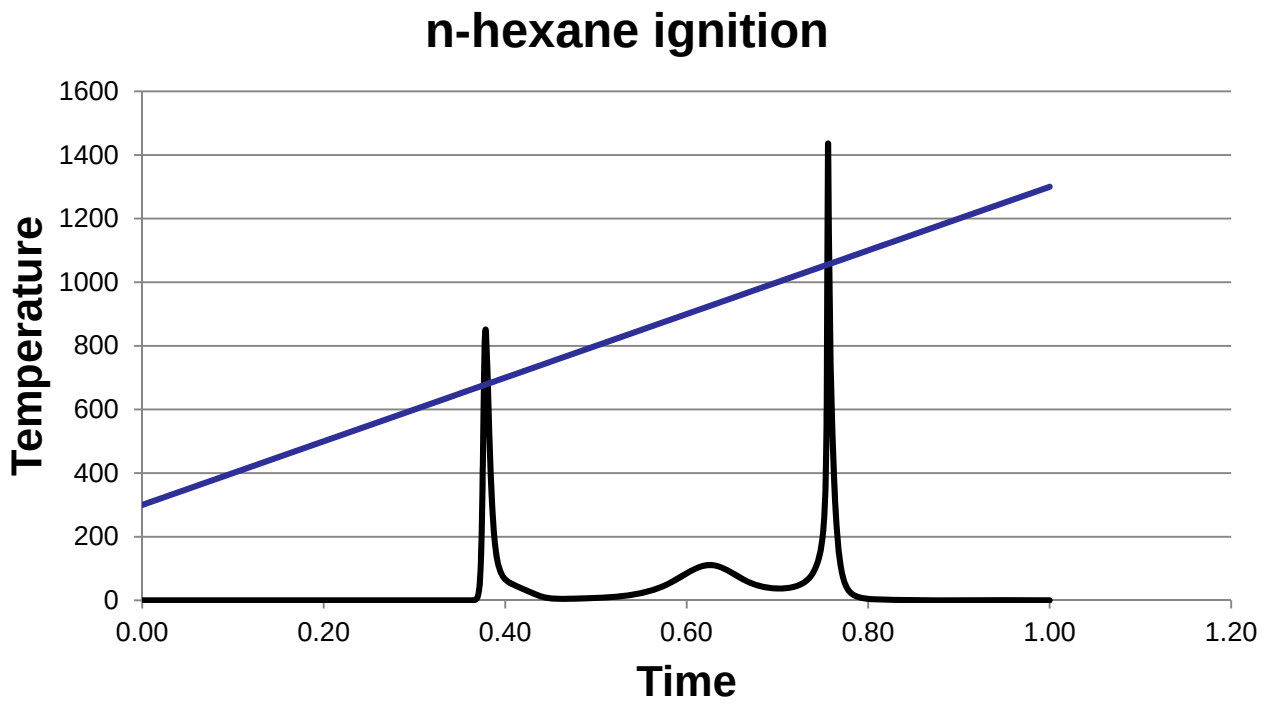
n-hexane ignition
Temperature
1600
1400
1200
1000
800
600
400
200
0
0.00
0.20
0.40
0.60
0.80
1.00
1.20
Time

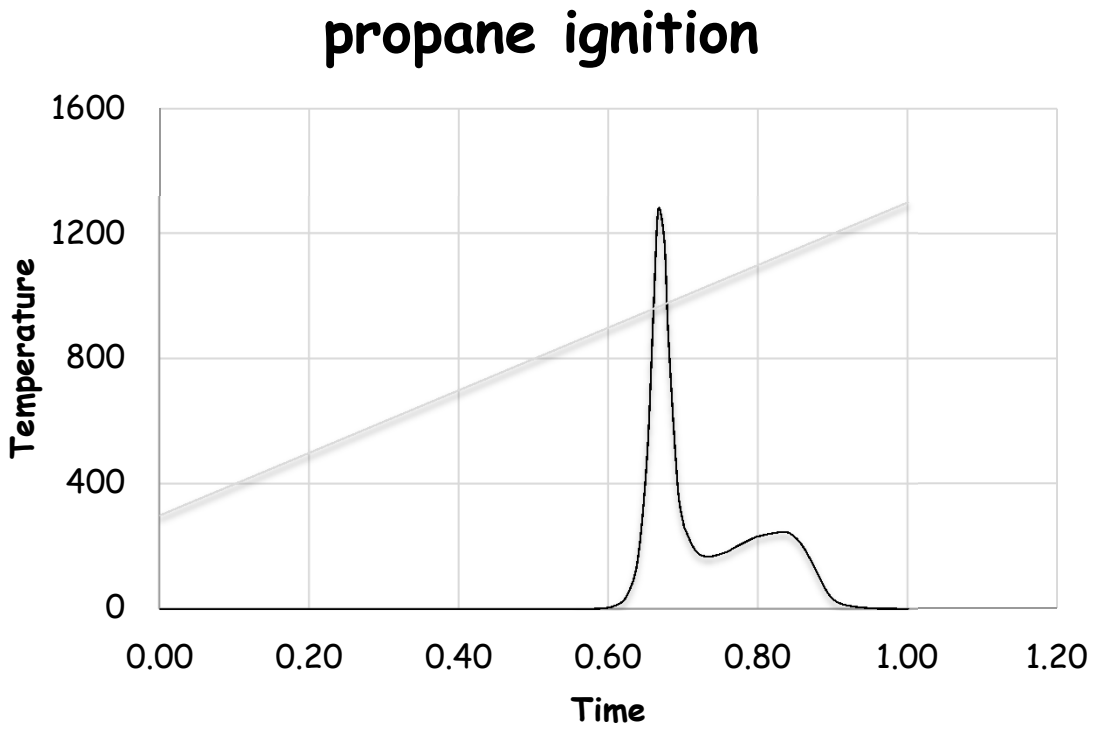
propane ignition
1600
1200
800
400
0
Temperature
0.00
0.20
0.40
0.60
0.80
1.00
1.20
Time

ST and RCM contribution to mechanism generation and validation

Shock Tube Ignition Delay Studies

Karlsruhe Inst. For Technology Shock Tube (Olzmann et al.)

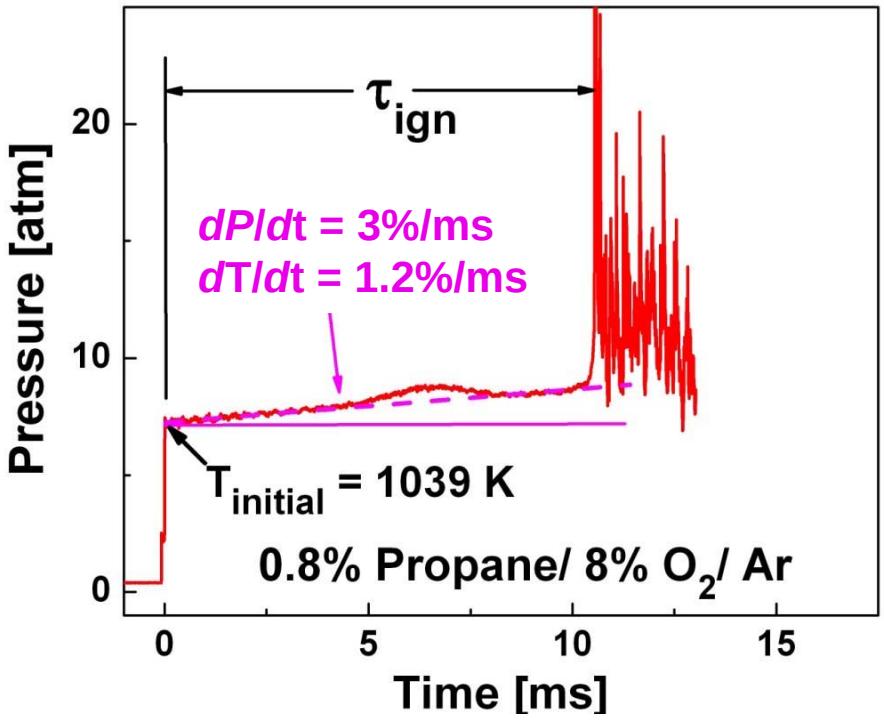

Shock Tubes are ideal for measuring homogeneous gas phase reaction kinetics

Ideally a zero-dimensional system after reflected shock departs from the end wall

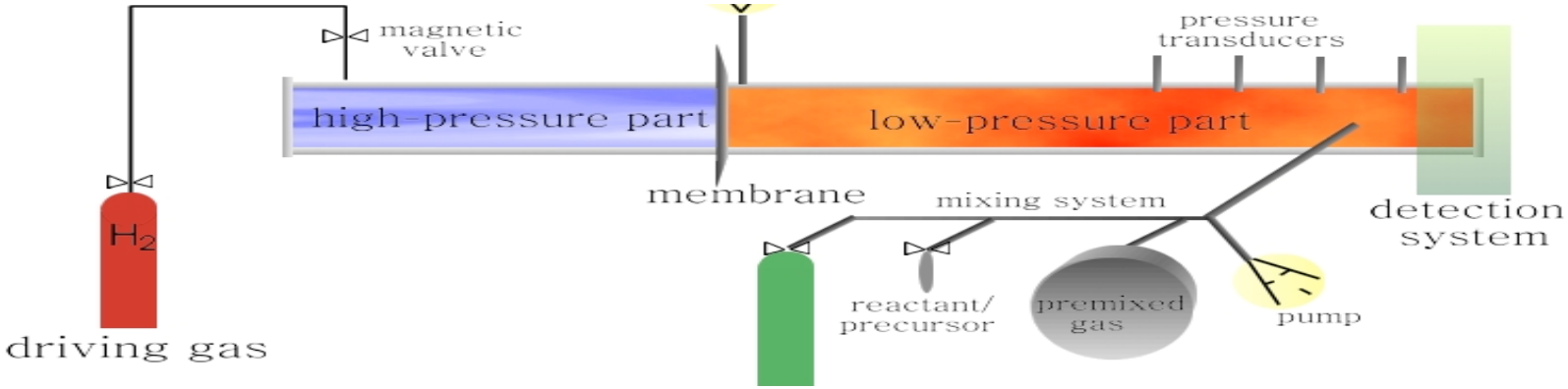

Stanford Shock Tubes

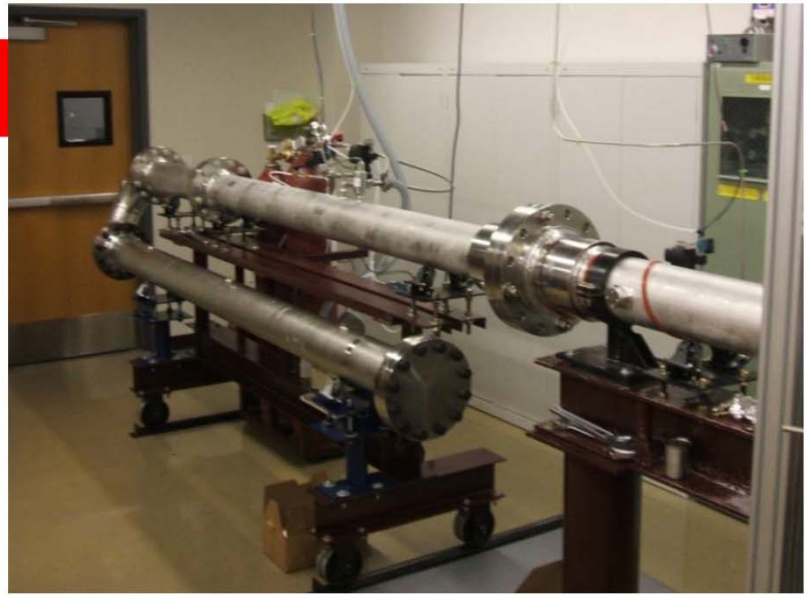

Kinetics Shock Tube 1 (30 atm)

Kinetics Shock Tube 2 (30 atm)

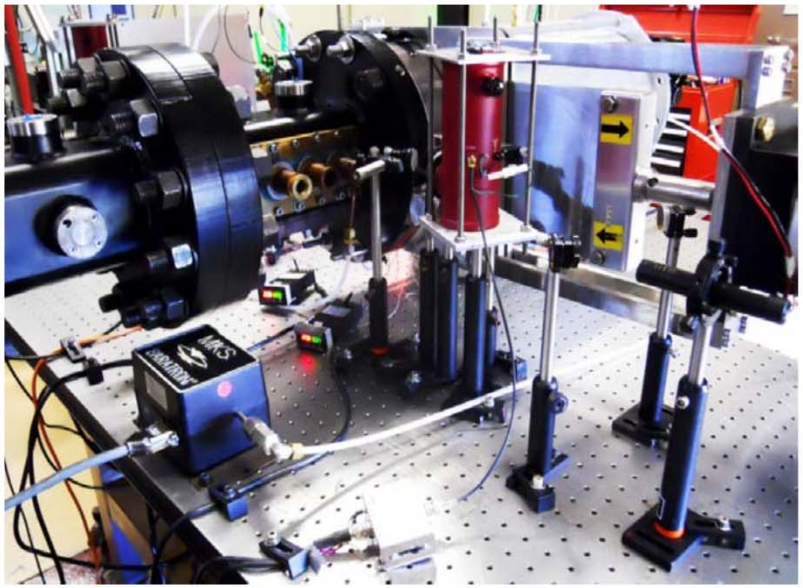

Aerosol Shock Tube (10 atm)

High Pressure Shock Tube (500 atm)

ST Ignition Delay Results

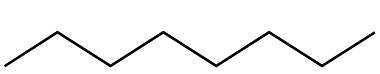

n-octane

RON

-19.0

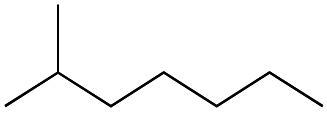

2-methylheptane

21.7

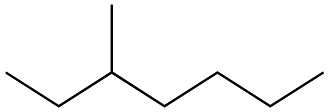

3-methylheptane

36.8

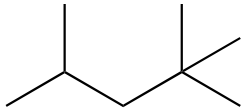

2,2,4-trimethylpentane

iso-ioctane

100

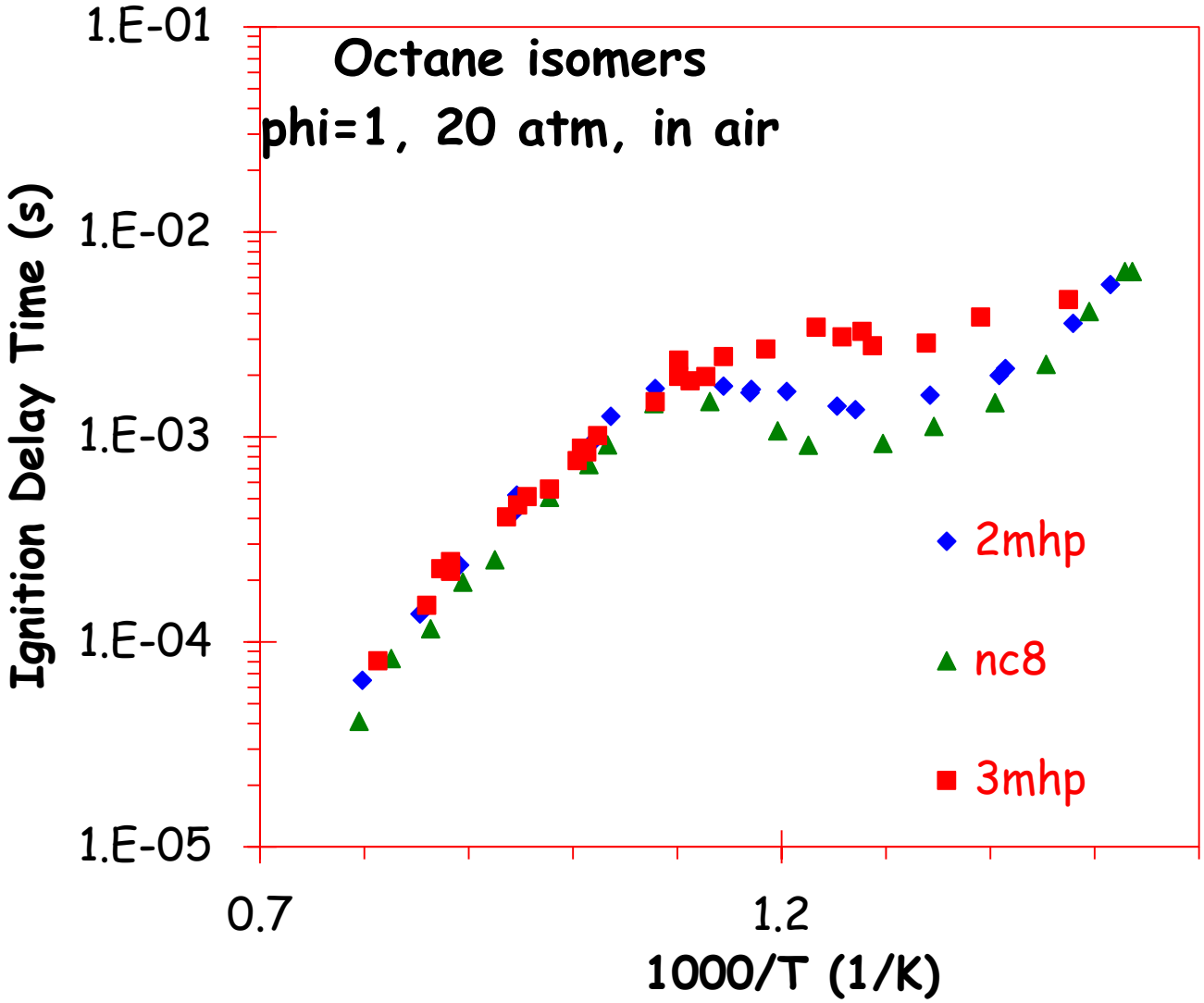

Reactions in shock waves

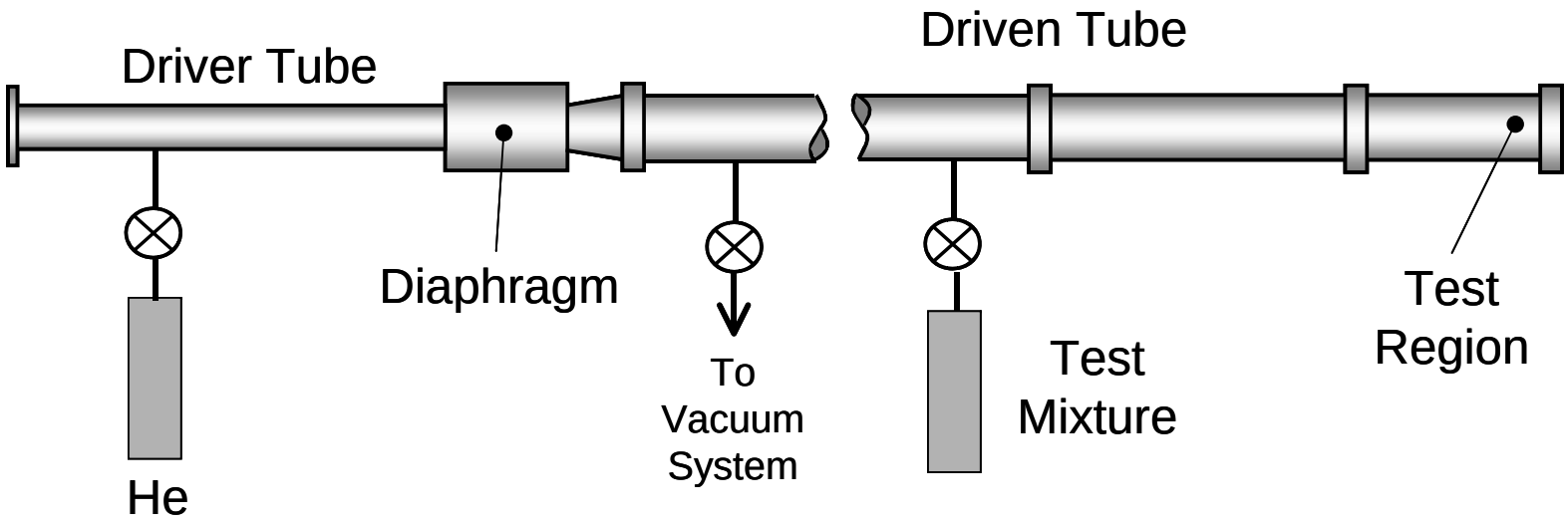

- Wide range of **T**'s & **P**'s accessible; **2,000** K, **50** bar routine
- Thermodynamics of high-T species eg **Ar** up to **5,000** K
- Study birth of compounds: $\mathbf{C_6H_5CHO \rightarrow CO^* + C_6H_6}$
- Energy transfer rxns.: $\mathbf{CO_2 + M \rightarrow CO_2^* + M}$
- Relative rates, use standard rxn as "clock"

Mode of action of shock tube

- Fast bunsen-burner (ns)
- Shock wave acts as a piston compressing & heating the gas ahead of it
- Study rxns behind incident shock wave or reflected shock wave (ms-ms times)
- Non-invasive techniques
- ***T*** & ***p*** by computation from measured shock velocity

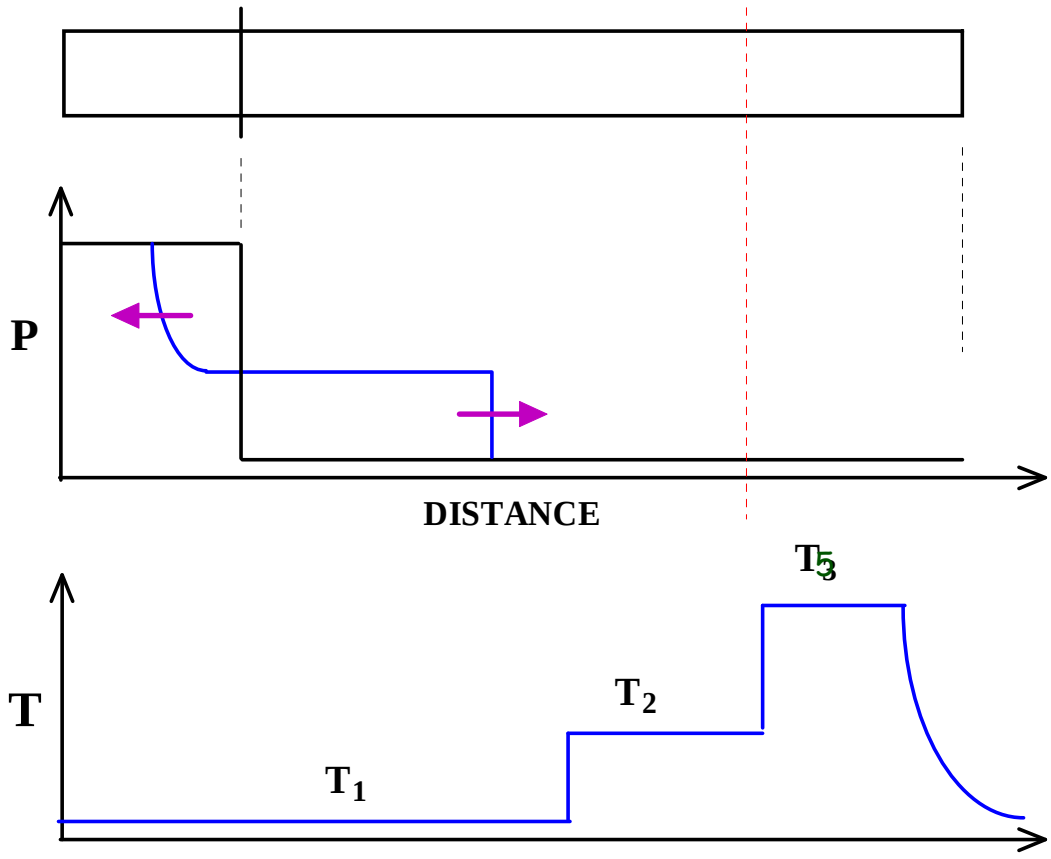

Shock Tube Operation and New Strategies

Advantages of Reflected Shock Wave Experiments

- **Accurately known initial T, P and time-zero**
- **Lack of transport effects**

Weakness

- **Non-uniformity in T_5, P_5 with time and location; we call this the dP_5/dt problem**

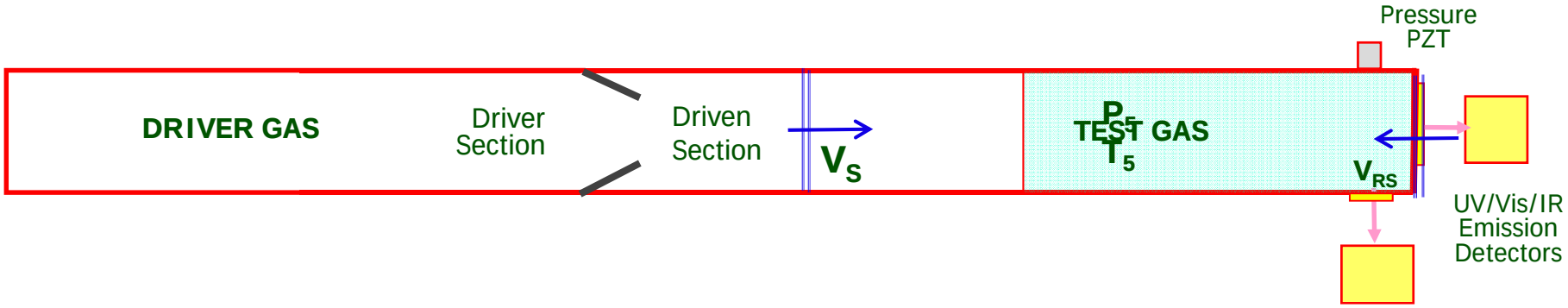

Slide courtesy of Prof. Ron Hanson Stanford University

Shock Tube Simulation

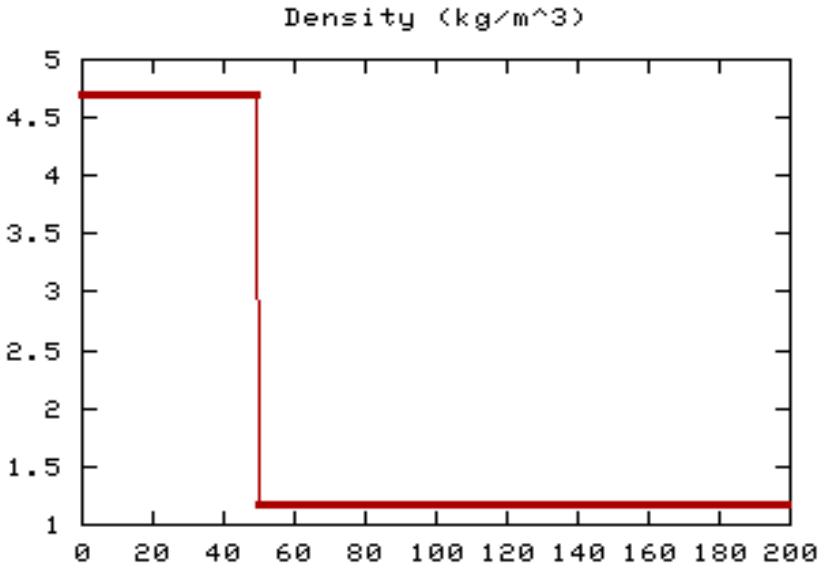

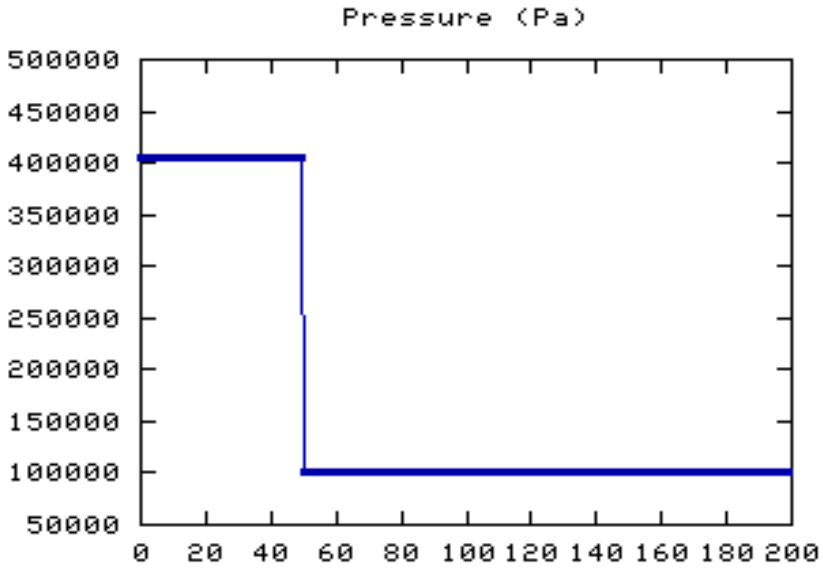

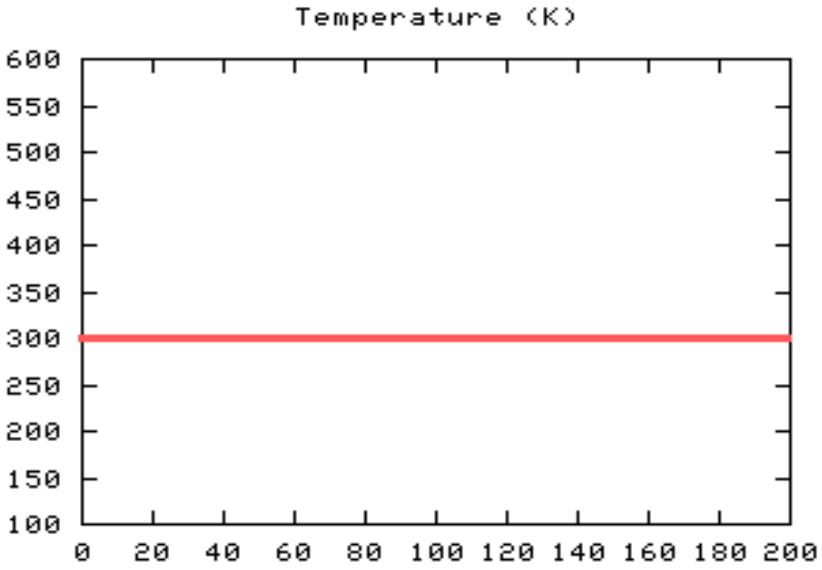

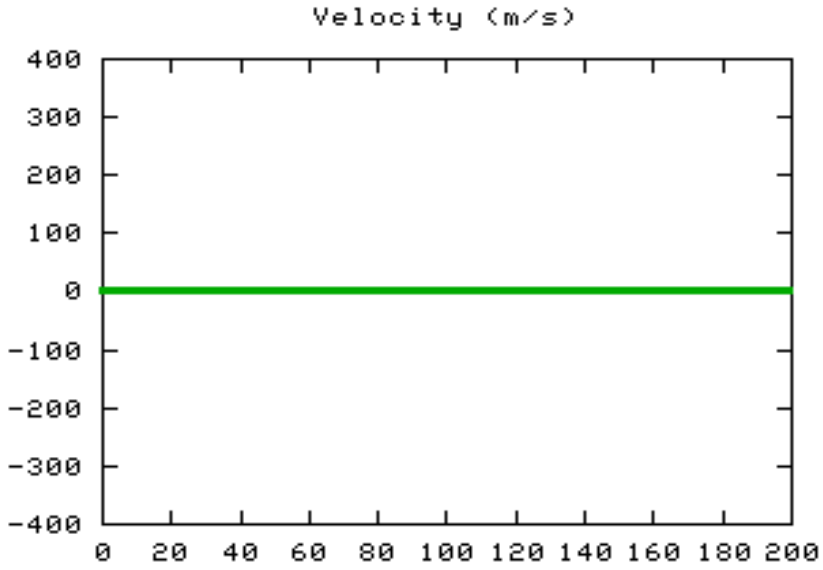

Time available in ST

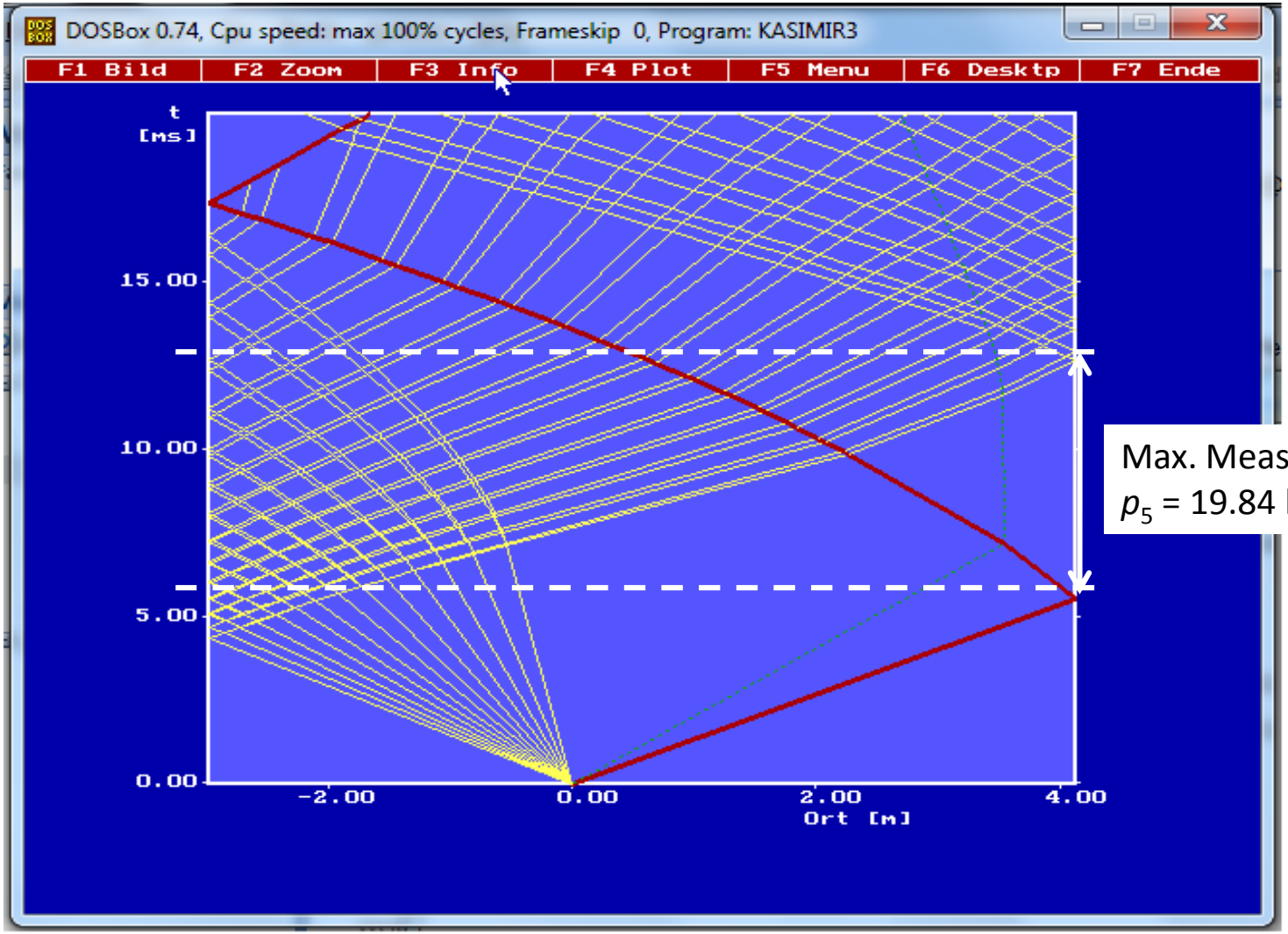

Max. Meas. Time ≈ 7 ms
p_5 = 19.84 bar, T_5= 806 K

Driver gas: 10% Ar / 90% He Driven gas: air
p_4 = 20 bar, p_1 = 1 bar

Real available measuring time around 5.3 ms (estimation)

Ignition delay times

CH **Chemiluminescence (431 nm)** Detected at Endwall and Sidewall*

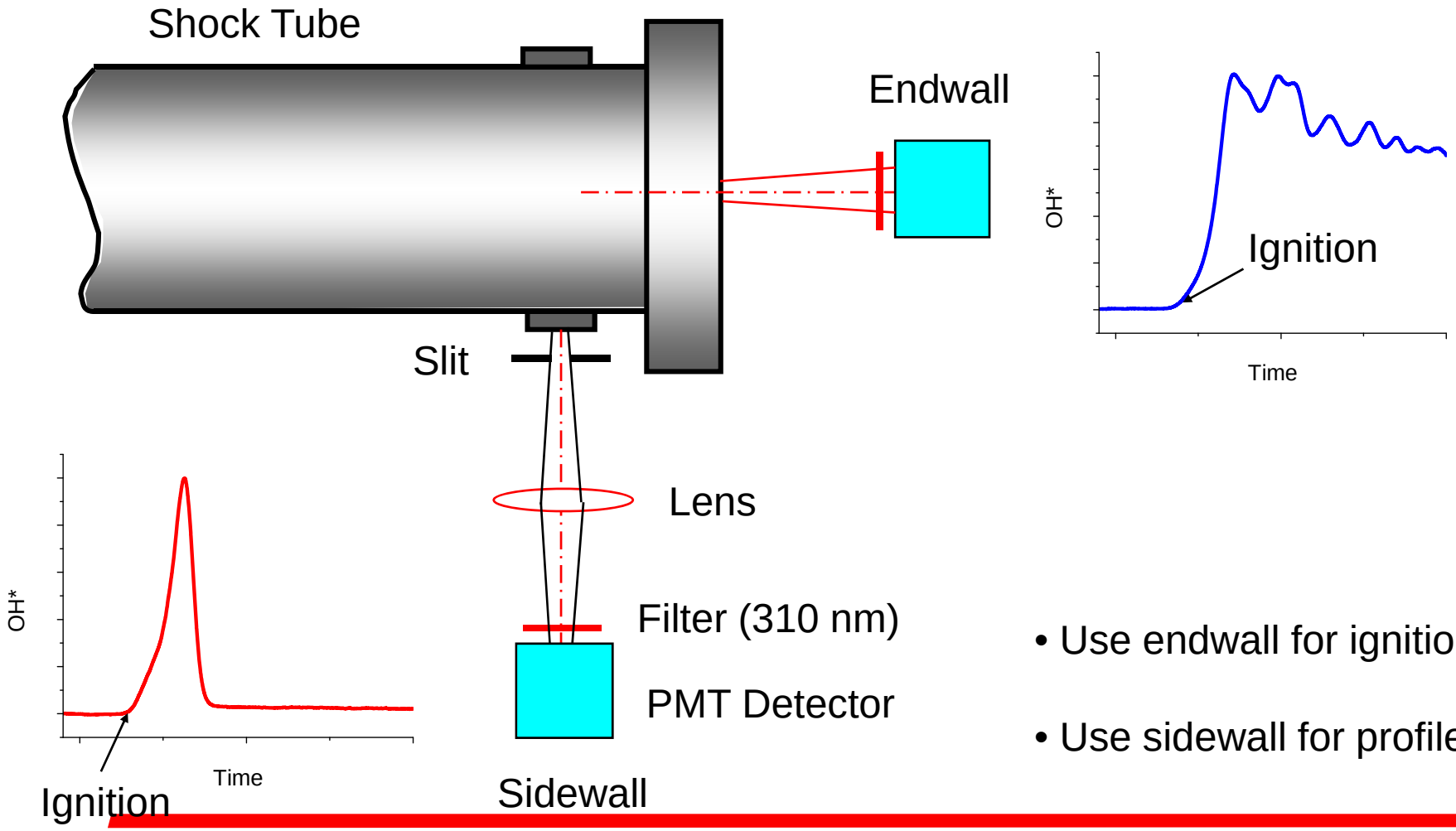

- Use endwall for ignition
- Use sidewall for profiles

Slide courtesy of Prof. E. Petersen

Typical ST experimental record

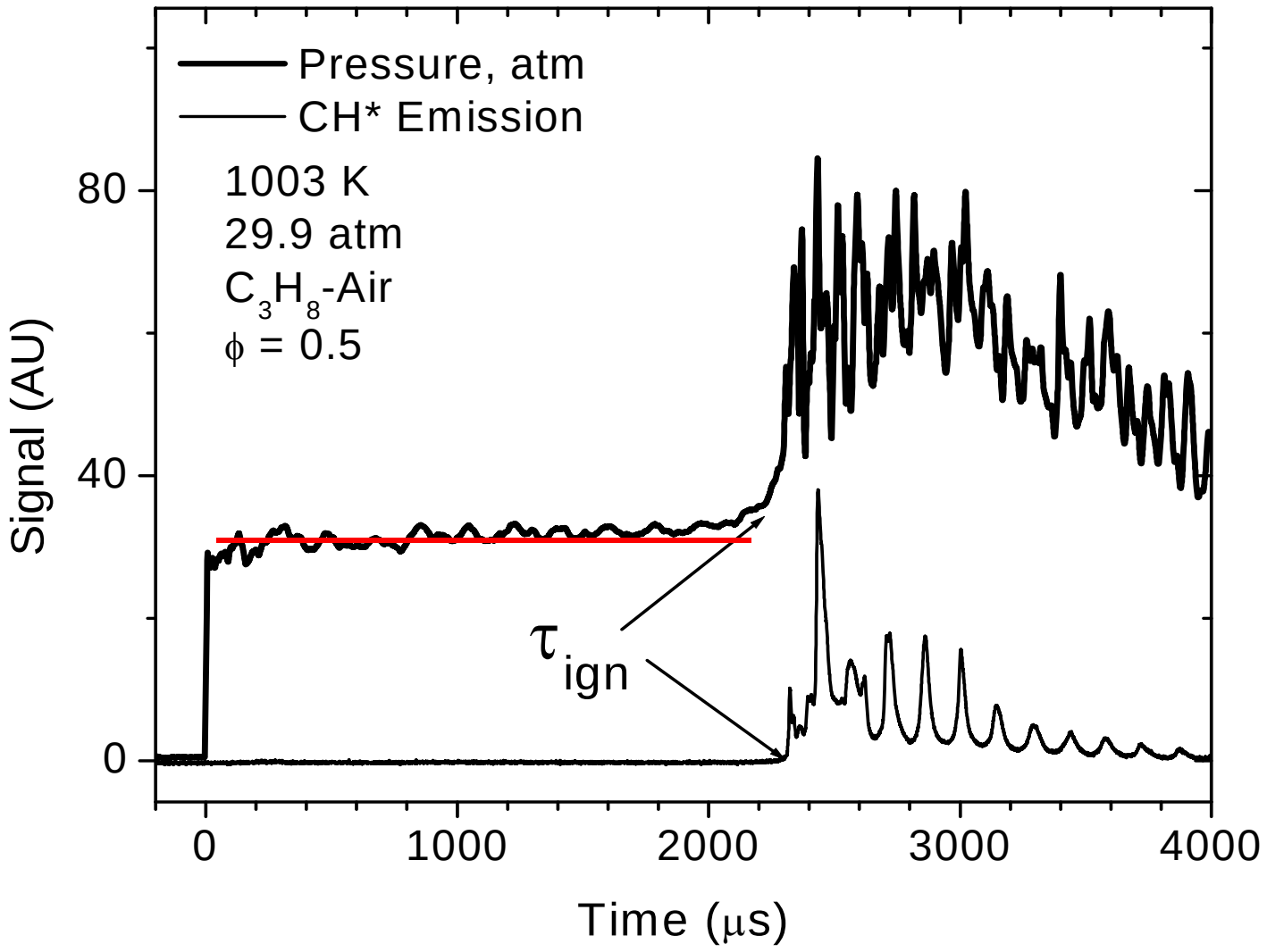

Slide courtesy of Prof. E. Petersen

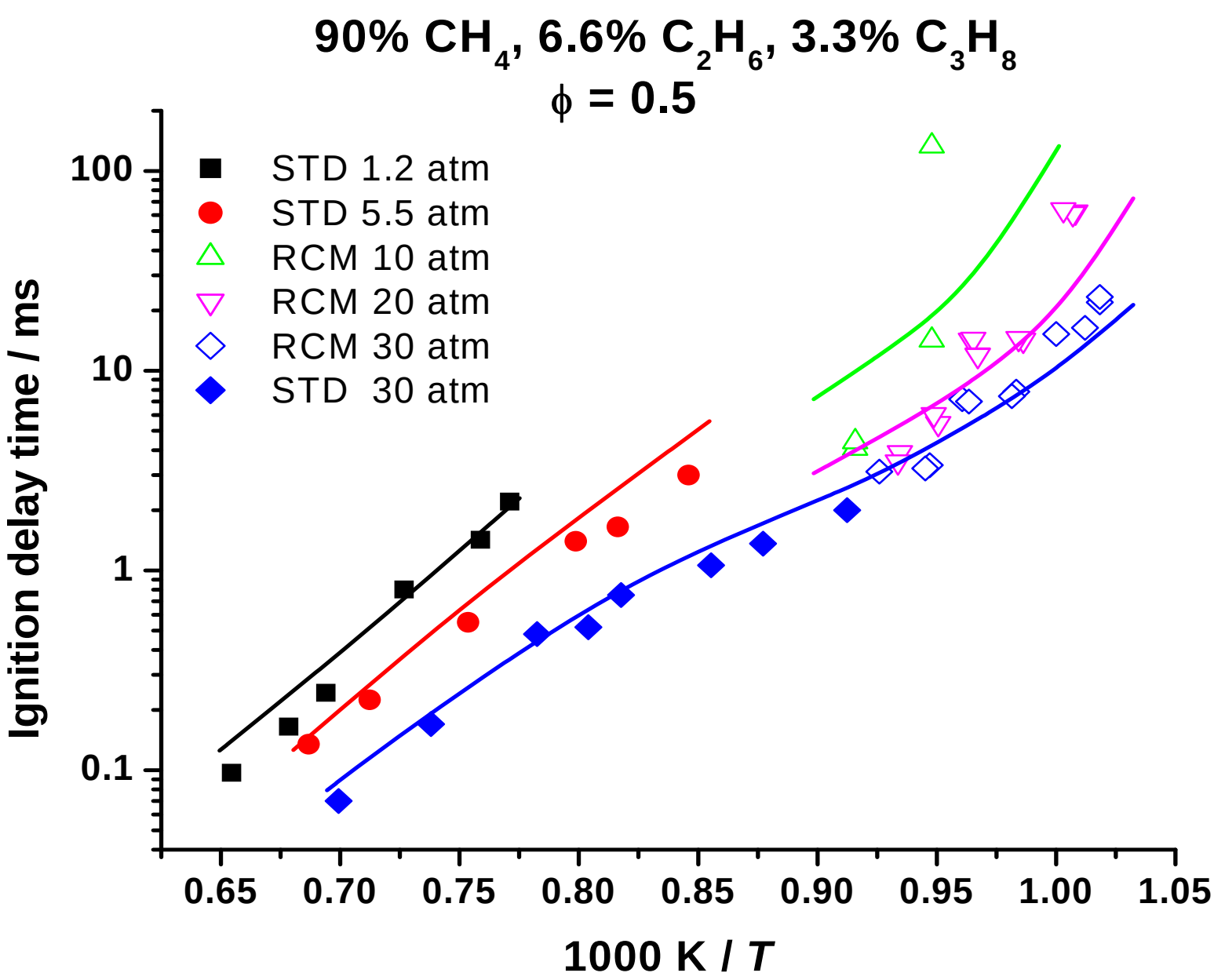
90% CH4, 6.6% C2H6, 3.3% C3H8
ϕ = 0.5
STD 1.2 atm
STD 5.5 atm
RCM 10 atm
RCM 20 atm
RCM 30 atm
STD 30 atm
Ignition delay time / ms
100
10
1
0.1
0.65
0.70
0.75
0.80
0.85
0.90
0.95
1.00
1.05
1000 K / T

Ignition delay times

- Important indicator of fuel reactivity
  - *T*, *p*, ϕ, dilution
    - » RCM: 600—1100 K, ST: 1100—2000 K
    - » based on time available
  - Problems at intermediate *T*, High *p*

Propane Results Show Discrepancy between RCM and Shock Tube

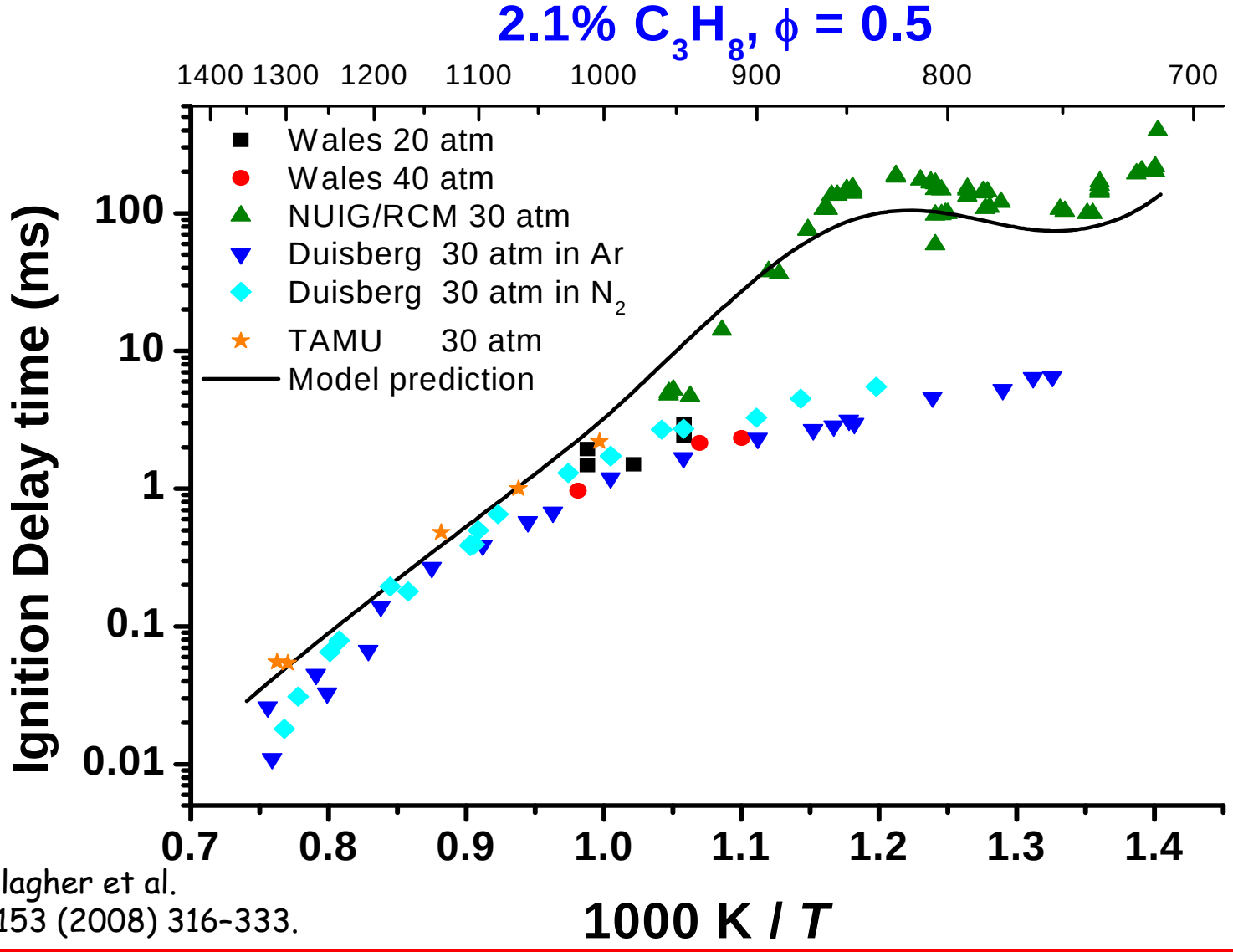

S. M. Gallagher et al.
Combust. Flame, 153 (2008) 316–333.

Typical data

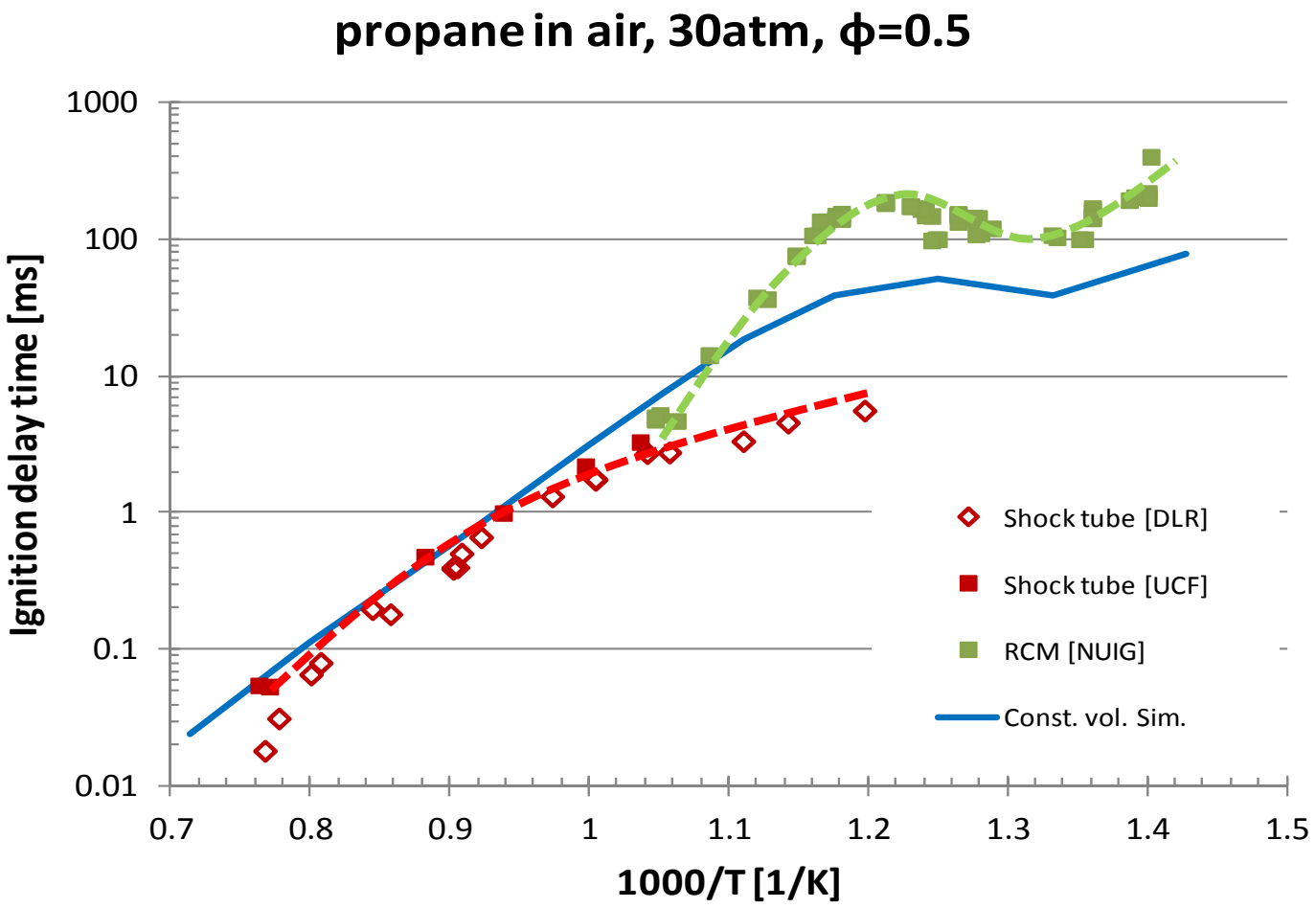

Lower-Temp Runs Exhibit Early Pressure Rise

Standard Ignition

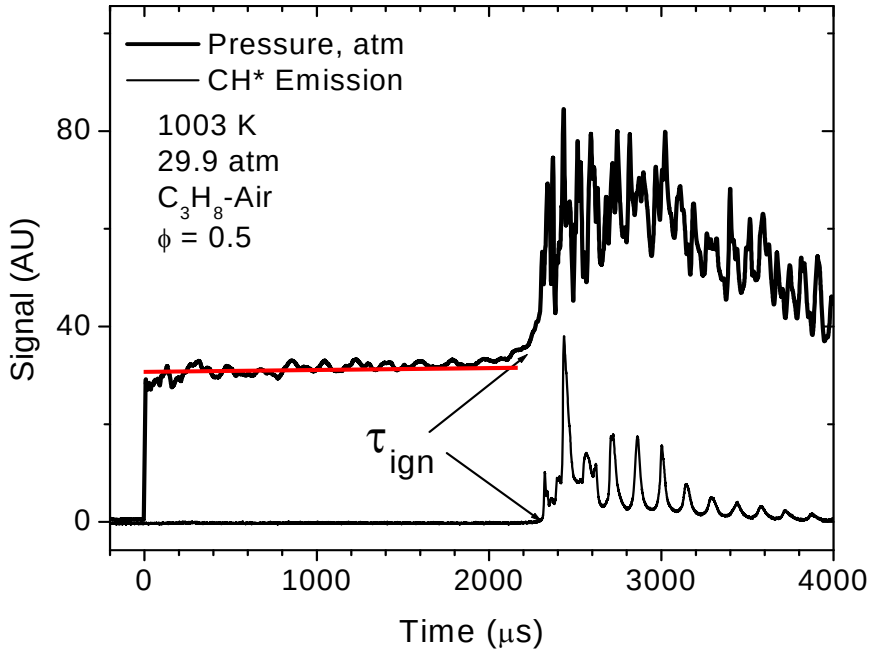

Early Pressure Rise

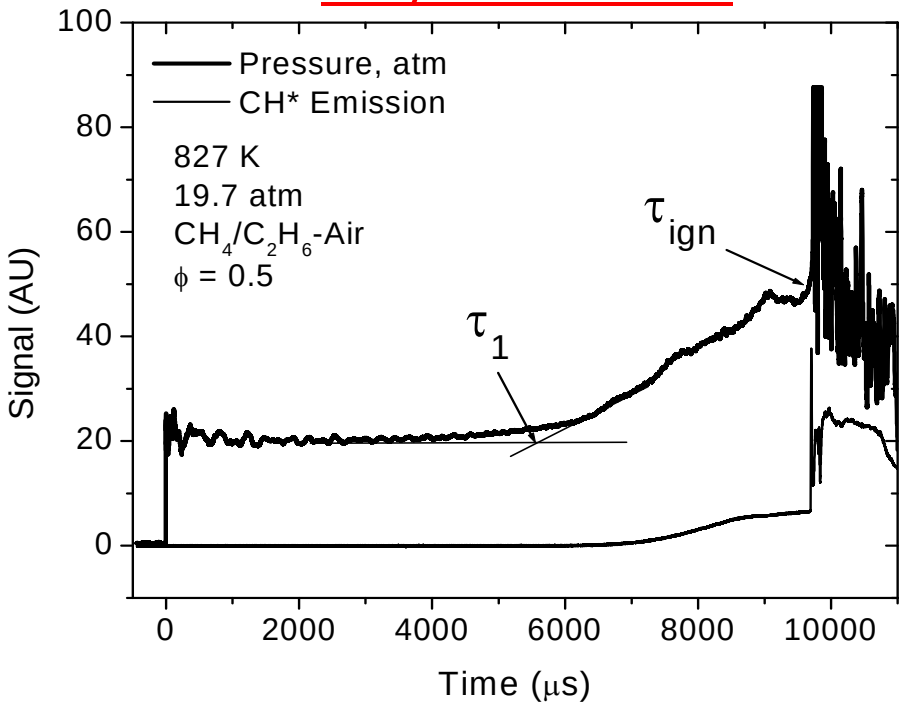

Slide courtesy of Prof. E. Petersen

Lower-Temp Runs Exhibit Early Pressure Rise

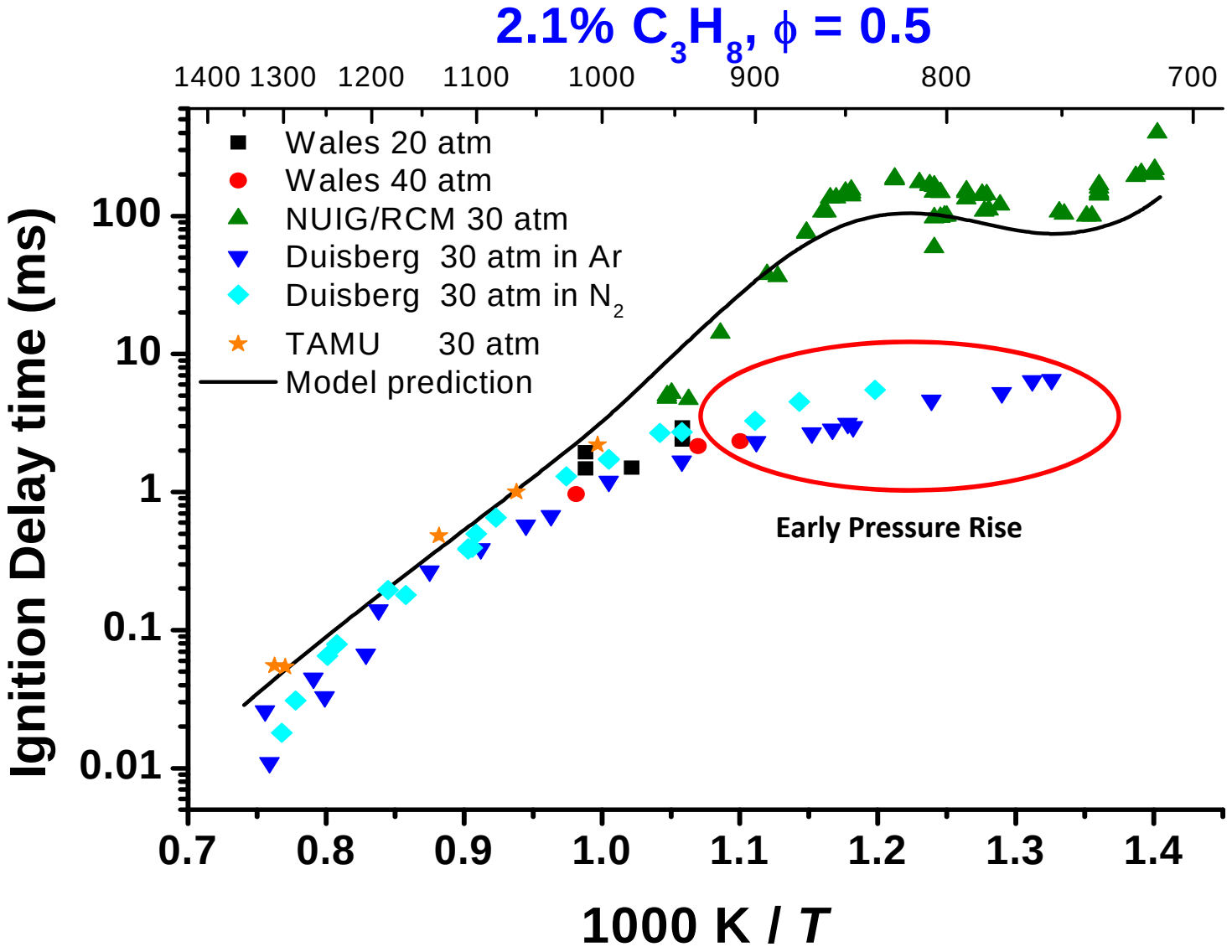

H_2 / O_2 in Ar

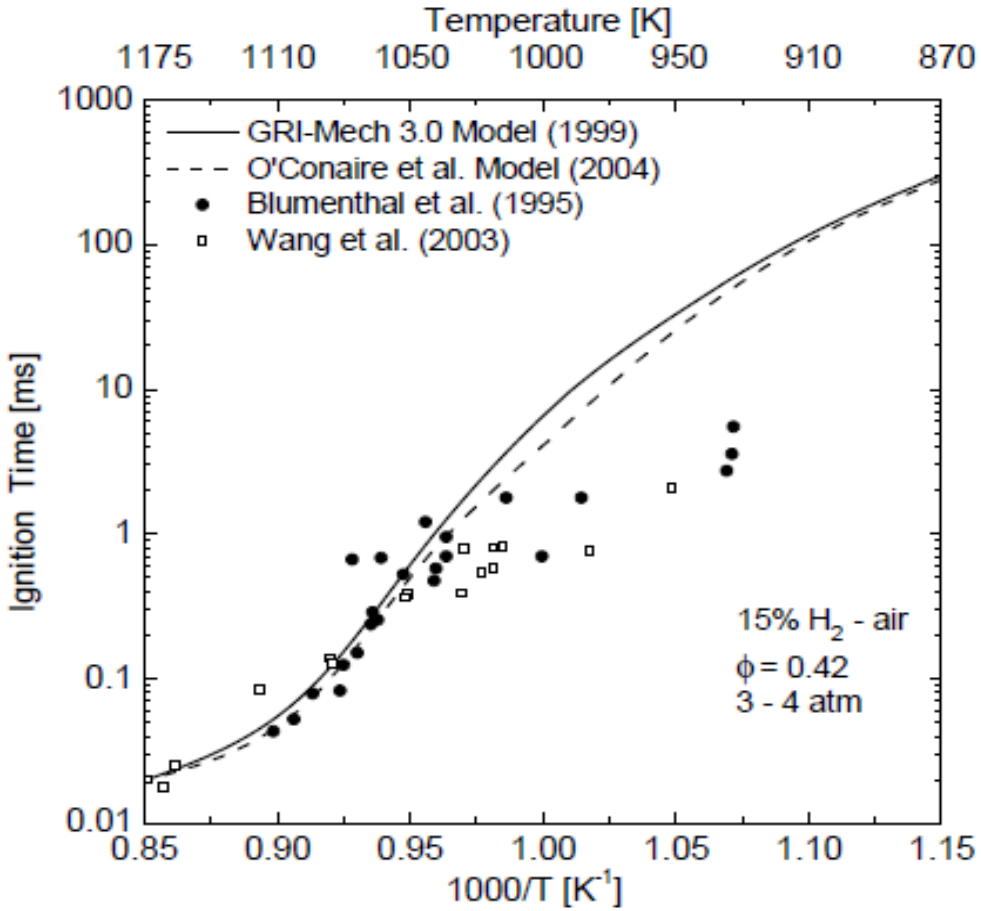

Fig. 1. Reflected-shock ignition delay time data compared to current kinetic models.

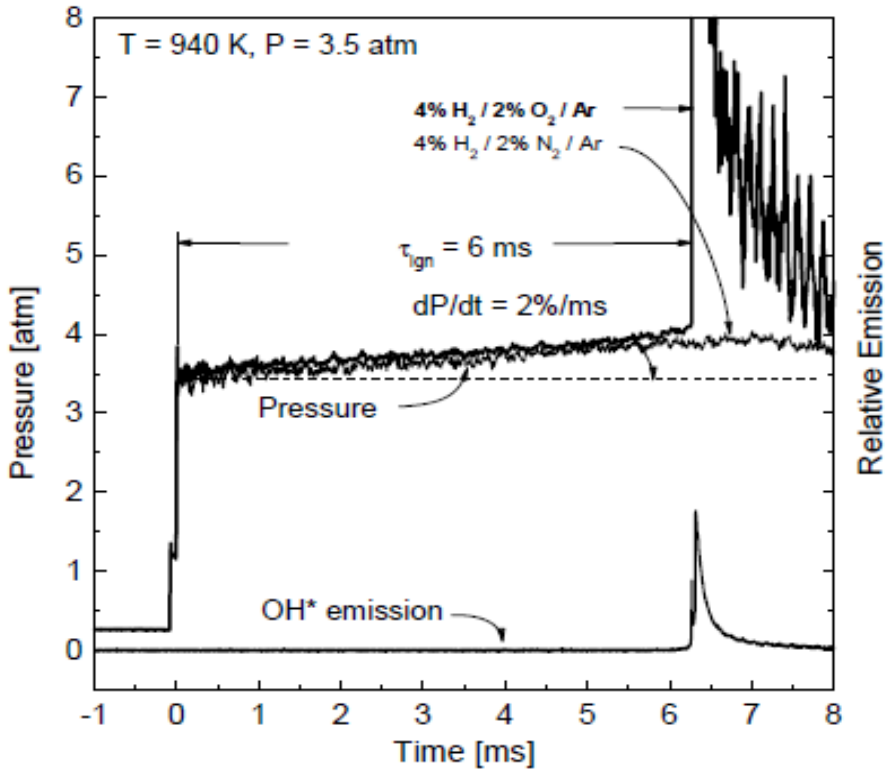

Fig. 2. Experimental data for a 4% H_2/2% O_2/Ar test gas mixture at initial post-shock conditions of 940 K and 3.5 atm for reactive and inert mixtures.

G.A. Pang, D.F. Davidson and R.K. Hanson *Proc. Combust. Inst.*, 32 (2009) 181–188.

Early pressure rise used to estimate Temp rise

Assume Temperature and Pressure are Related by:

$$\frac{T}{T_i} = \left(\frac{P}{P_i}\right)^{\frac{\gamma-1}{\gamma}}$$

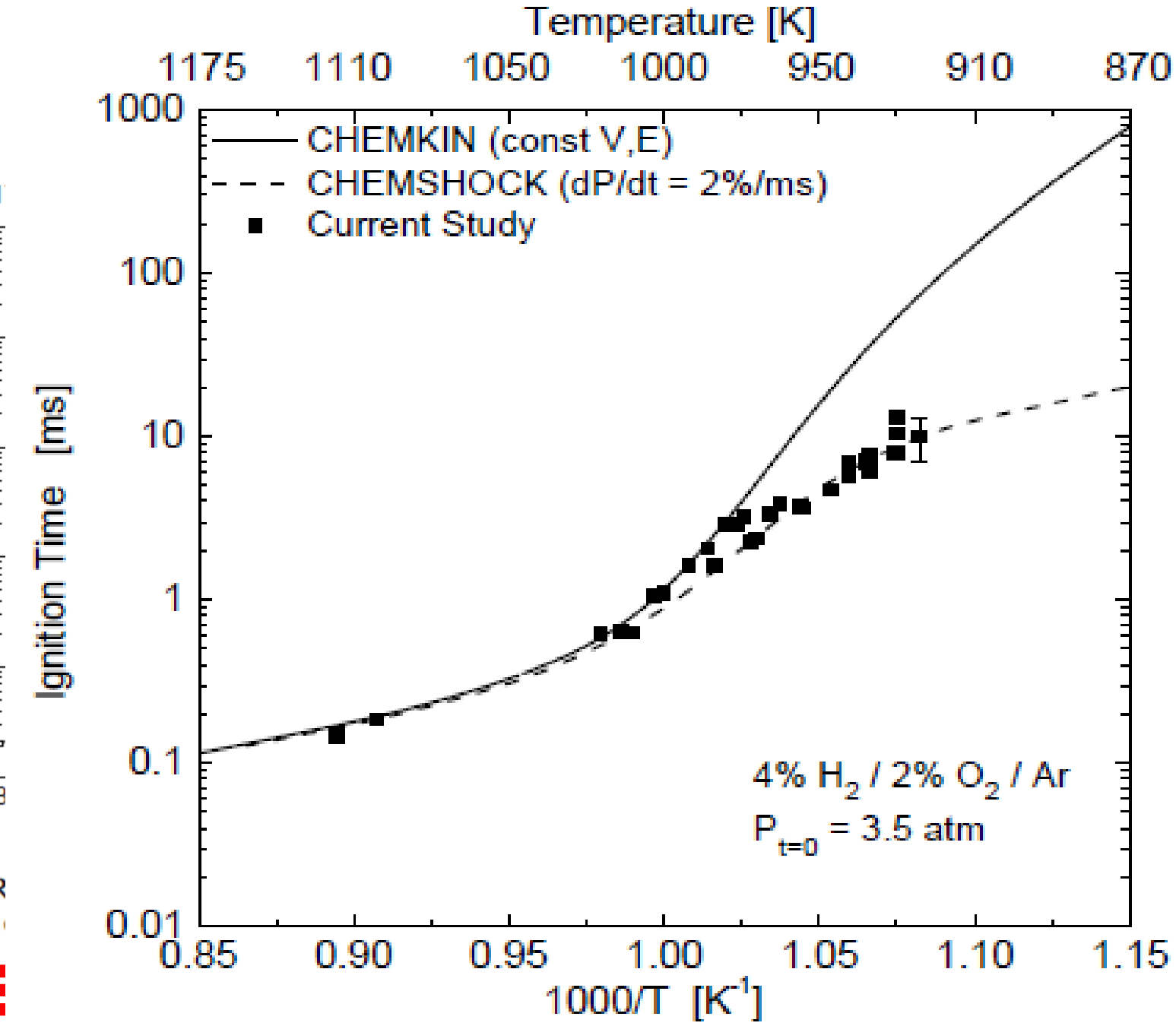

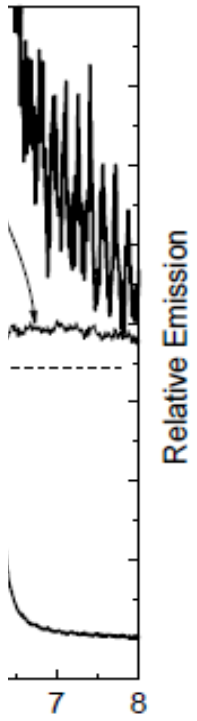

Fig. 1. R
pared to

% O_2/Ar test
of 940 K and

Important characteristics for shock tubes

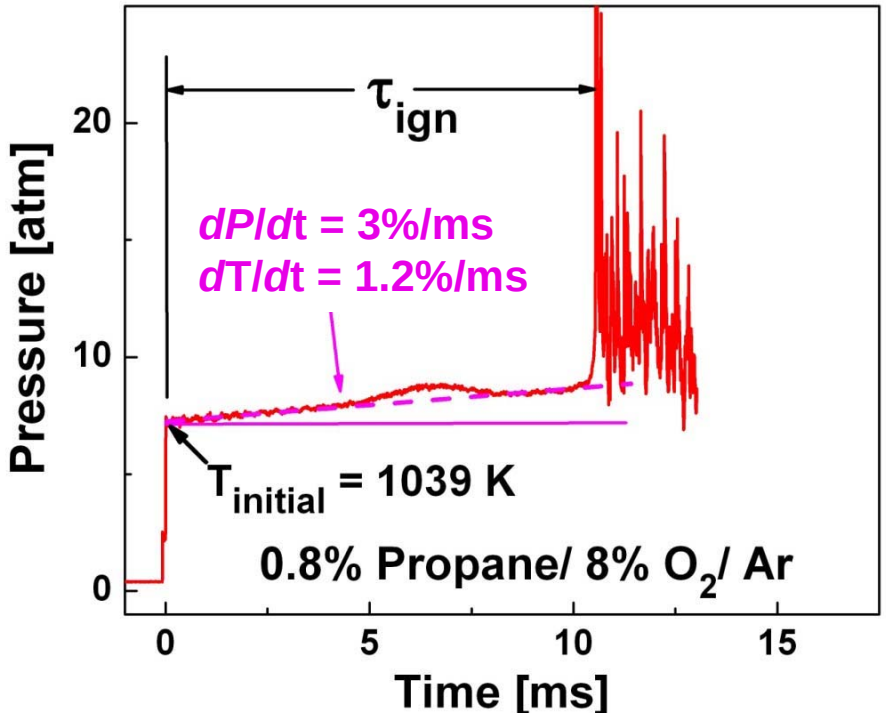

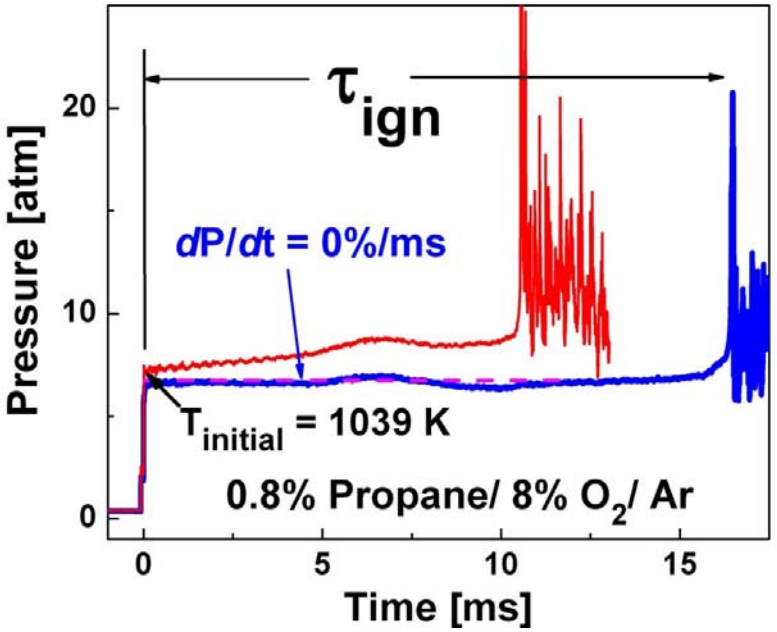

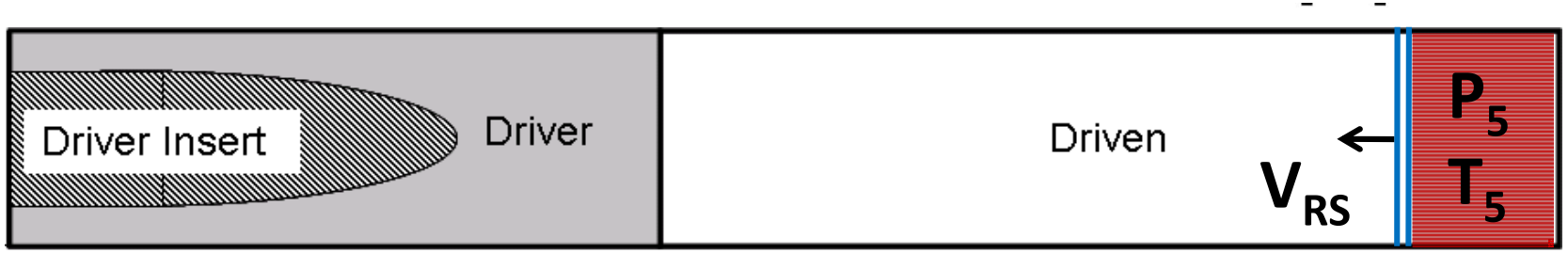

- **Driver inserts modify flow to achieve uniform T and P at long test times**

Laser absorption measurements

- OH measurement at 306.7 nm
  - Peak of $R_1(5)$ absorption line in the OH A-X(0,0) band
  - CW laser light at 613.4 nm generated using dye laser
  - Light at 306.7 nm generated by intracavity frequency-doubling, using a temperature-tuned AD*A crystal.
  - OH concentration calculated using Beer's law:

$$I/I_o = \exp(-k_v p_{total} X_{OH} L)$$

- I and I_o are the transmitted and incident beam intensities
- k_v is the line-center absorption coefficient at 306.7 nm for OH
- p_{total} total test gas mixture
- X_{OH} is the OH mole fraction
- L is the path length

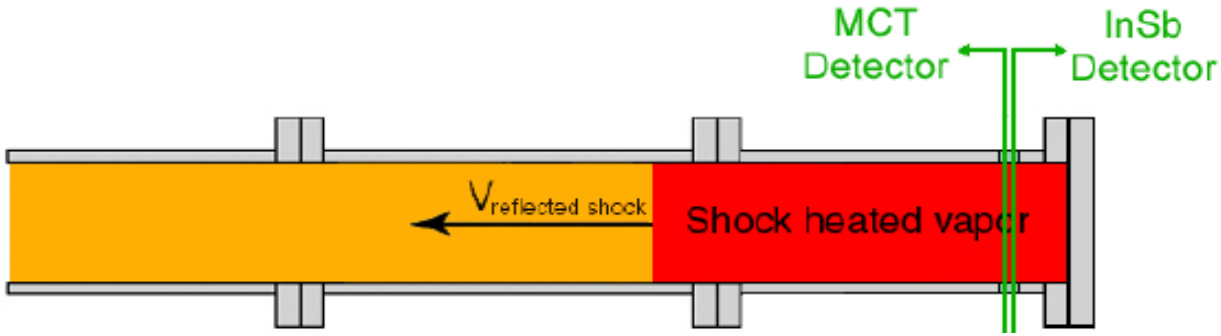

613.4 nm using Spectra Physics 380 ring Dye laser

Laser absorption measurements

- CO_2 measured at 2752.5 nm
- H_2O measured at 2550.96 nm
- Concentration calculated using Beer's law:

$$I/I_o = \exp(-k_v p_{total} X_{species} L)$$

- I and I_o are the transmitted and incident beam intensities
- k_v is the line-center absorption coefficient at 2752.5 nm for CO_2
- p_{total} total test gas mixture
- X_{CO2} is the CO_2 mole fraction
- L is the path length

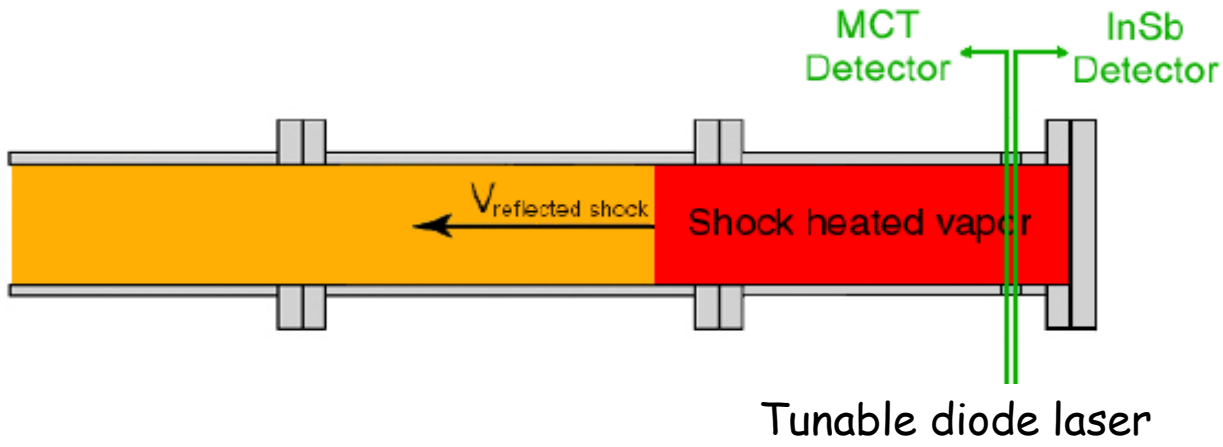

Laser absorption measurements

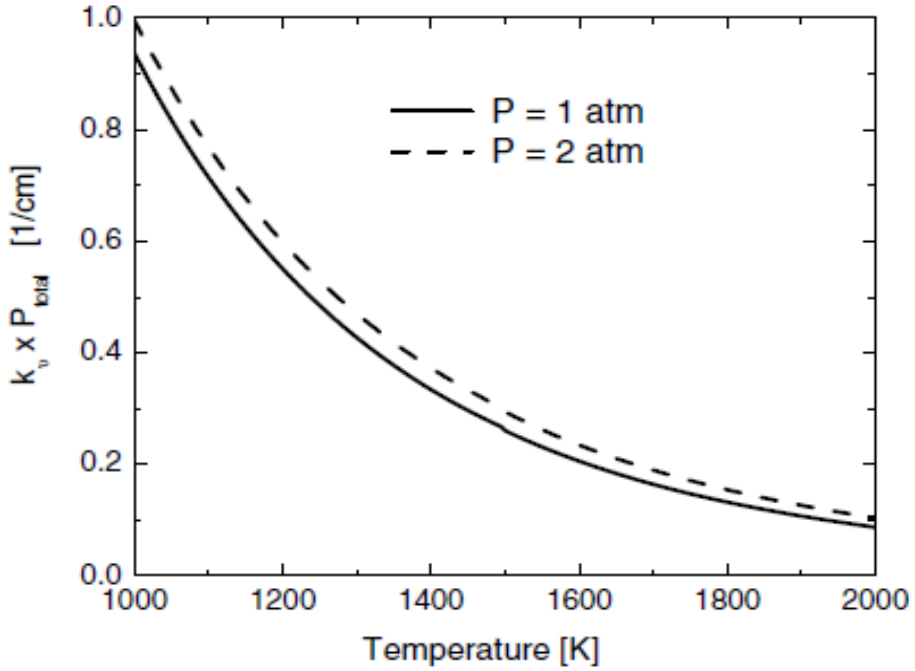

Fig. 1. Absorption coefficient × pressure product, $k_\nu \times P_{\text{total}}$ [cm^{-1}] for the R(28) CO_2 transition near 3633.08 cm^{-1} (2752.5 nm) at $P = 1$ and 2 atm.

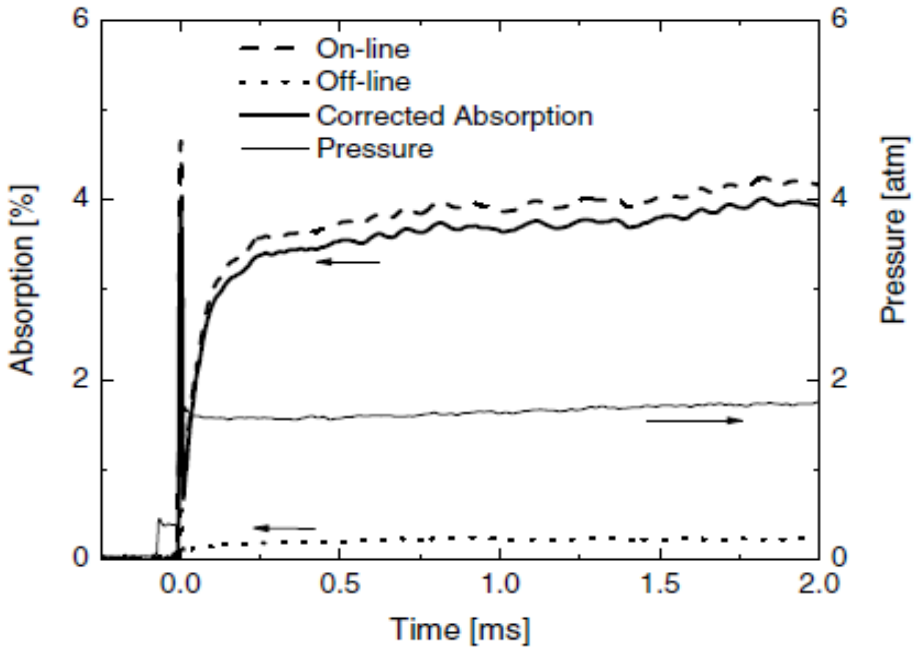

Fig. 2. Example on-line and off-line absorption measurement in 2% MB/Argon. Reflected shock conditions: $T_5 = 1426$ K, $P_5 = 1.58$ atm. On-line wavenumber = 3633.08 cm^{-1}; Off-line wavenumber = 3633.25 cm^{-1}.

A. Farooq, D.F. Davidson, R.K. Hanson, L.K. Huynh, A. Violi
Proc. Combust. Inst. 32 (2009) 247—253.

Laser absorption measurements

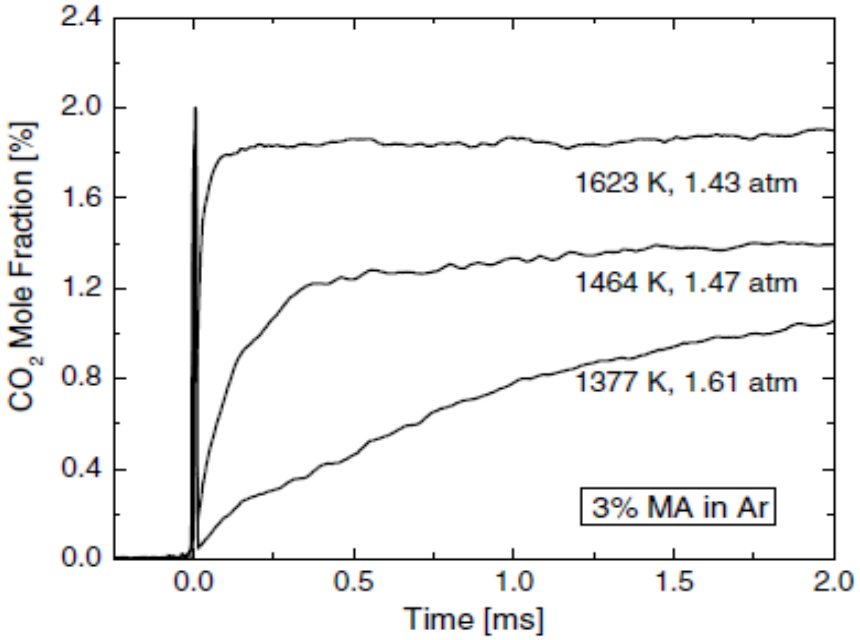

Fig. 3. Measured CO_2 time-histories behind reflected shock waves (T_5, P_5 shown) for methyl acetate pyrolysis (3% MA in Ar).

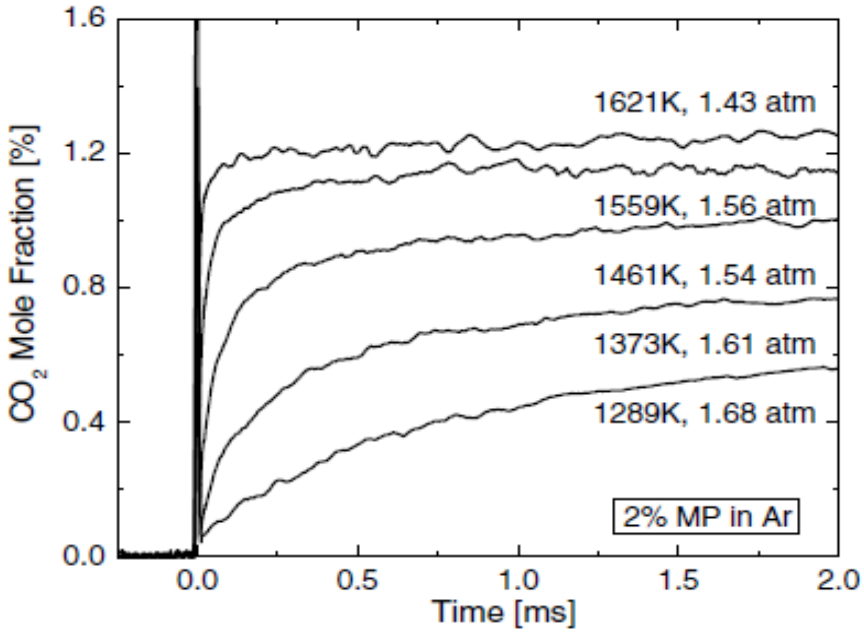

Fig. 4. Measured CO_2 time-histories behind reflected shock waves (T_5, P_5 shown) for methyl propionate pyrolysis (2% MP in Ar).

A. Farooq, D.F. Davidson, R.K. Hanson, L.K. Huynh, A. Violi
Proc. Combust. Inst. 32 (2009) 247—253.

Laser absorption measurements

- Fuel measurement at 3.39 μm
- C_2H_4 measurement at 10.5 μm

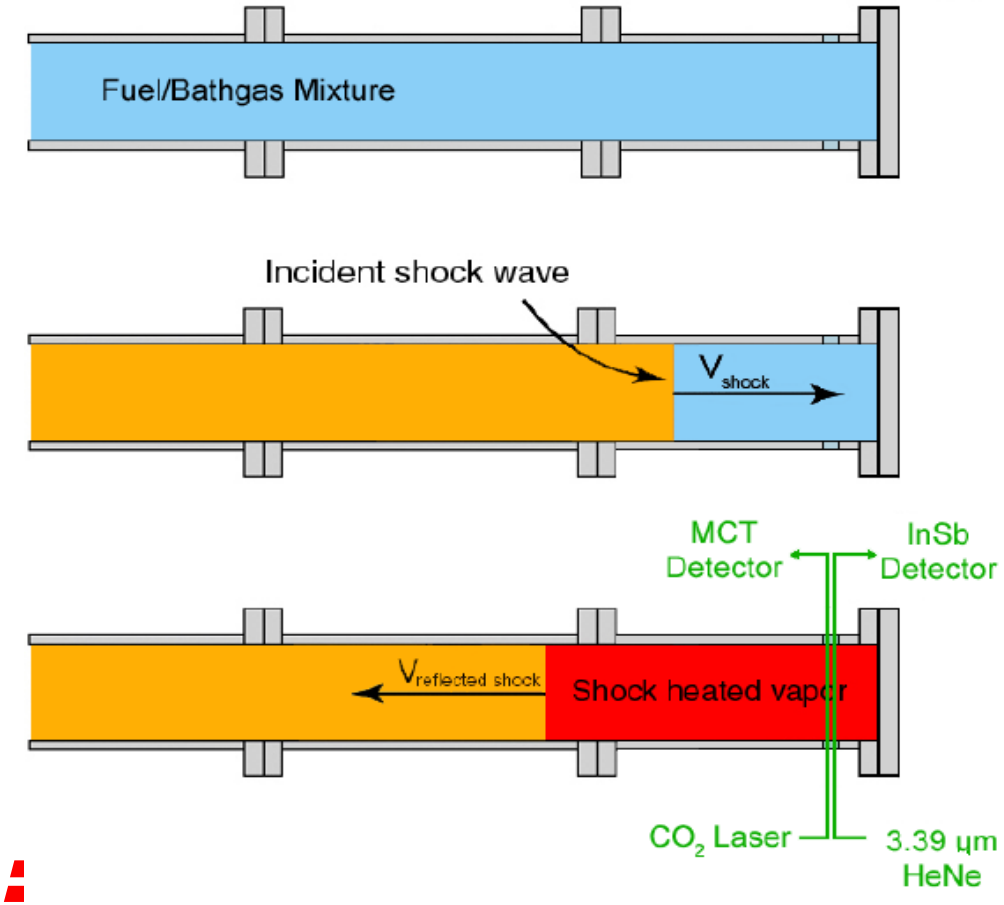

Beer's Law

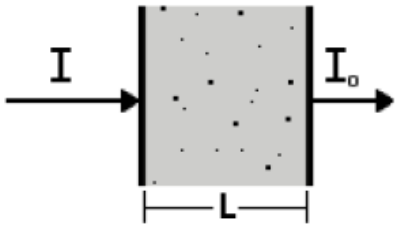

$$\frac{I}{I_o} = \exp(-\sigma NL)$$

Absorption cross section

IR Fuel Diagnostic (3.39 μm)

- 3.39 μm strongly absorbed by all HC fuels
- Beer's Law + Absorption cross sections →Fuel mole fraction
- **Need fuel cross section at 3.39 μm**

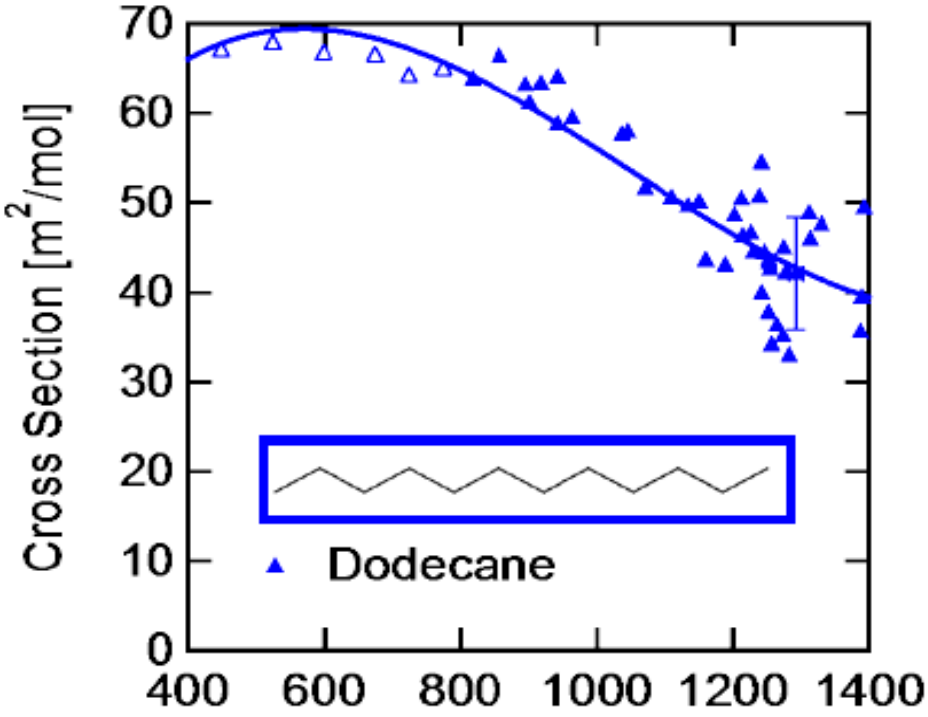

MacDonald et al., J. Prop. Power, 2011

IR Ethylene Diagnostic (10.5 μm)

- CO_2 gas laser P14 line is strongly absorbed by C_2H_4
  - but also other alkenes
- Need to measure two wavelengths
  - 10.532 μm P14 line (on-line)
  - 10.675 μm P28 line (off-line)

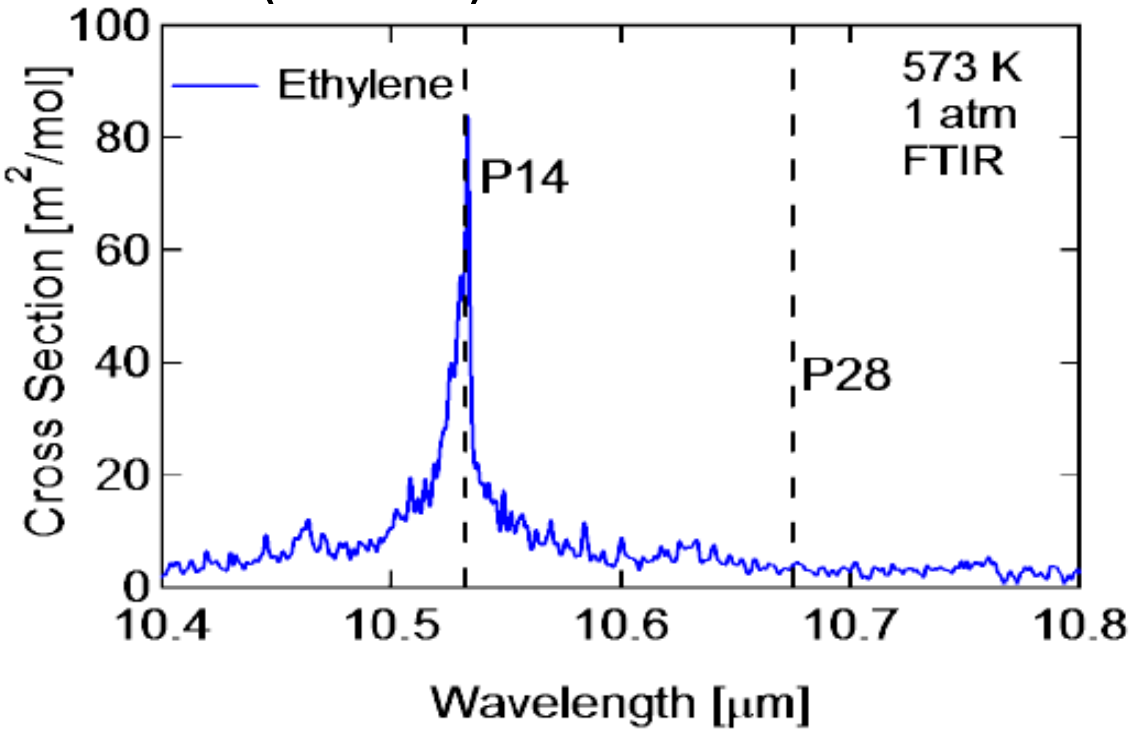

IR Ethylene Diagnostic (10.5 μm)

- **Need ethylene cross sections at both lines**
- Other alkenes absorb at 10.5 μm
- Interfering species have a constant cross section
- Differential absorption at 2 wavelengths permits isolation of C_2H_4 absorption

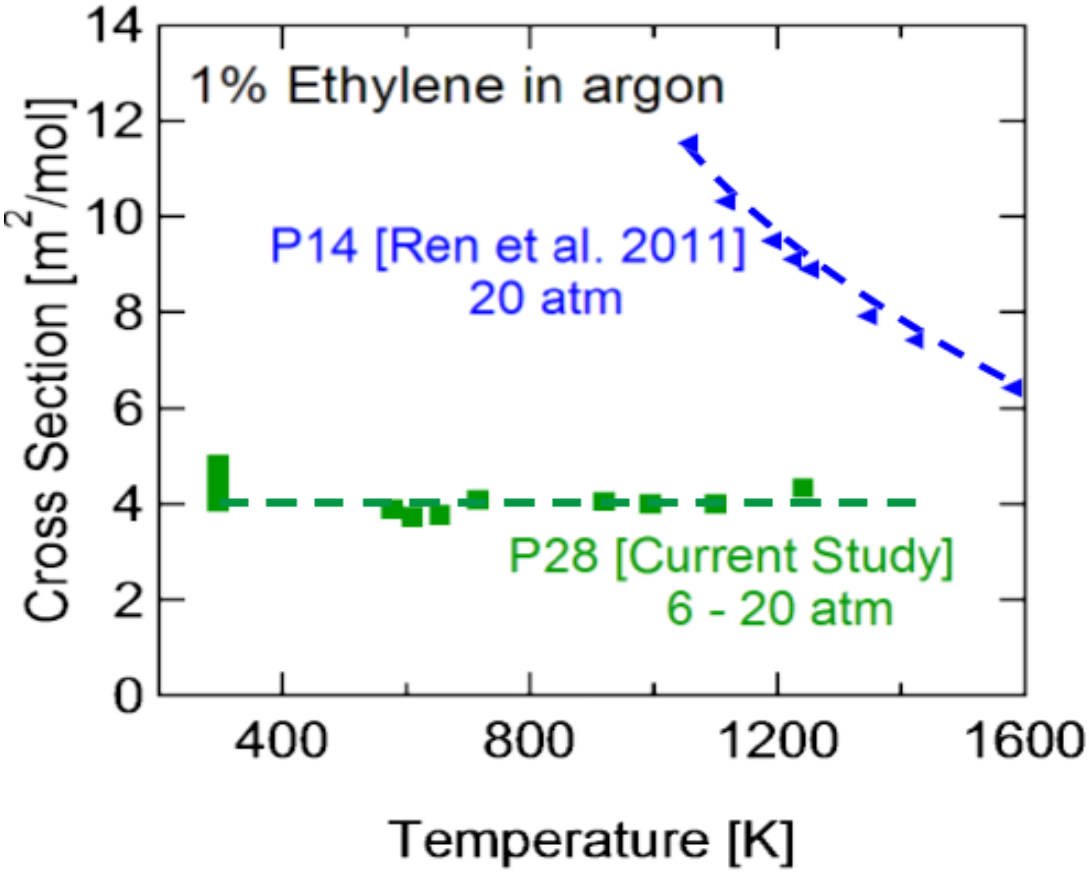

Need to check cross sections of interfering species to ensure they are constant at 10.5 μm

Cross sections of interfering species

- Small absorption by propene and 1-butene

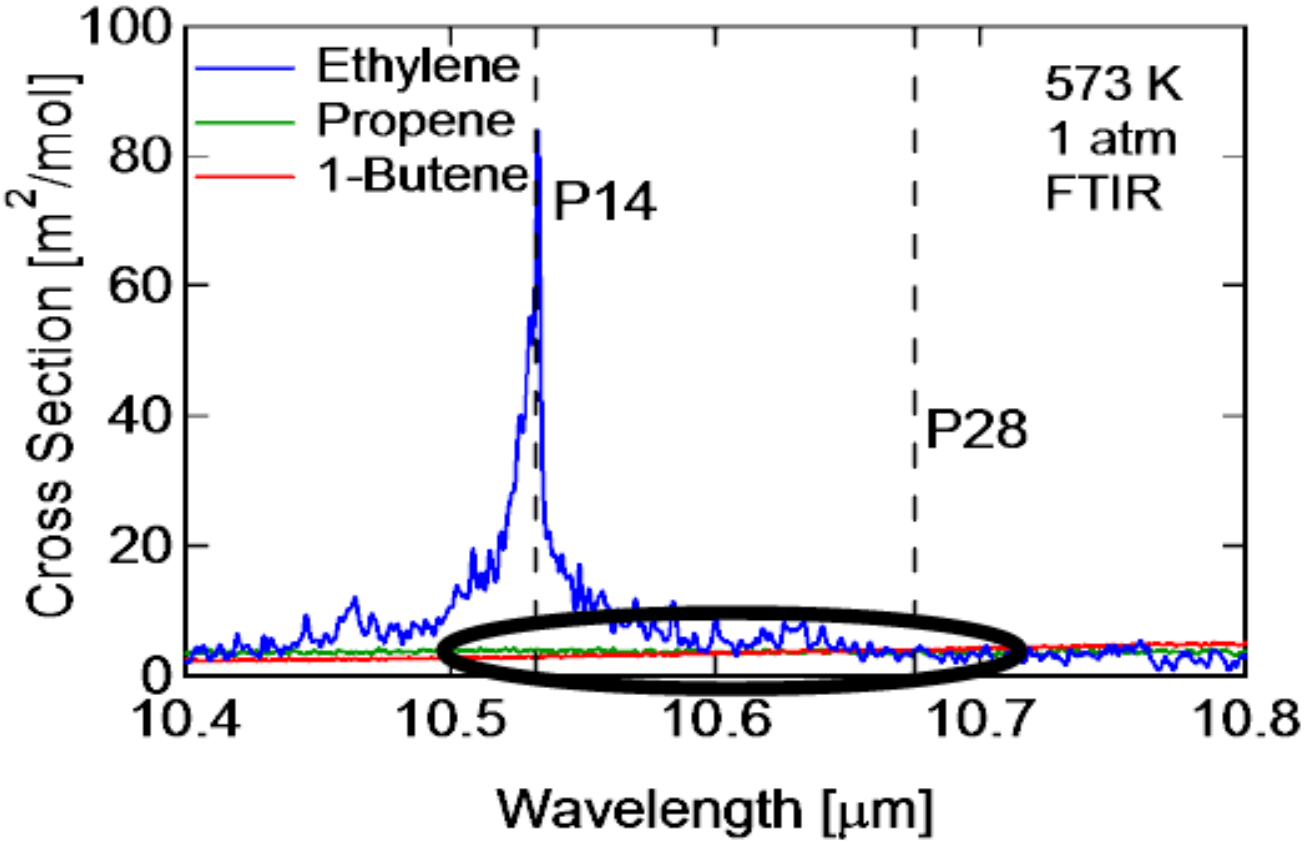

Cross sections of interfering species

- Small absorption by propene and 1-butene with nearly constant cross-sections at P14 and P28

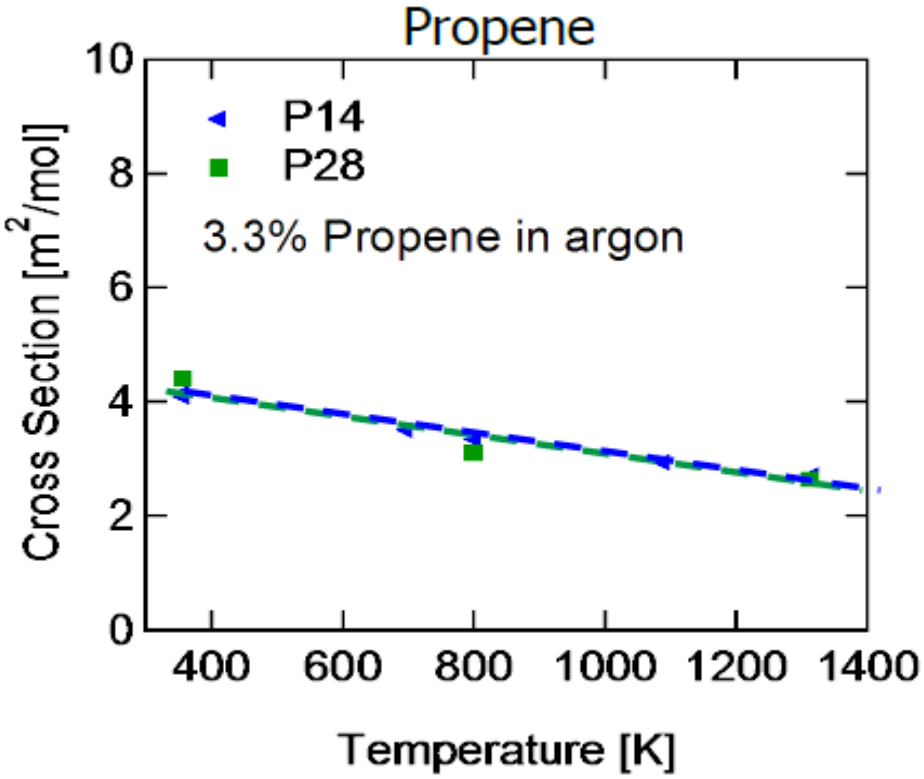

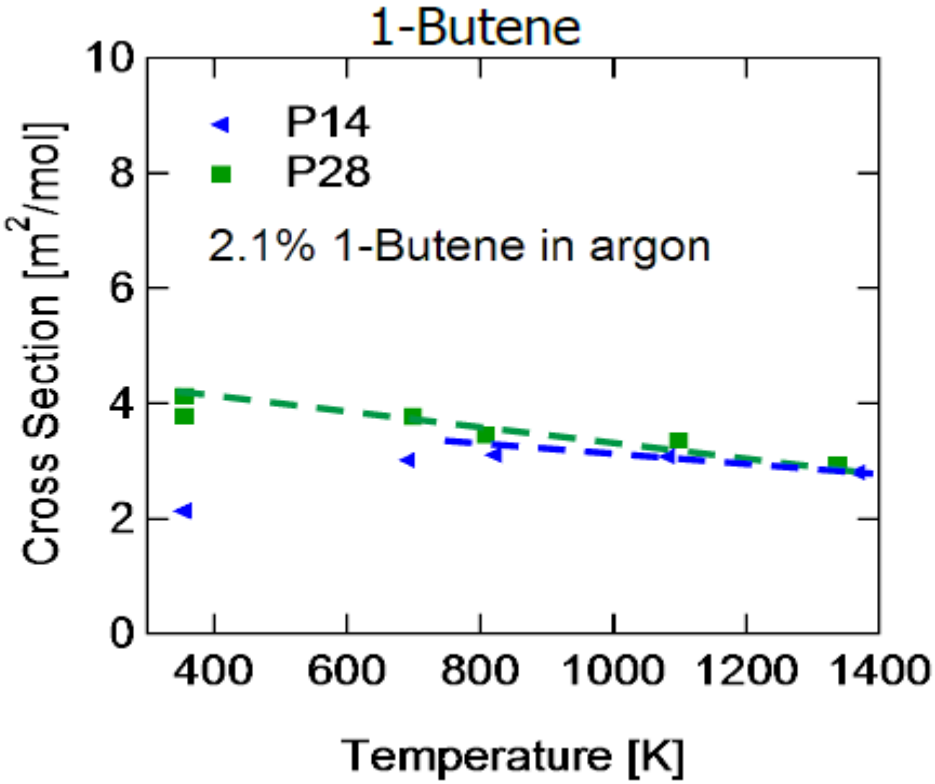

Species time-history measurements

457 ppm *n*-Dodecane/O_2/Argon
ϕ = 1.0, 1410 K, 2.3 atm

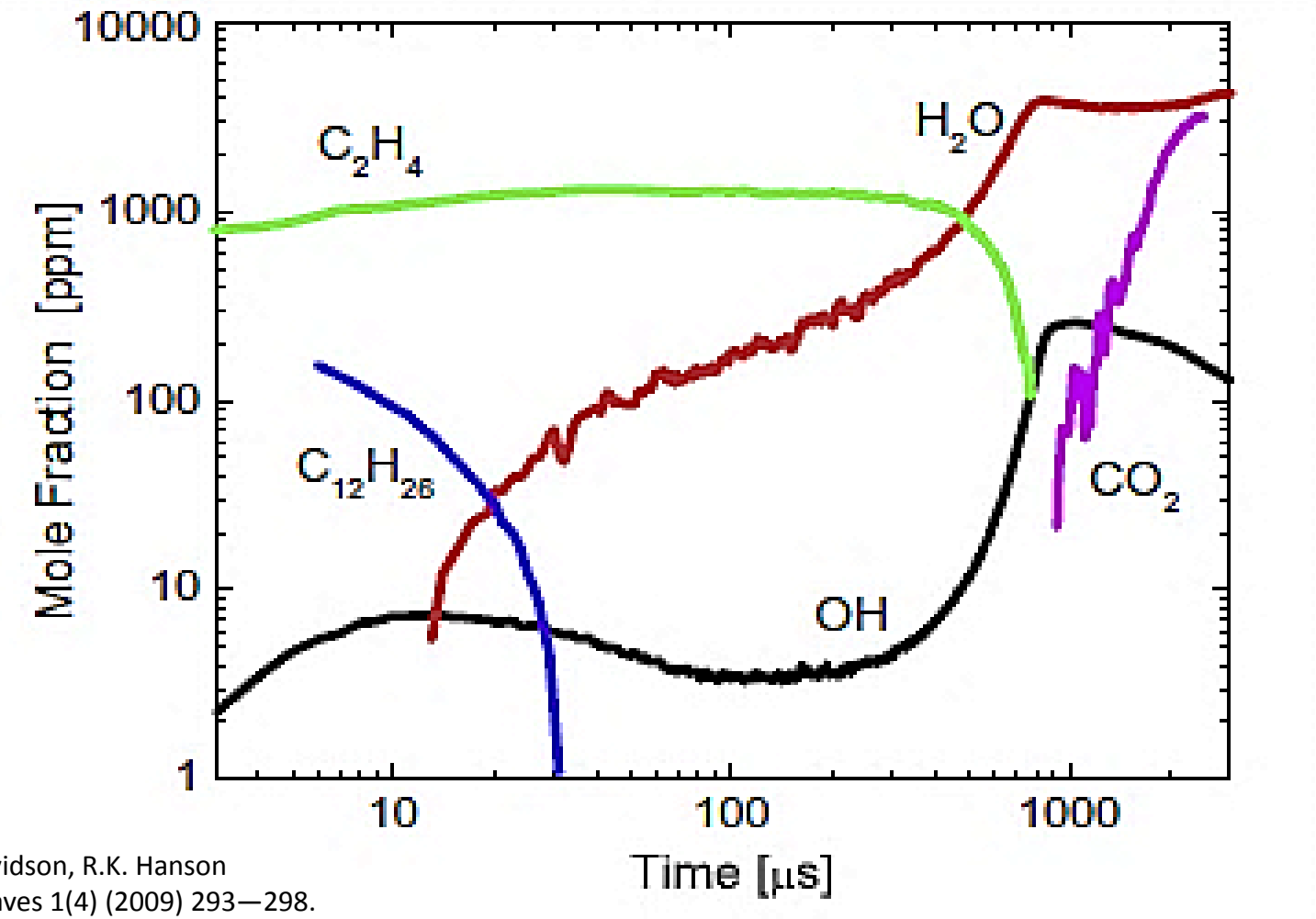

S.S. Vasu, D.F. Davidson, R.K. Hanson
26th Intl. Symp. Shock Waves 1(4) (2009) 293—298.

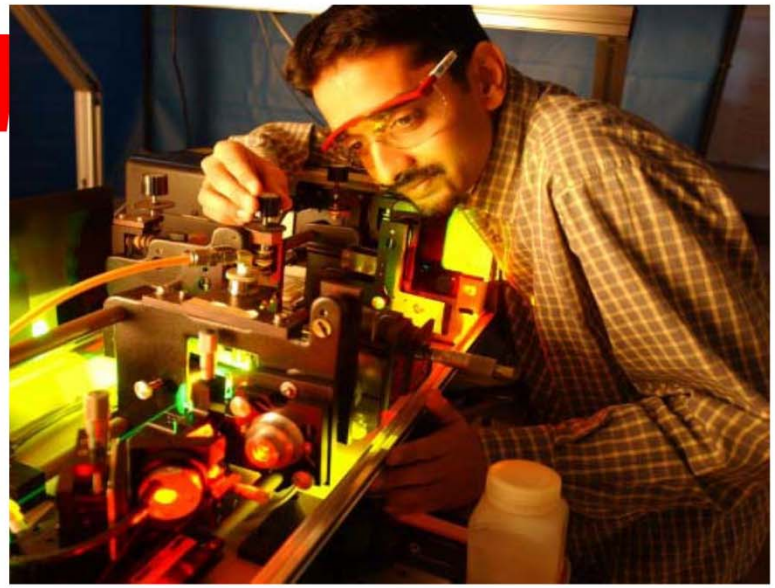

First use of tunable dye lasers in shock tubes (1982)

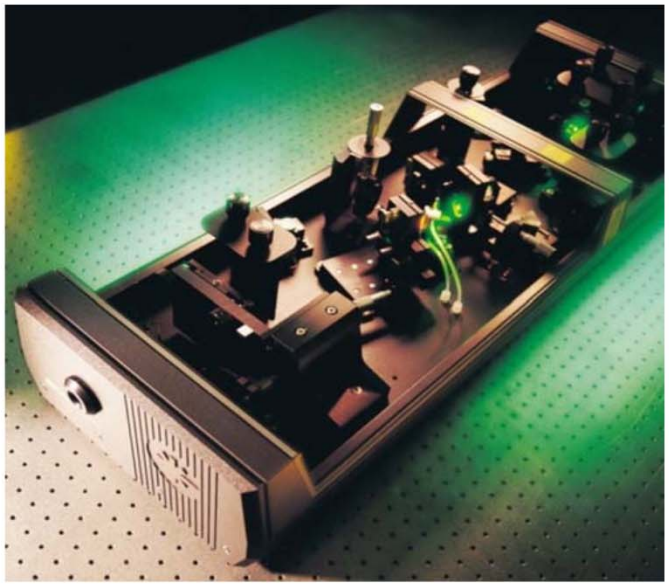

Ultra-fast lasers used to extend UV tuning range (2009)

Stanford Laser Diagnostics

New lasers allow simple access to mid-IR (2007-10)

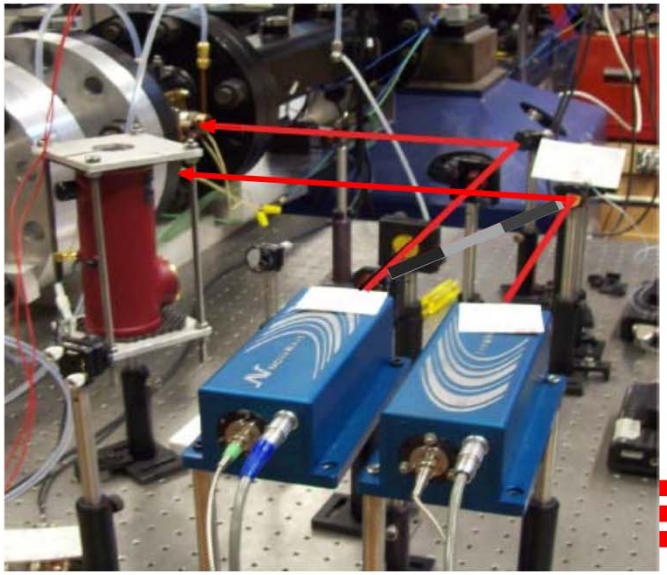

Ultraviolet

CH_3	216 nm
NO	225 nm
O_2	227 nm
HO_2	230 nm
OH	306 nm
NH	336 nm

Visible

CN	388 nm
CH	431 nm
NCO	440 nm
NO_2	472 nm
NH_2	597 nm
HCO	614 nm

Infrared

H_2O	2.5 μm
CO_2	2.7 μm
CH_4	3.4 μm
CH_2O	3.4 μm
CO	4.6 μm
NO	5.2 μm
C_2H_4	10.5 μm

Species time histories in shock tubes

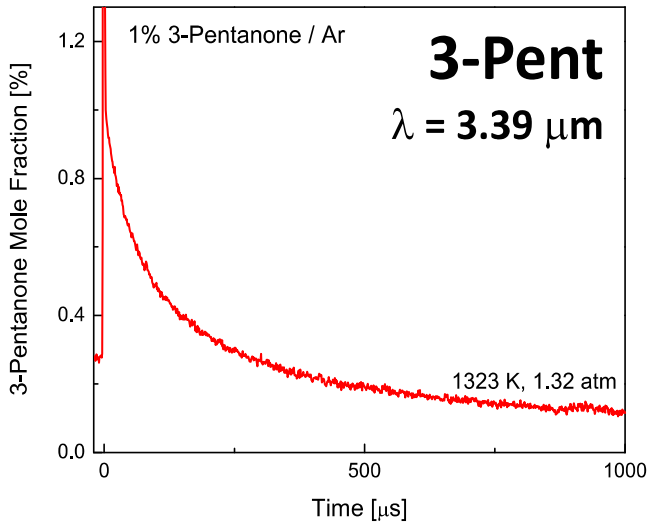

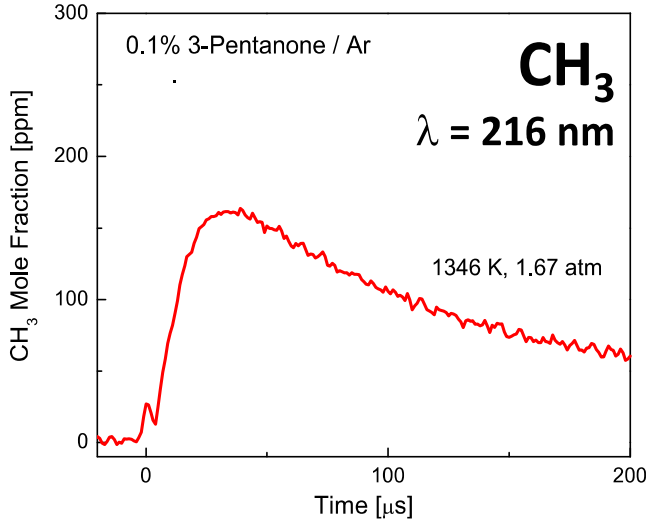

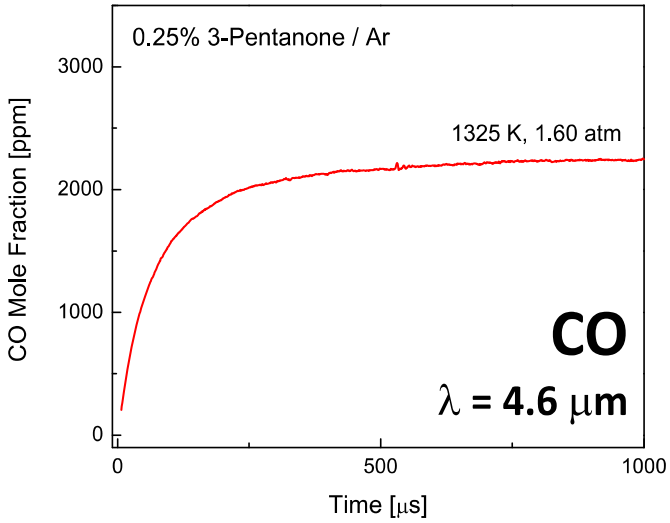

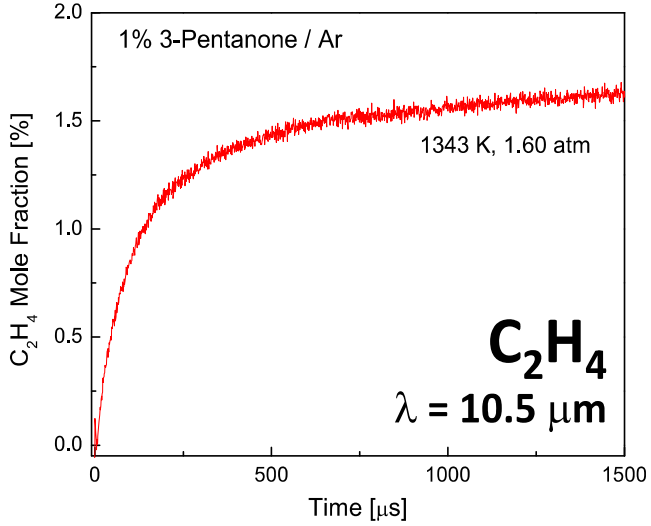

KAUST Laser Sensors Laboratory

Other diagnostics available in our laboratory:

Species	Laser	Wavelength
OH	Ring-Dye w/ external doubling	306 nm
CH_2O	Difference-frequency-generation laser	3.6 μm
CO_2	Quantum-cascade laser (QCL)	4.3 μm
N_2O	Quantum-cascade laser (QCL)	4.5 μm
CO	Quantum-cascade laser (QCL)	4.6 μm
H_2O	Quantum-cascade laser (QCL)	7.6 μm
H_2O_2	Quantum-cascade laser (QCL)	7.7 μm
CH_4	Quantum-cascade laser (QCL)	7.7 μm
C_2H_2	Quantum-cascade laser (QCL)	7.8 μm
NH_3	Quantum-cascade laser (QCL)	9.0 μm
C_2H_4	Quantum-cascade laser (QCL)	10.5 μm
C_2H_2	Quantum-cascade laser (QCL)	13.3 μm

Laser absorption measurements

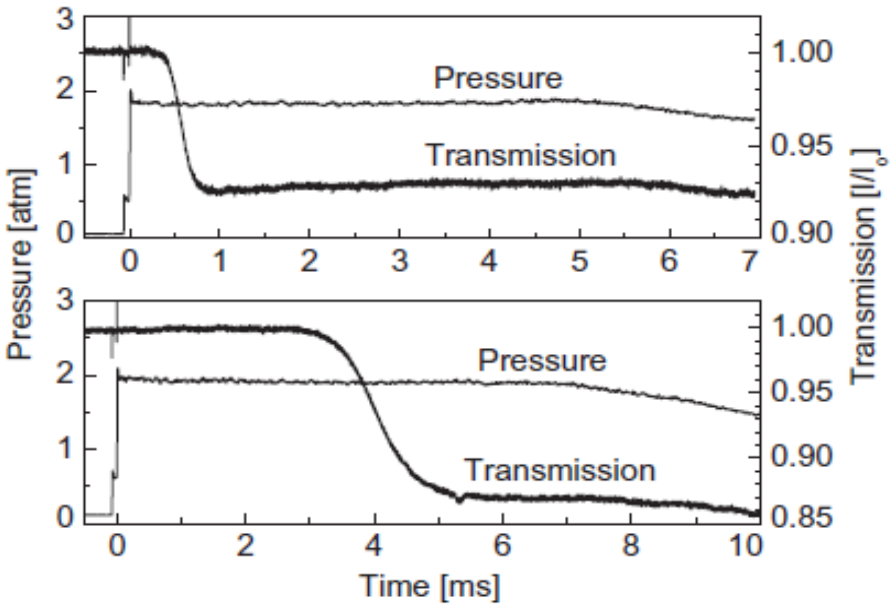

Fig. 1. Typical pressure and laser transmission histories in reflected-shock experiments: (a. upper) 0.1% O_2, 0.9% H_2, 99% Ar, 1472 K, 1.83 atm; (b. lower) 0.1% O_2, 2.9% H_2, 97% Ar, 1100 K, 1.95 atm.

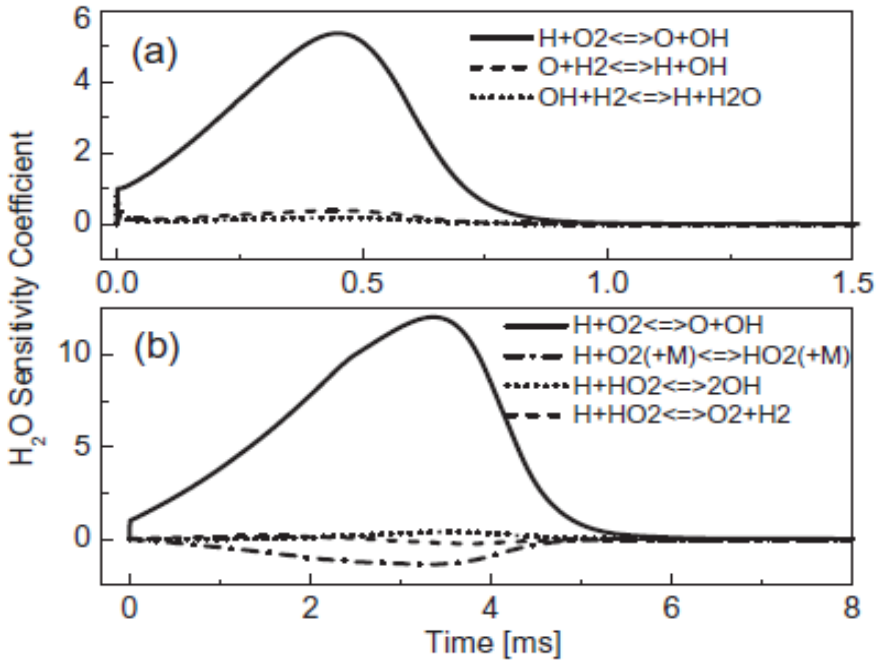

Fig. 2. H_2O sensitivity plot at conditions of the corresponding panels of Fig. 1.

Z. Hong, D.F. Davidson, E.A. Barbour, R.K. Hanson
Proc. Combust. Inst. 33 (2011) 309–316.

Laser absorption measurements

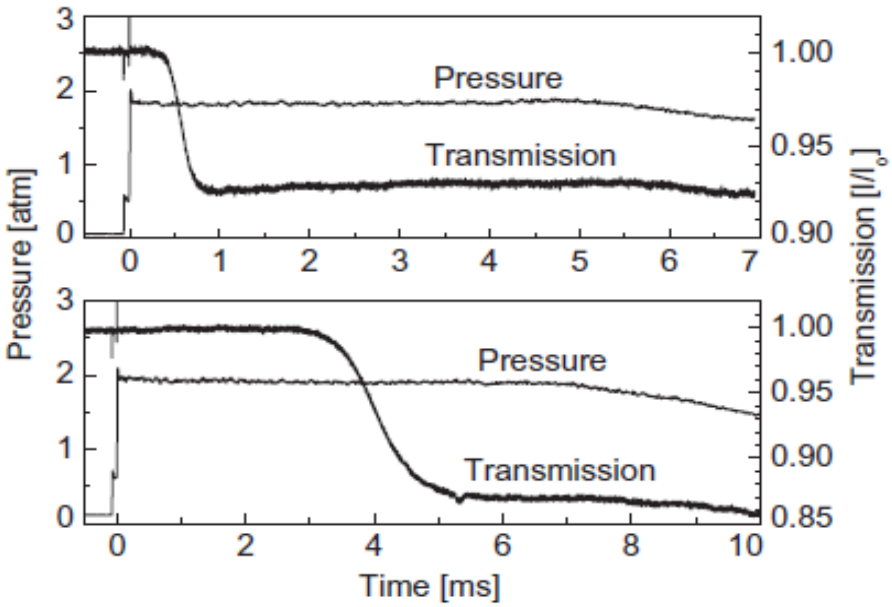

Fig. 1. Typical pressure and laser transmission histories in reflected-shock experiments: (a. upper) 0.1% O_2, 0.9% H_2, 99% Ar, 1472 K, 1.83 atm; (b. lower) 0.1% O_2, 2.9% H_2, 97% Ar, 1100 K, 1.95 atm.

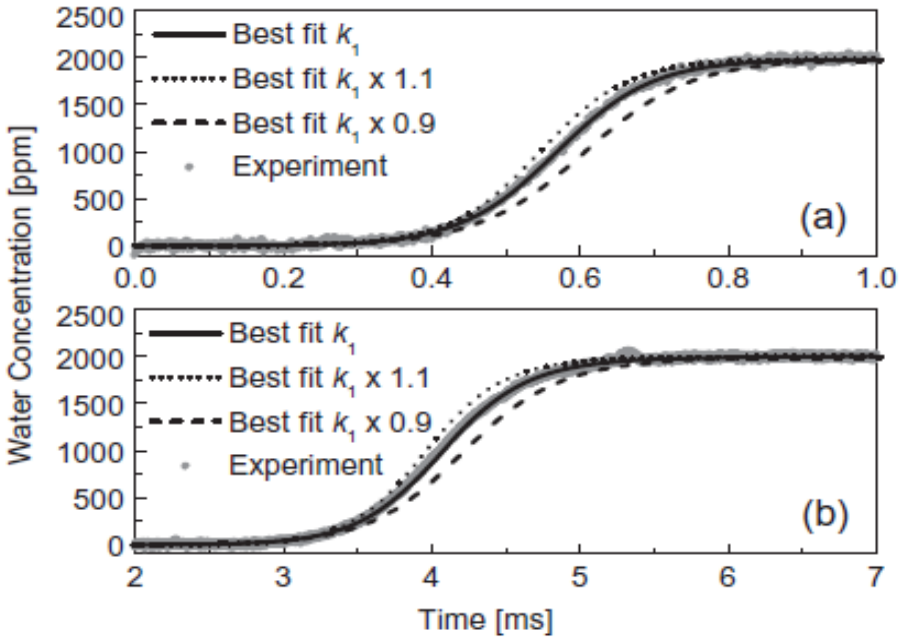

Fig. 3. Comparison of experimental and Senkin calculated H_2O profiles using best-fit k_1 with effect of ±10% variation on k_1 at conditions of the corresponding panels of Fig. 1.

Z. Hong, D.F. Davidson, E.A. Barbour, R.K. Hanson
Proc. Combust. Inst. 33 (2011) 309–316.

$\dot{H} + O_2 = \ddot{O} + \dot{O}H$

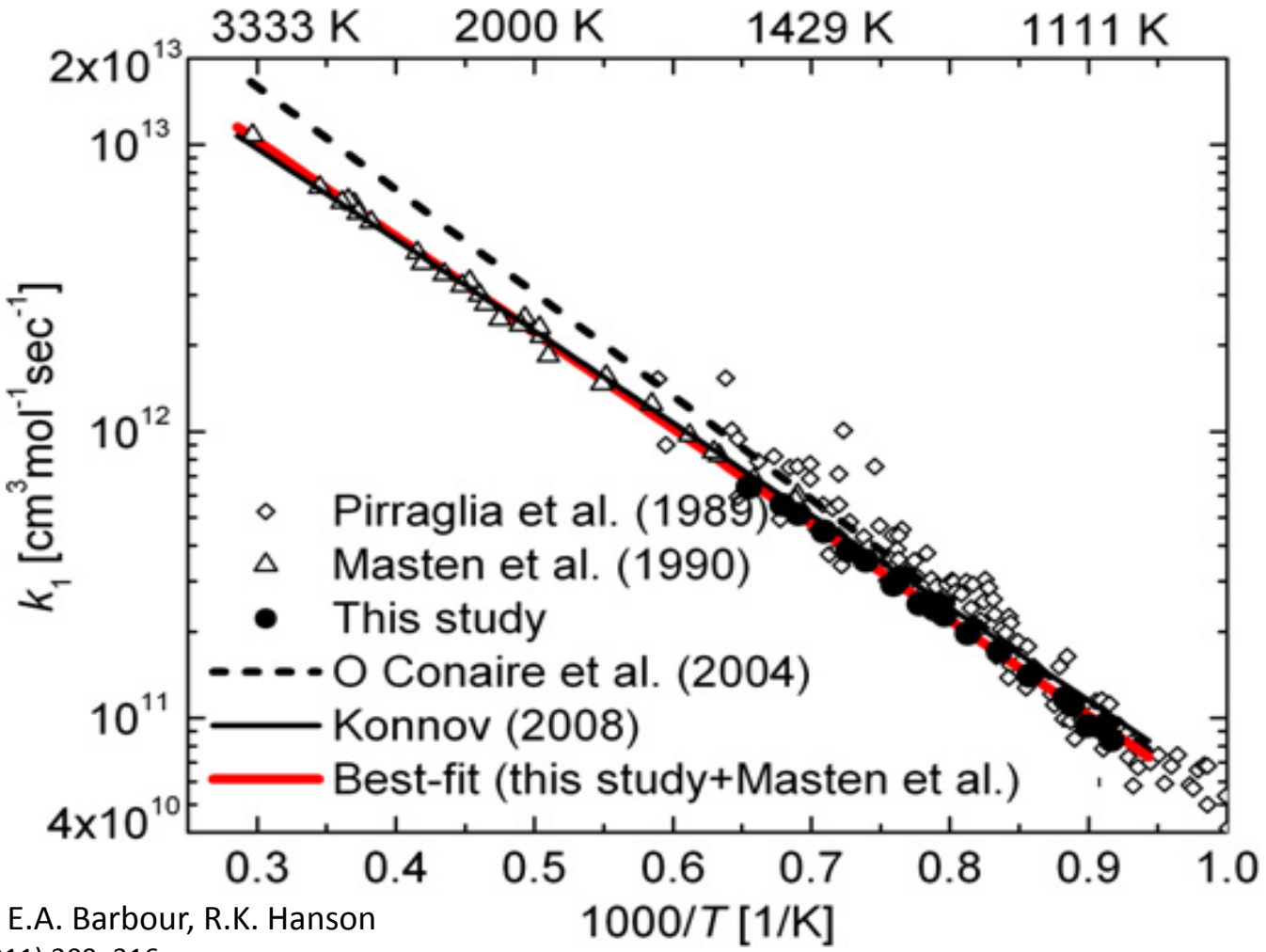

Z. Hong, D.F. Davidson, E.A. Barbour, R.K. Hanson
Proc. Combust. Inst. 33 (2011) 309–316.

$k = 1.04 \times 10^{14} \exp(-15286/RT)\ cm^3\ mol^{-1}\ s^{-1}$

Diesel relevant n-heptane fuel exhibits low temperature ignition

Experiments performed at RWTH Aachen (Ravi Fernandes)

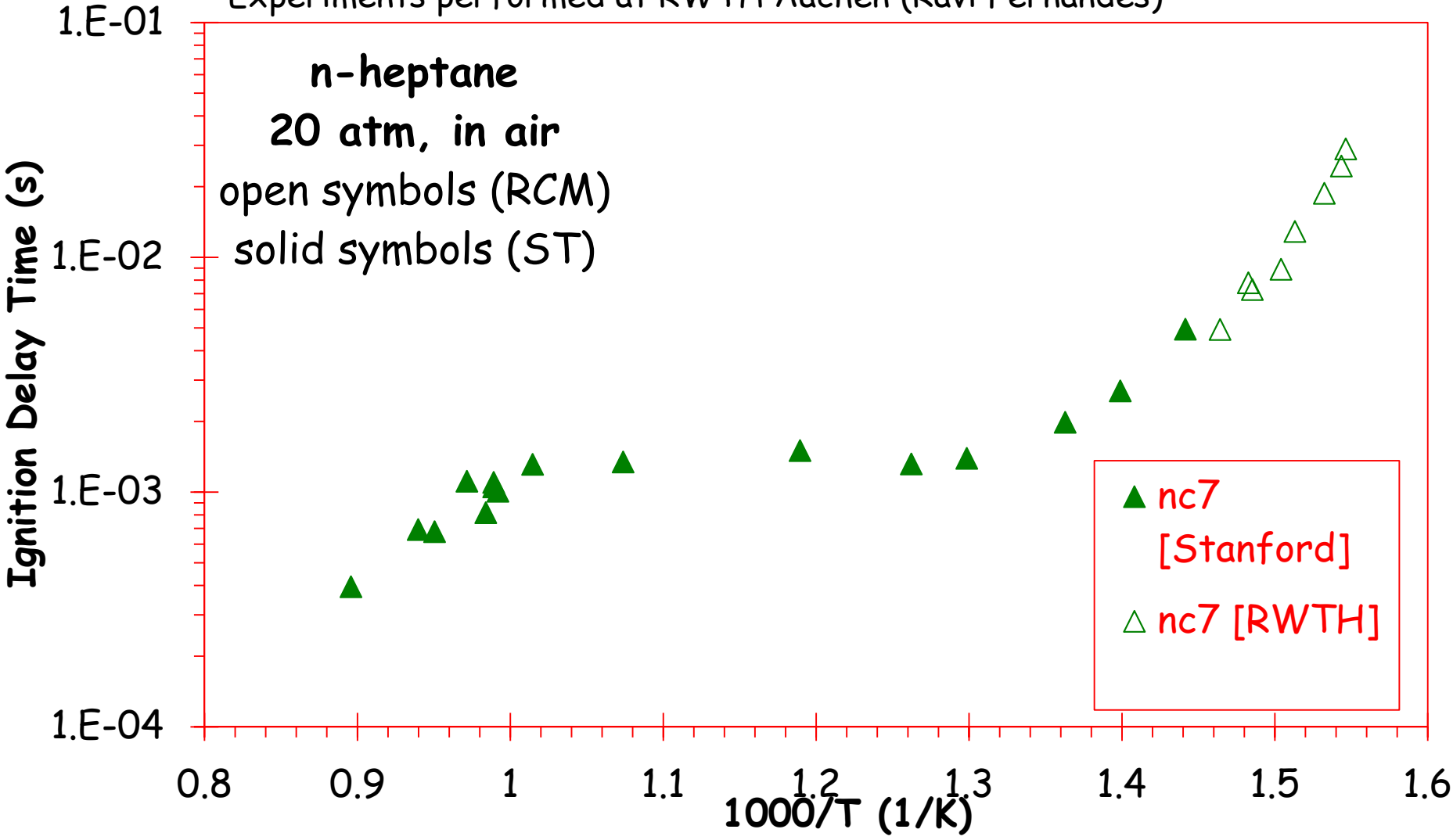

Frontiers of ignition delay research

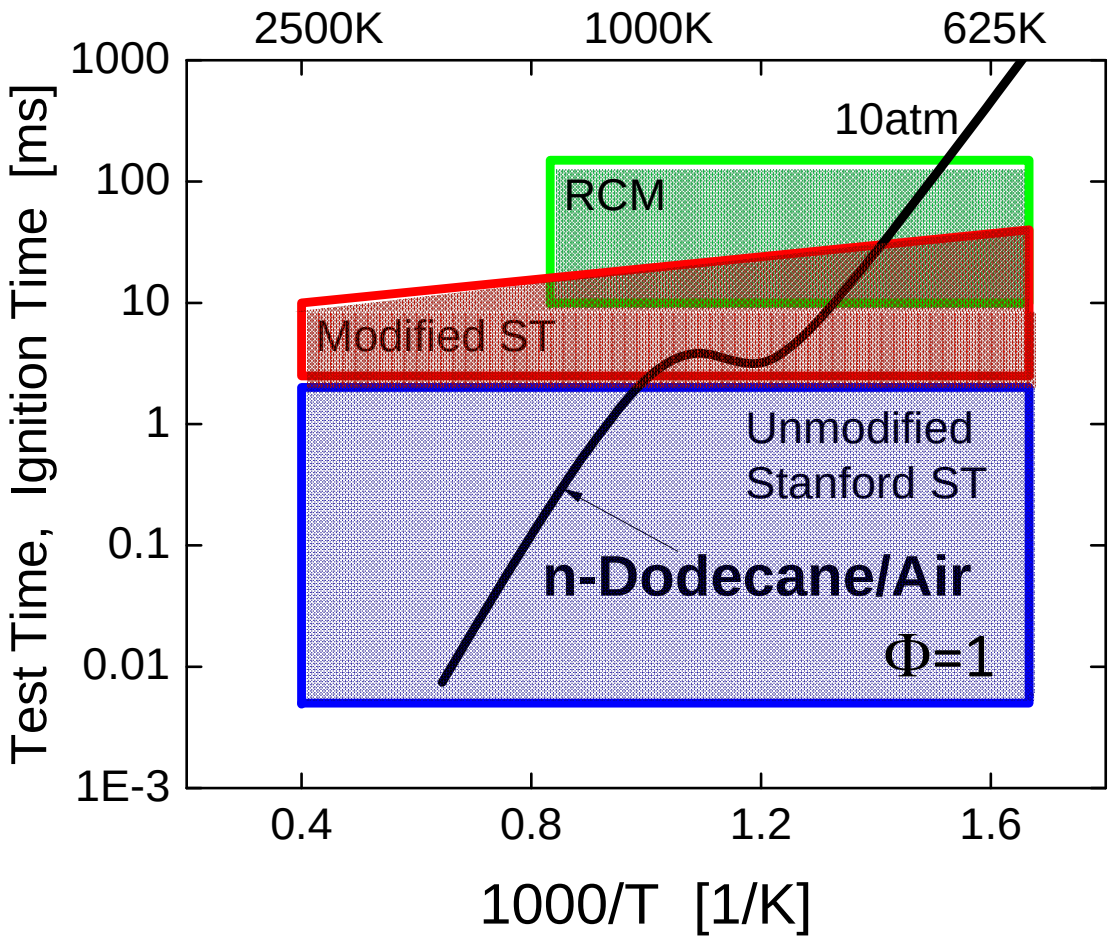

Similar activation energy trend as seen for methyl butanoate

NTC behavior not observed for combined data sets

- Unlikely due to short HC chain lengths

Shorter ignition delay times for ethyl propanoate are in agreement with experimental results

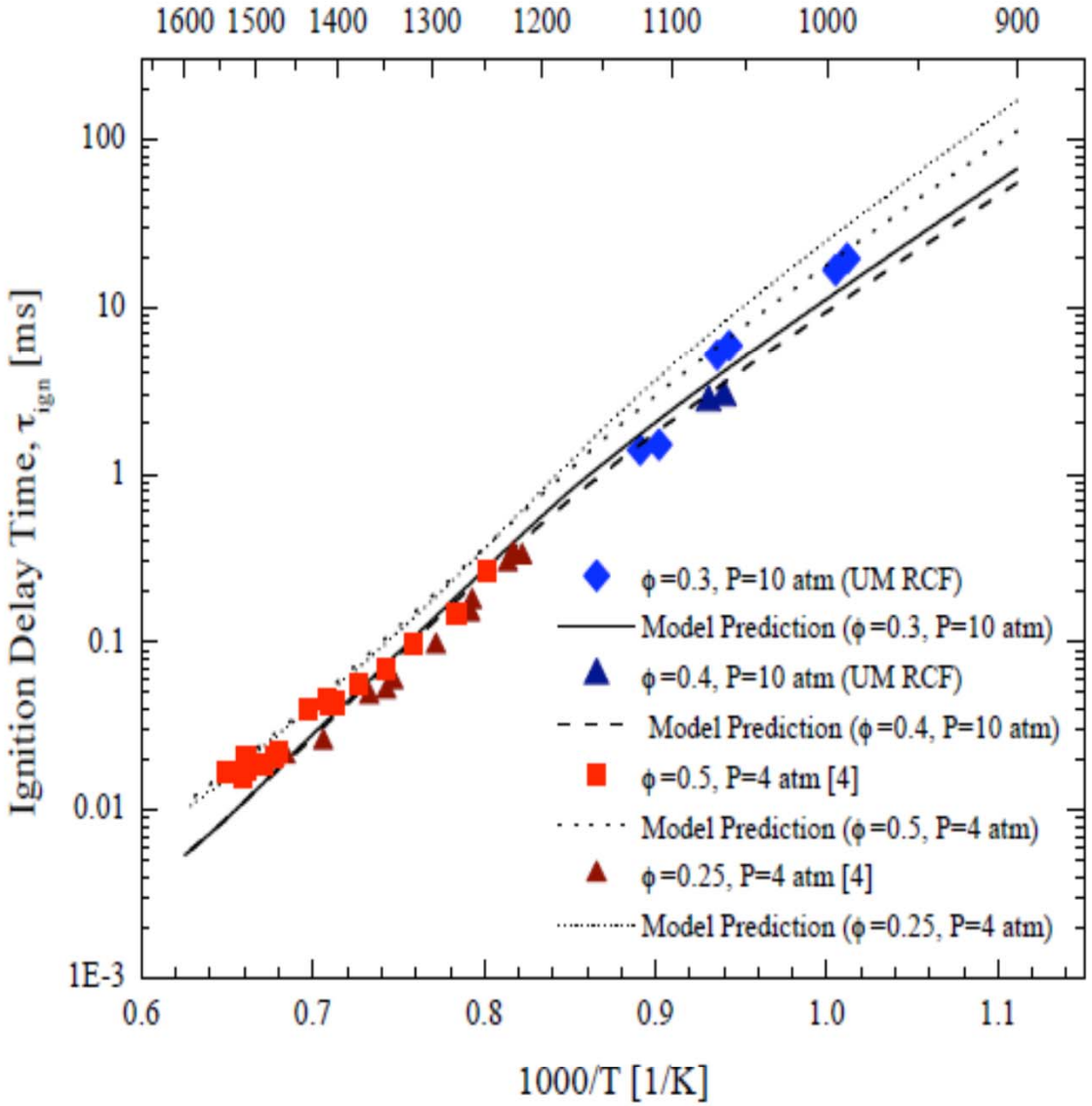

High temperatures, Metcalfe et al., JPCA 2007
Low temps, Walton et al., PROCI 2009

Premixed low pressure flames

Low pressure (10-100 Torr) premixed burner stabilized flames are ideal for measuring combustions intermediates and stable products.

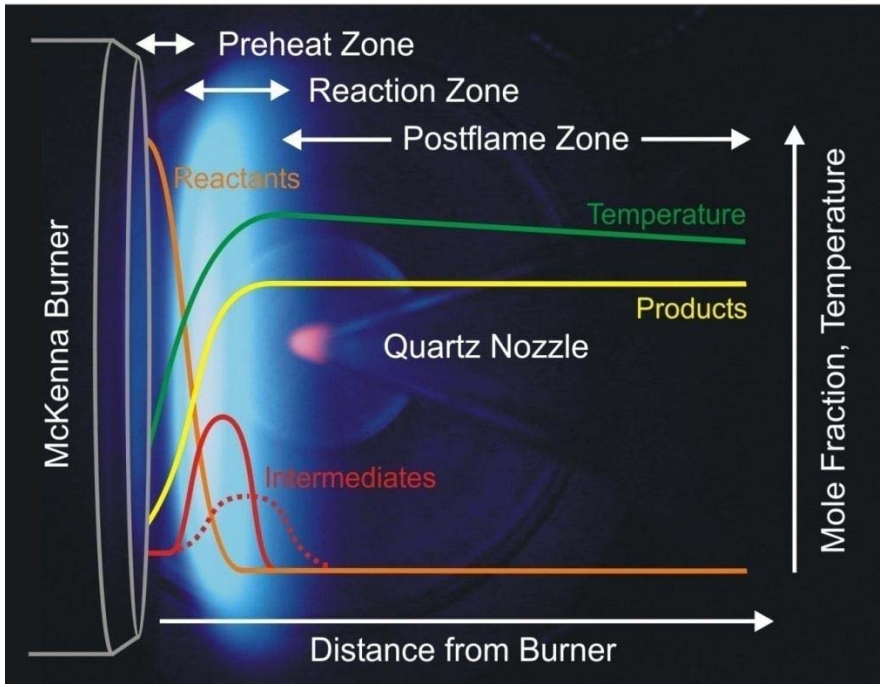

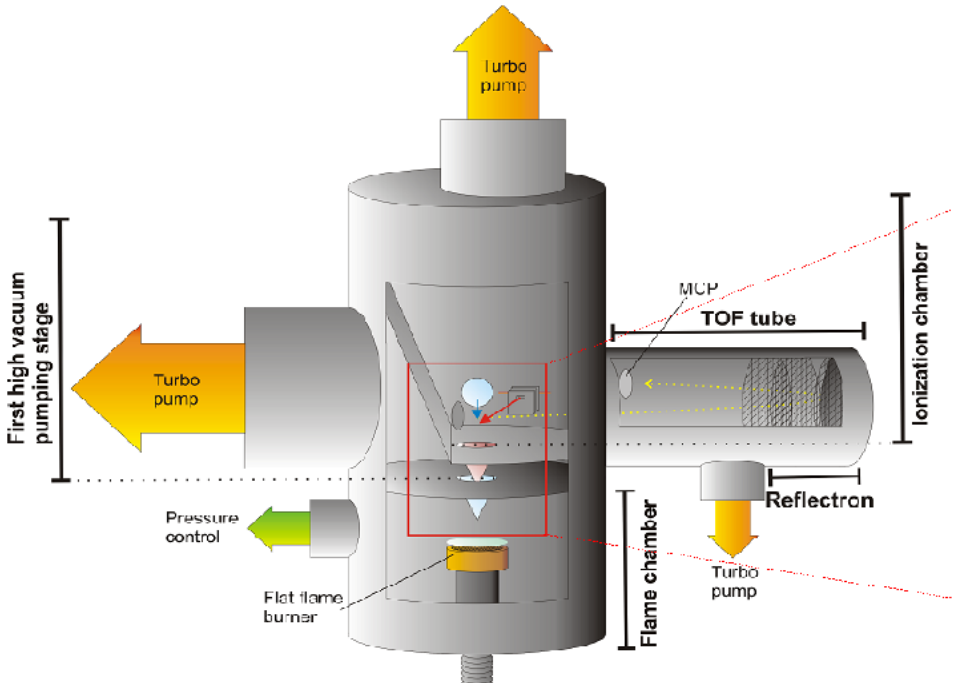

Premixed low pressure flames results

- ***T profile*** **for optical or MBMS sampling must be considered in comparison with models – no shifts!**
- ***Example:*** **butanol flames.**

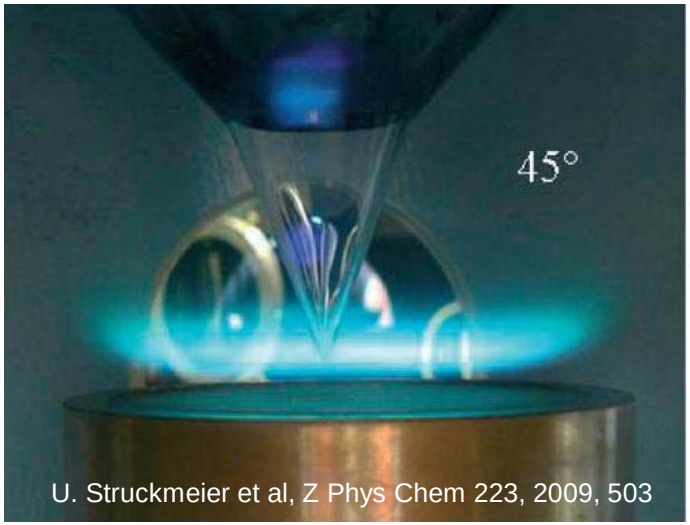

U. Struckmeier et al, Z Phys Chem 223, 2009, 503

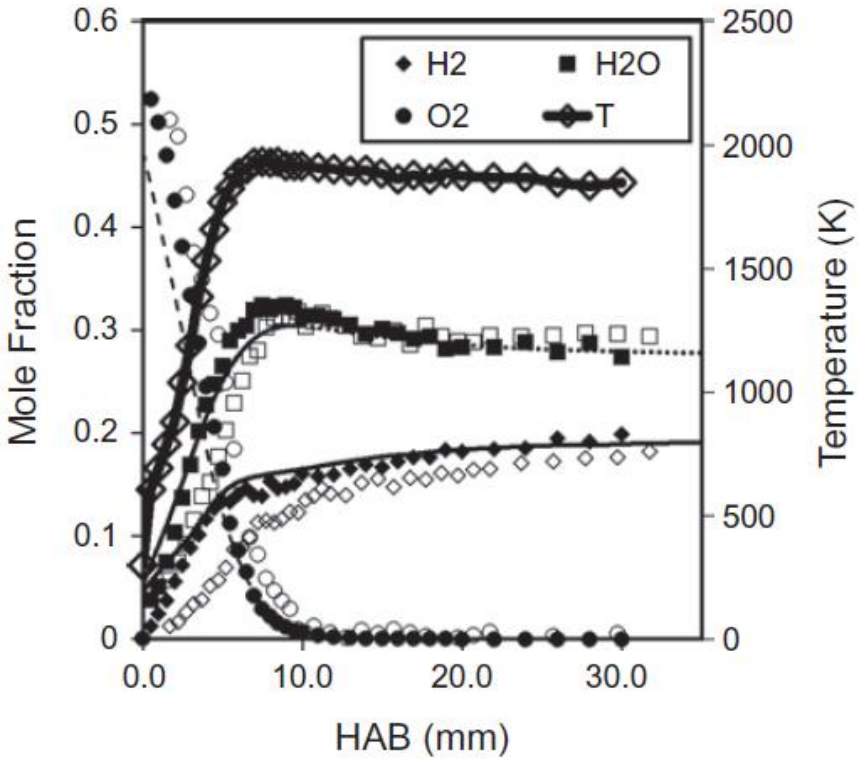

M. Sarathy et al, Combust Flame 159, 2012, 2028

Premixed Laminar Flame Speed

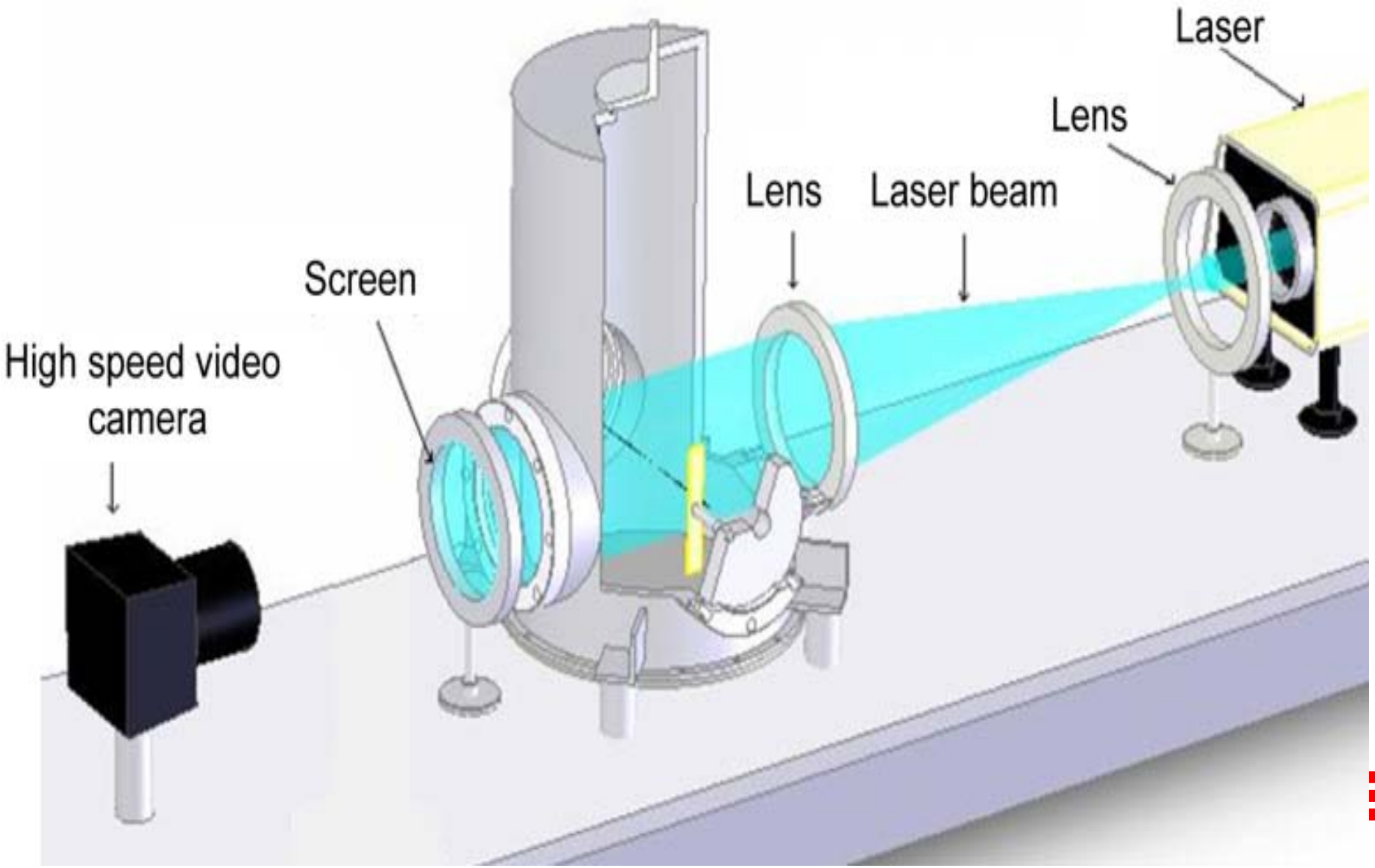

Premixed Laminar Flame Speed
Univ Southern California, F. Egolfopoulos

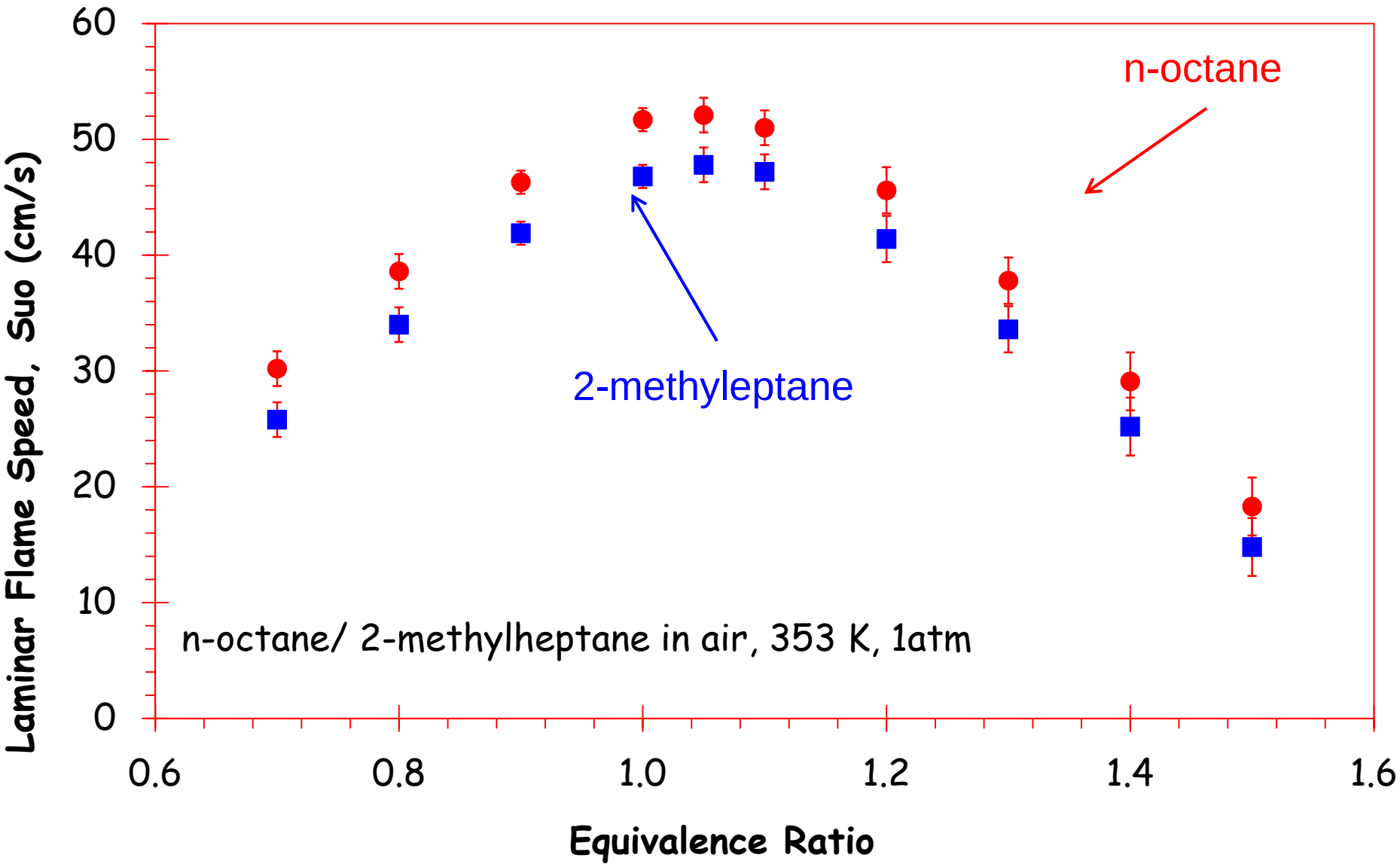

Premixed Laminar Flame Speed for n-octane

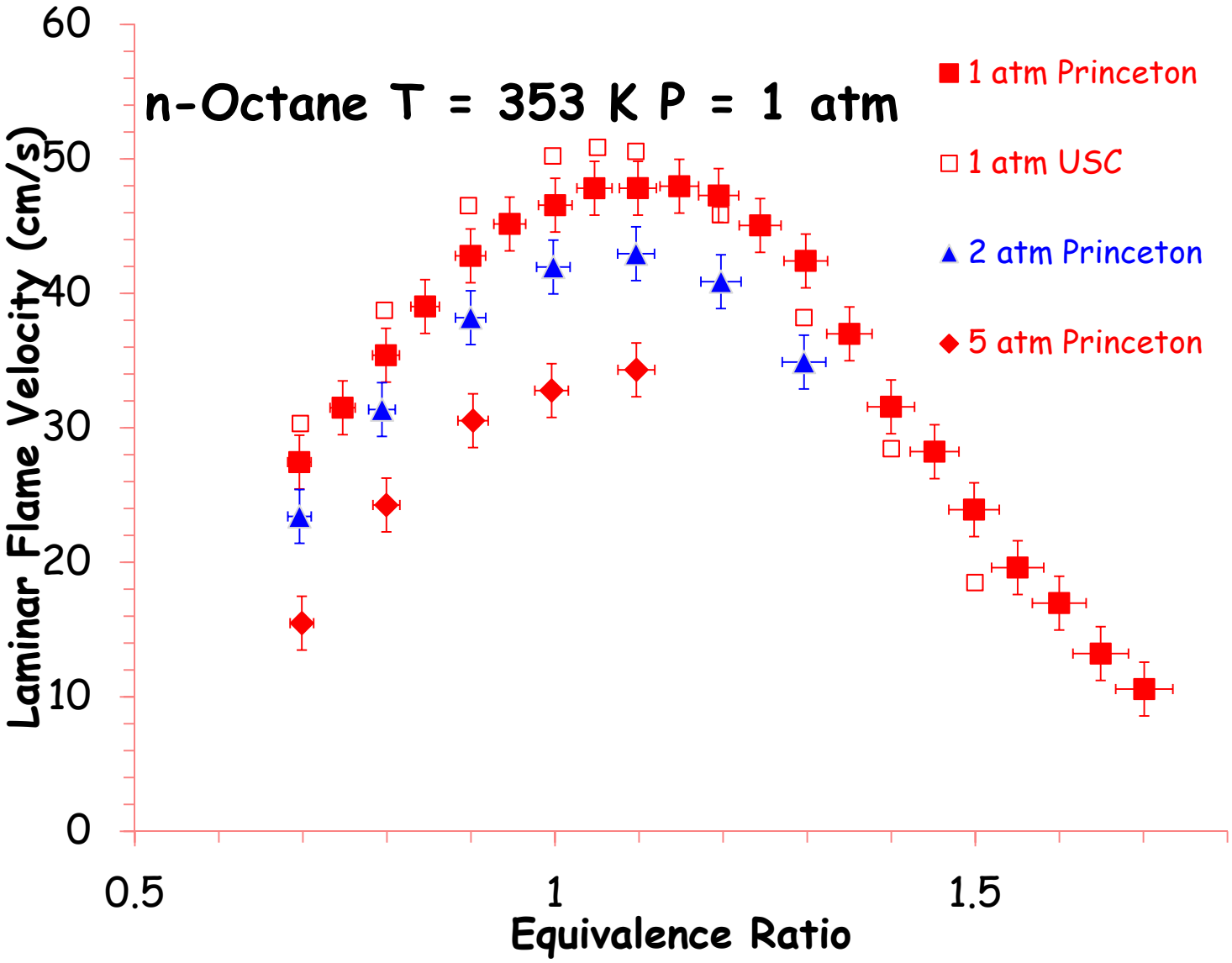

Opposed-flow Diffusion Flame (OPPDIF)

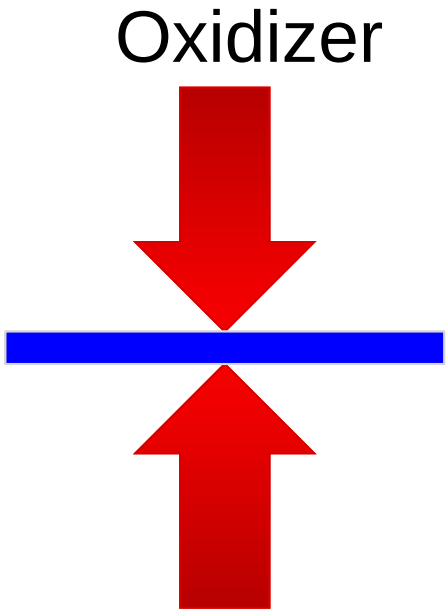

- The one dimensional flame structure is ideal for modeling.
- The emissions and temperature profiles are dependent on chemical kinetics due to the non-turbulent flame.

Port diameter = 25.4 mm
Port Gap = 20 mm

OPPDIF Experimental Setup

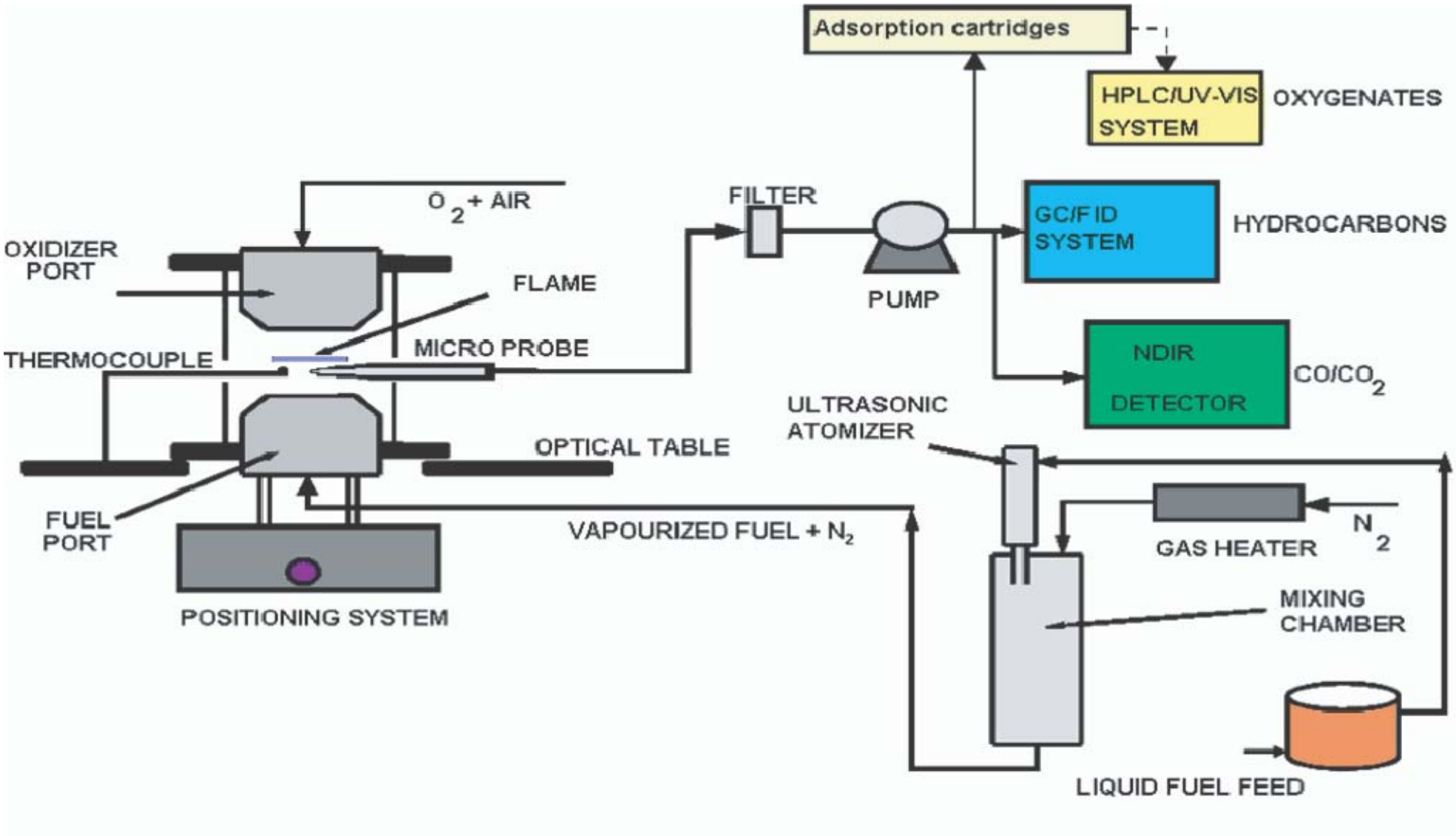

OPPDIF Plots

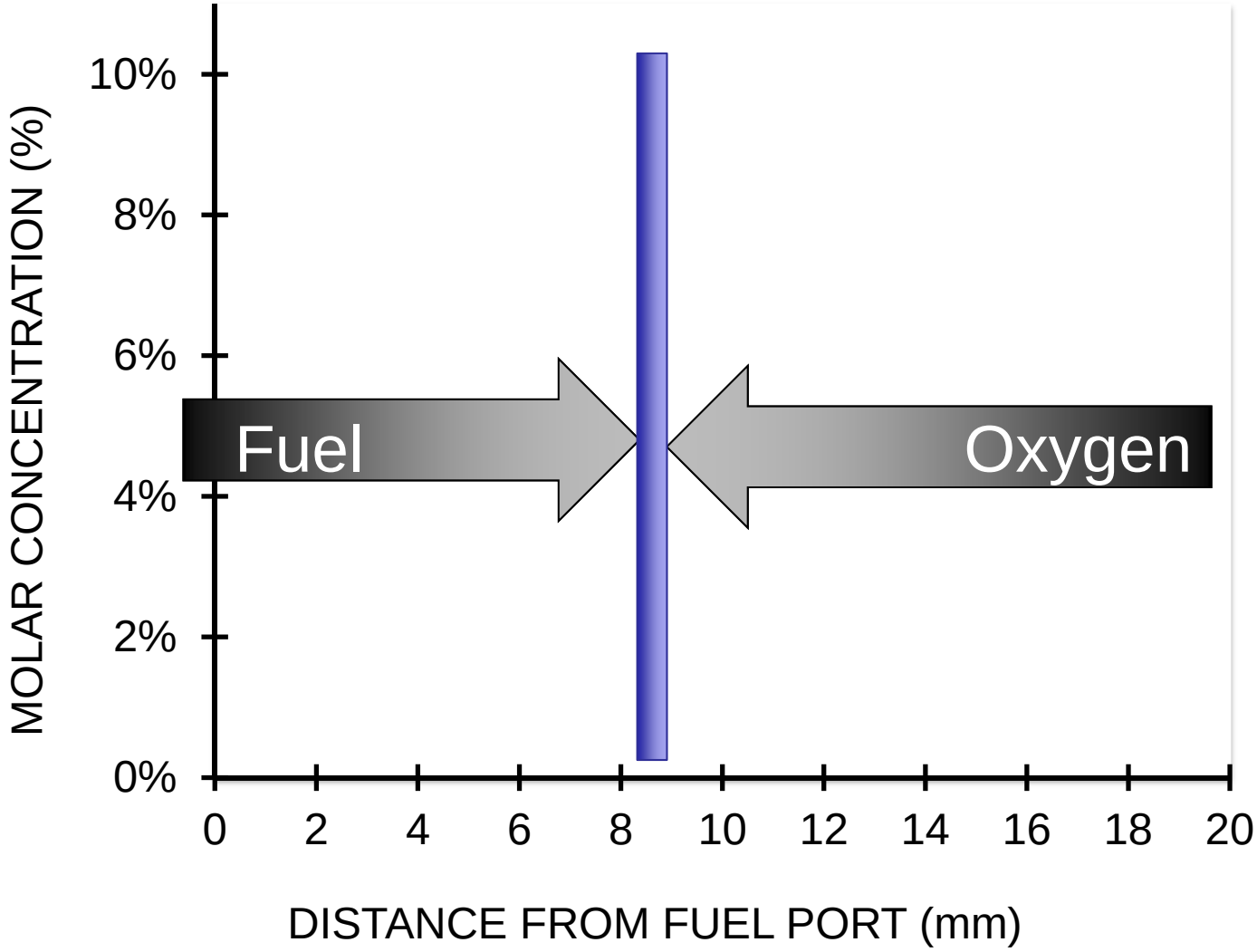

OPPDIF Results

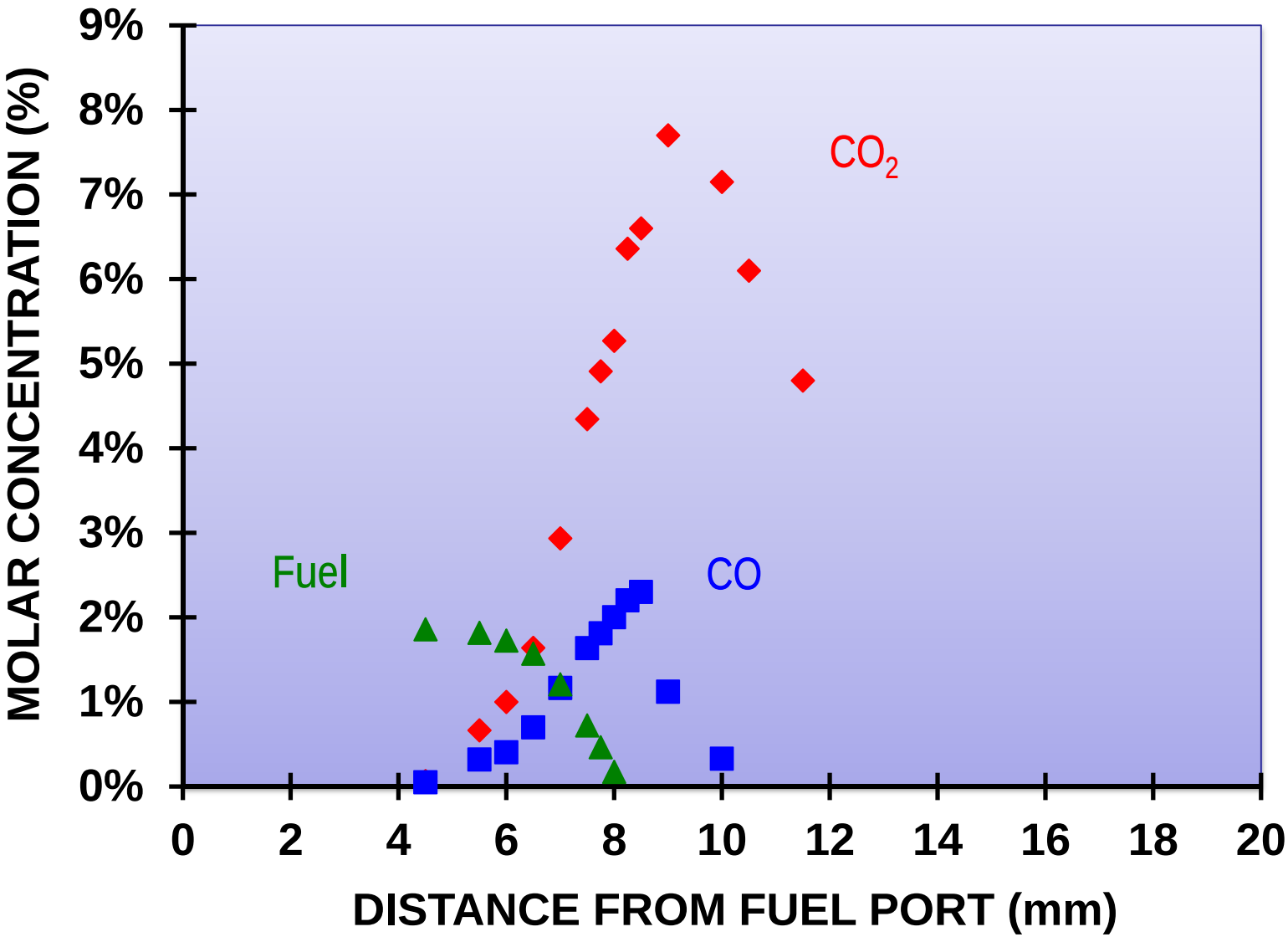

OPPDIF Minor Species Results

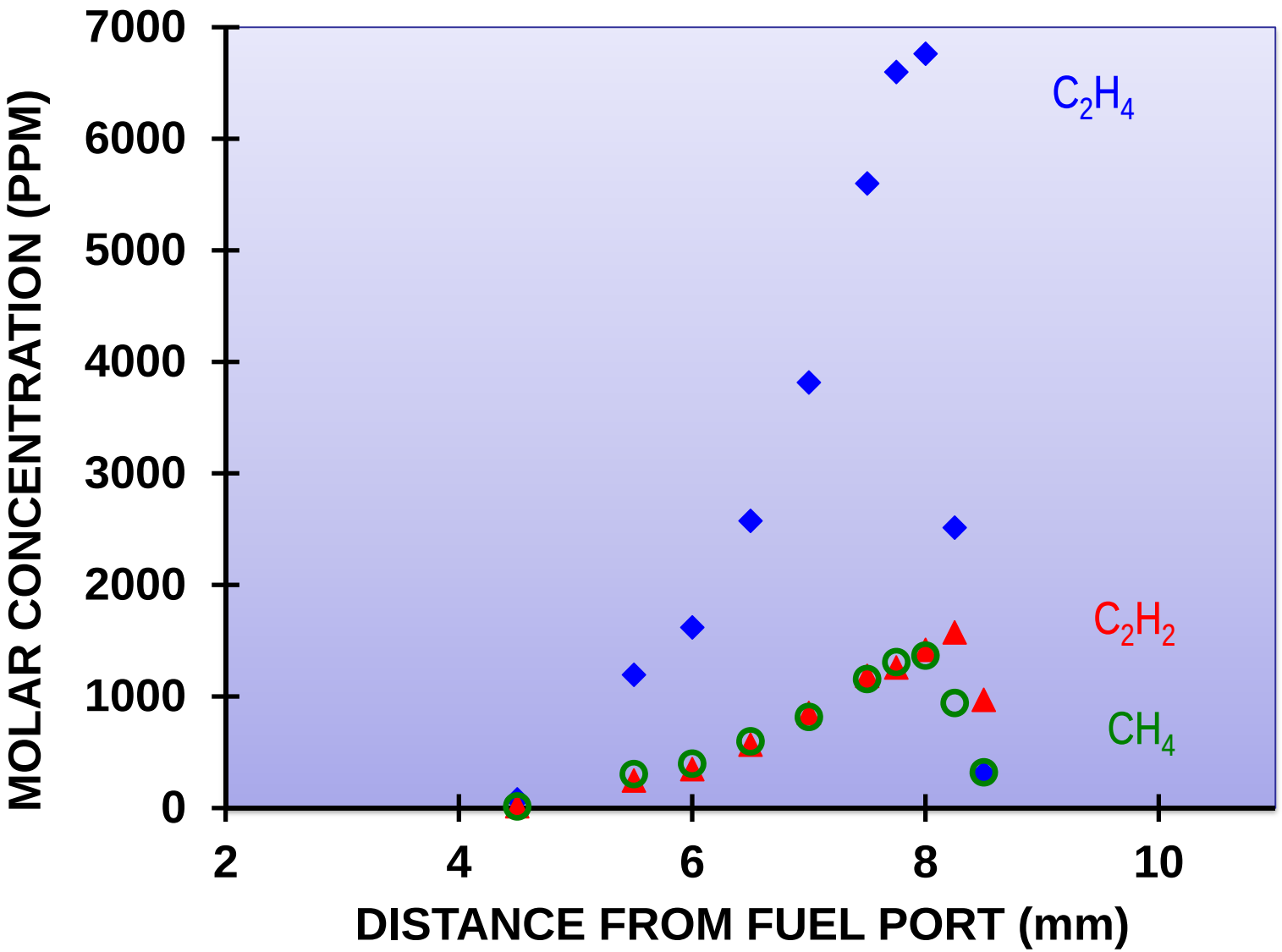

Strained extinction and ignition

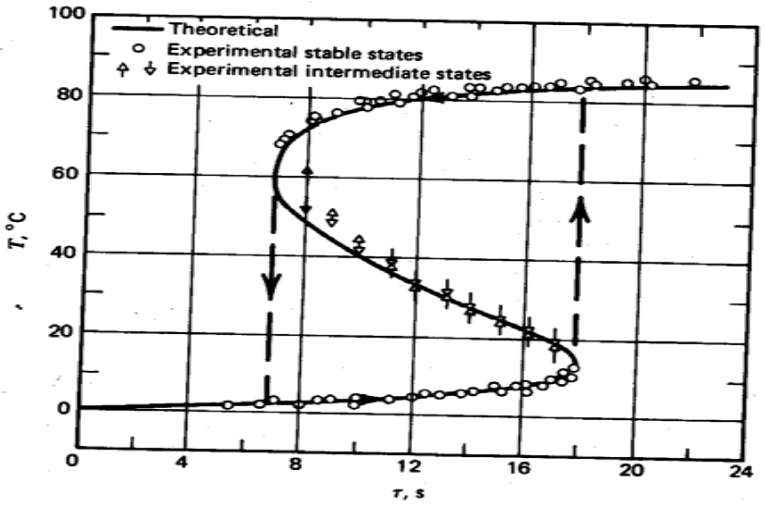

- Stable lower and upper branches are common in diffusive-convective reacting flows
- NTC-affected ignition phenomenon has also been observed

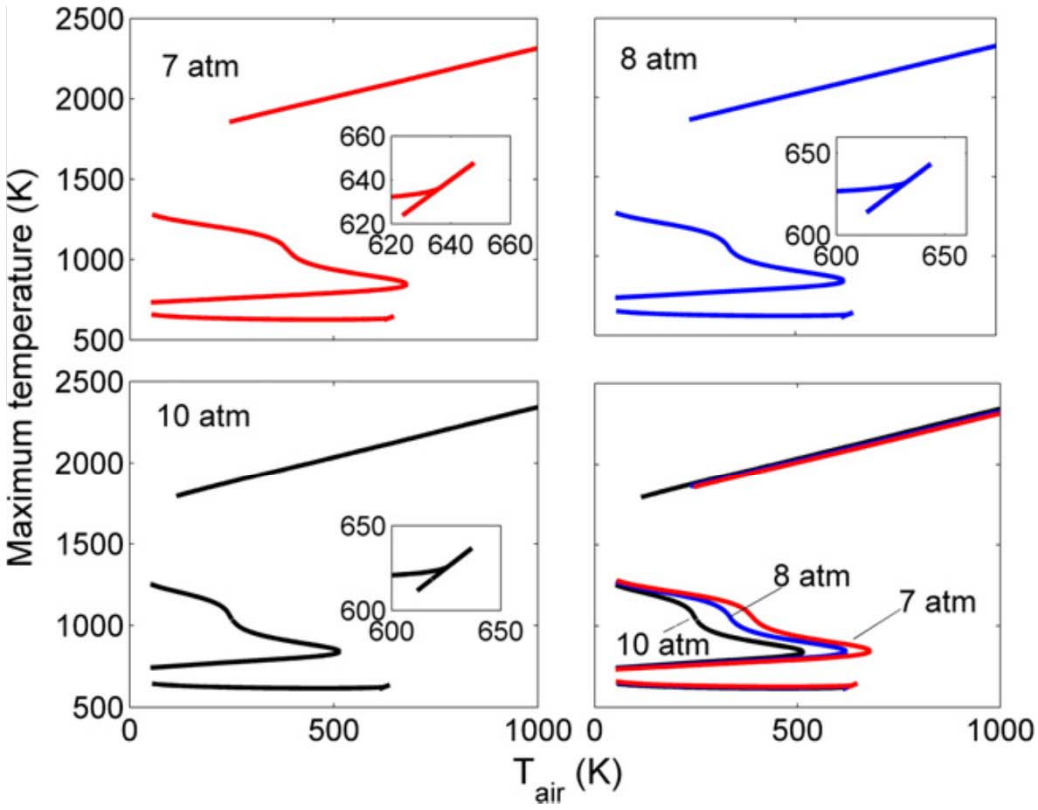

Fig. 19. The global response S-curve of the diffusion counterflow: maximum temperature versus air-side boundary temperature from 7 atm to 10 atm, with a pressure-weighted strain rate 100 $(1/s)$.

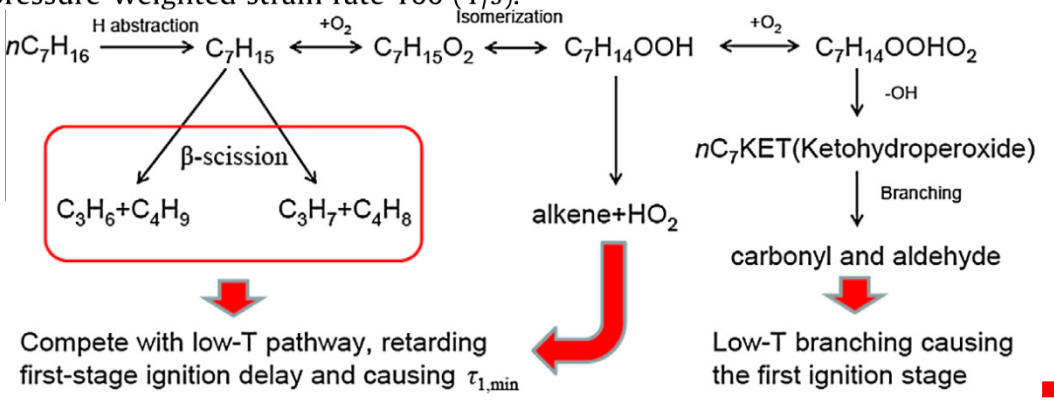

C.K. Law, P. Zhao, Combust. Flame (2011); P. Zhao, C.K. Law Combust. Flame (2013)

Counterflow Extinction/Ignition Results for branched alkanes

Sarathy et al. Combustion Flame (2011)

2-methylheptane

3-methylheptane

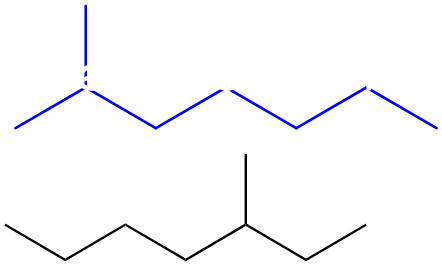

2,5-dimethylhexane

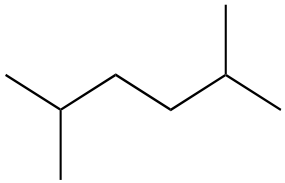

Extinction

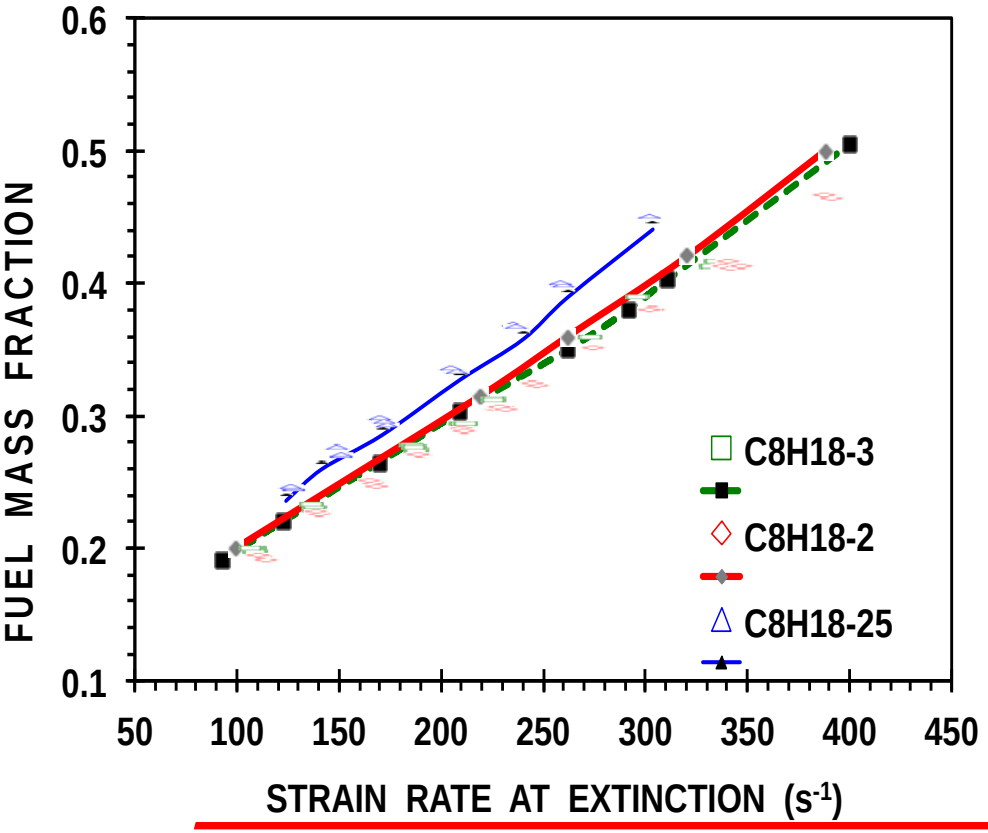

Ignition

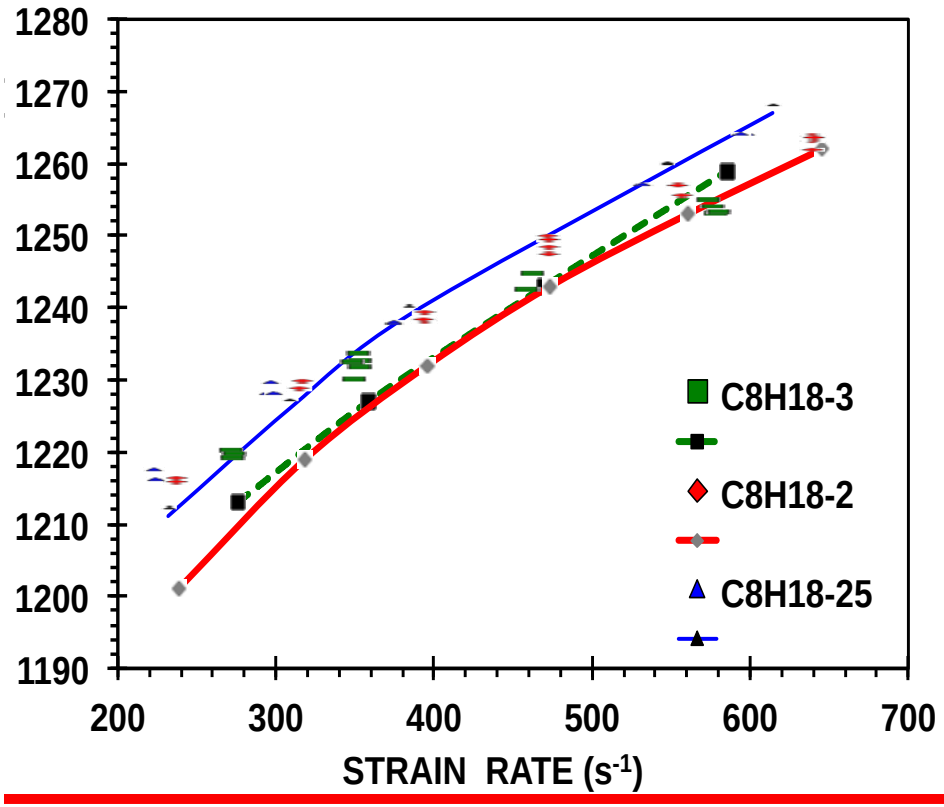

Simulating Comprehensive Combustion Chemistry

Combustion and Flame 160 (2013) 2712–2728

Contents lists available at SciVerse ScienceDirect

Combustion and Flame

journal homepage: www.elsevier.com/locate/combustflame

A comprehensive experimental and modeling study of iso-pentanol combustion

S. Mani Sarathy [a,*], Sungwoo Park [a], Bryan W. Weber [b], Weijing Wang [c], Peter S. Veloo [d], Alexander C. Davis [a], Casimir Togbe [e,1], Charles K. Westbrook [f], Okjoo Park [g], Guillaume Dayma [e], Zhaoyu Luo [b], Matthew A. Oehlschlaeger [c], Fokion N. Egolfopoulos [g], Tianfeng Lu [b], William J. Pitz [f], Chih-Jen Sung [b], Philippe Dagaut [e]

[a] *Clean Combustion Research Center, King Abdullah University of Science and Technology, Thuwal 23955-6900, Saudi Arabia*
[b] *Department of Mechanical Engineering, University of Connecticut, Storrs, CN, USA*
[c] *Mechanical, Aerospace, and Nuclear Engineering, Rensselaer Polytechnic Institute, Troy, NY, USA*
[d] *Department of Mechanical and Aerospace Engineering, Princeton University, Princeton, NJ, USA*
[e] *CNRS-INSIS, 1C, Ave de la Recherche Scientifique, Orleans Cedex 2, France*
[f] *Lawrence Livermore National Laboratory, Livermore, CA, USA*
[g] *Department of Aerospace and Mechanical Engineering, University of Southern California, Los Angeles, CA 90089, USA*

Simulating Comprehensive Combustion Chemistry

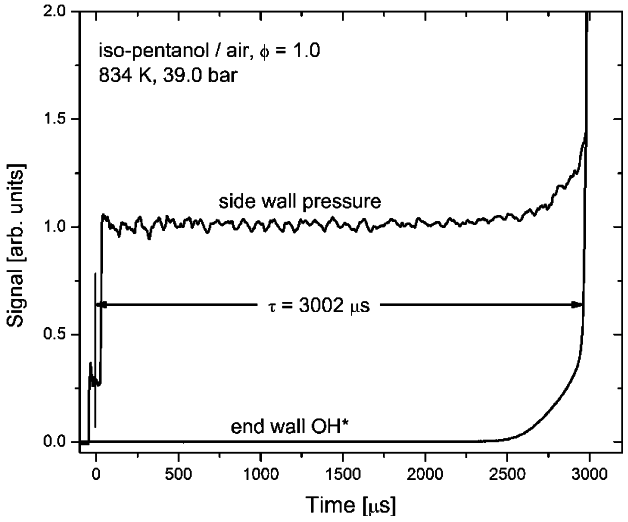

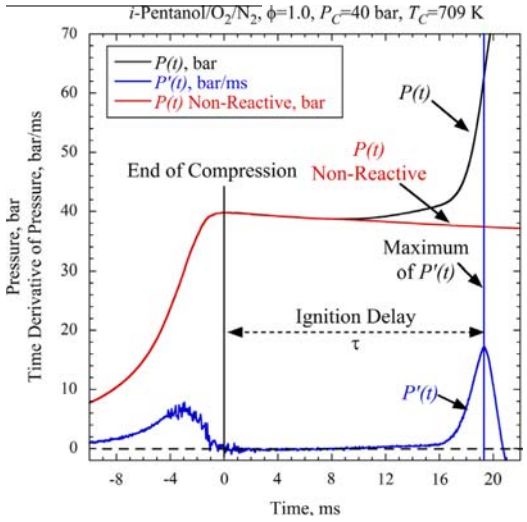

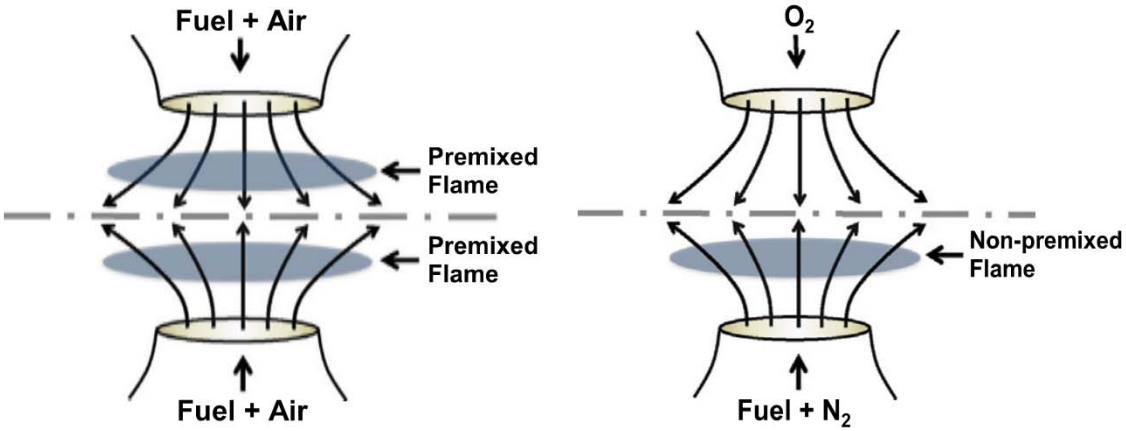

Simulations of ignition delay in STs and RCMs

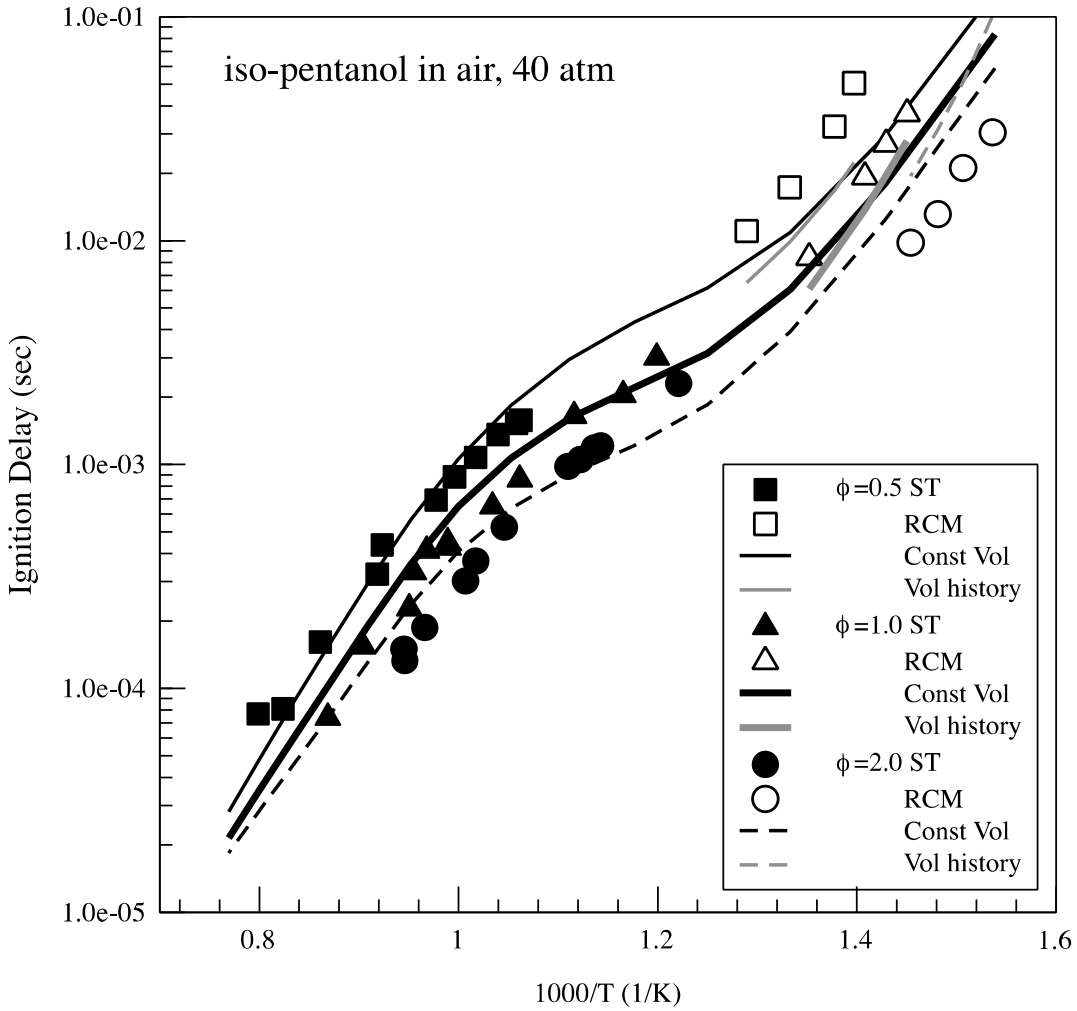

- RCM simulations with heat loss exhibit longer ignition delays than constant volume simulations at low T and shorter ignition delays at higher temperatures.

Sensitivity analysis on ignition delay time

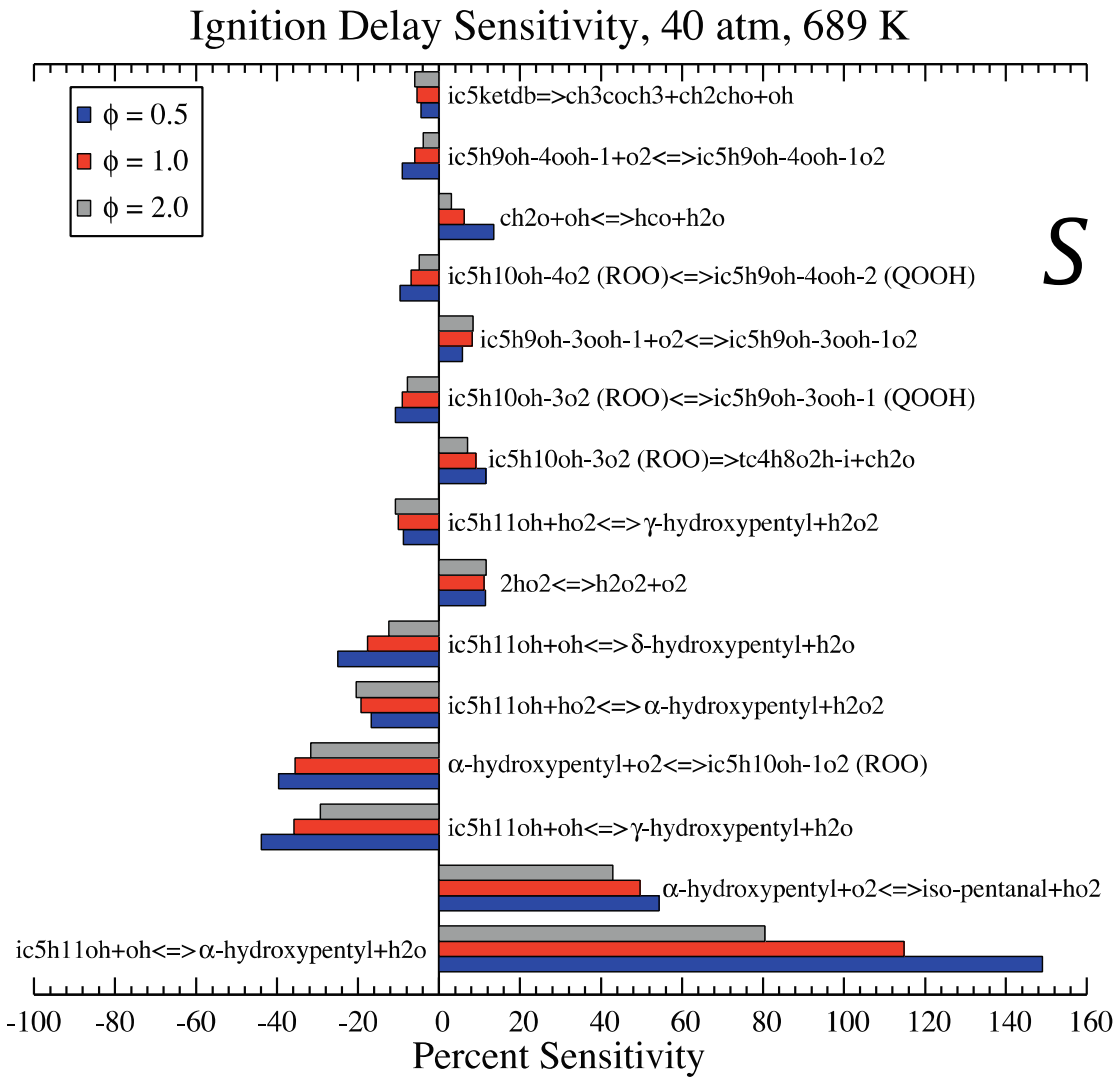

$$S = \frac{\tau(2k_i) - \tau(k_i)}{\tau(k_i)} \times 100\%$$

where

$\tau(2k_i)$ is ign del when rate const of rxn i is doubled

$\tau(k_i)$ is the nominal ign del

Perfectly stirred reactor simulations

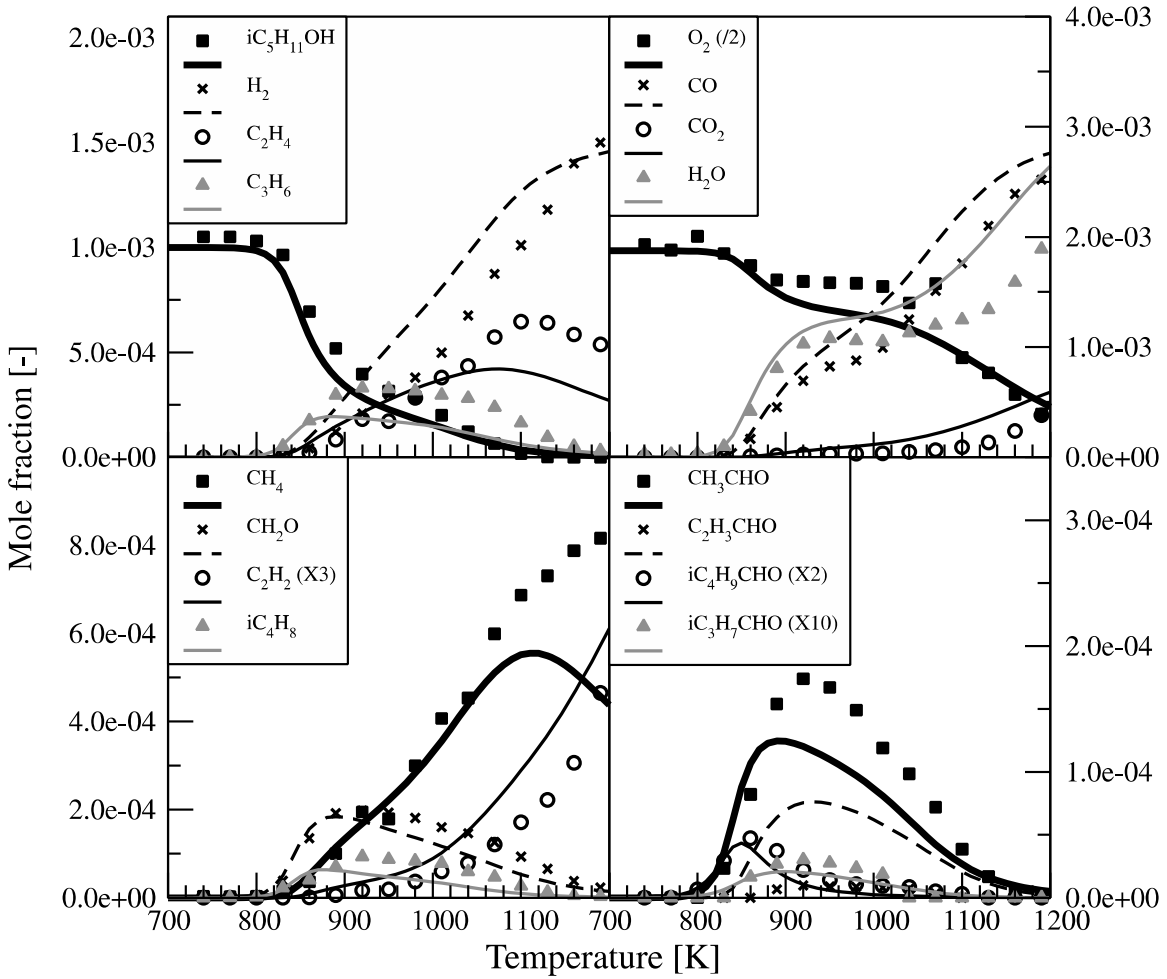

Fig. 20. iso-Pentanol oxidation in a JSR at 5 atm, $t = 0.35$ s and $\phi = 2.0$. The initial fuel mole fraction was 0.1%. Experimental data (symbols) are compared to calculations (lines).

Reaction flux analysis

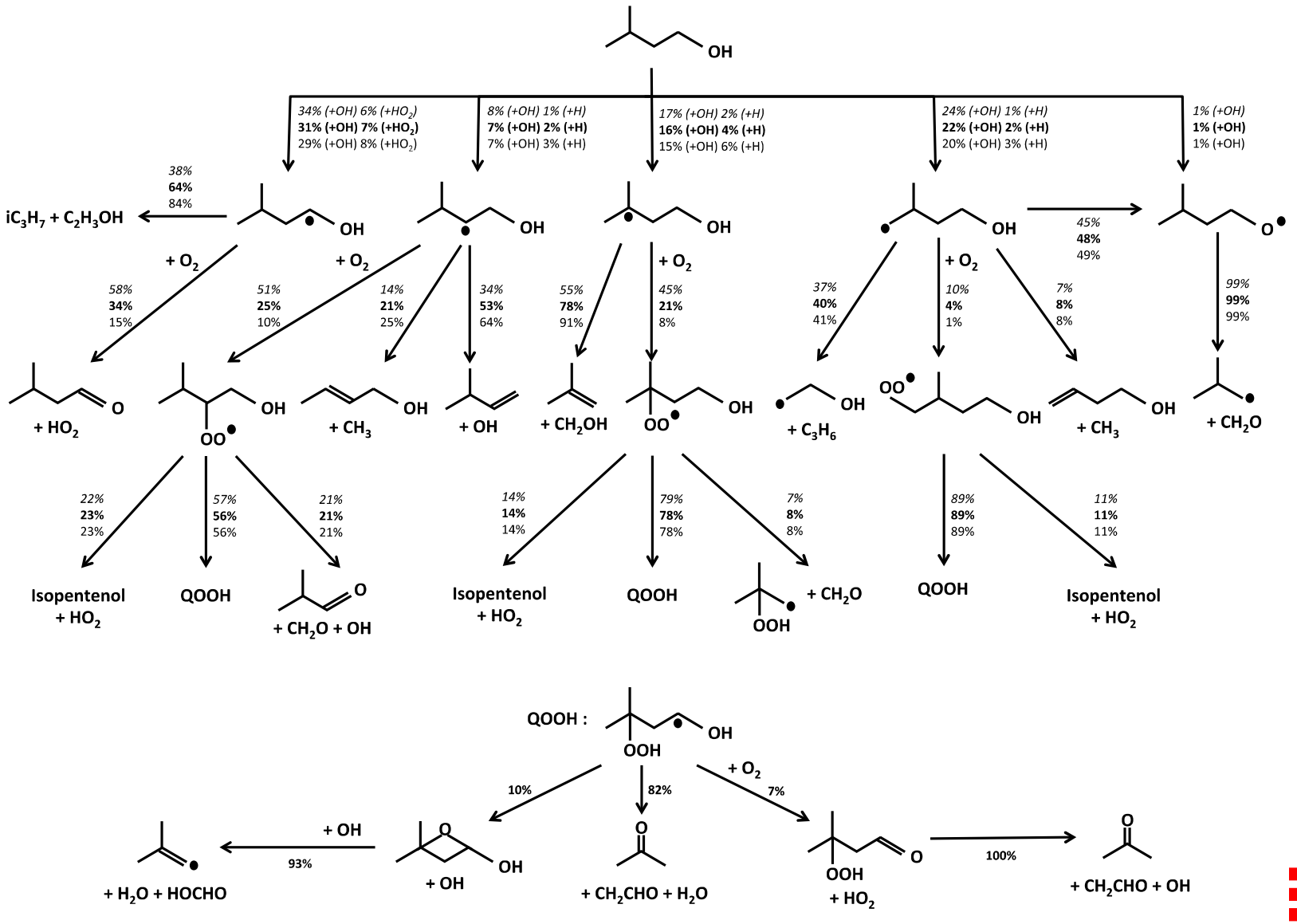

Fig. 22. Reaction path analysis for iso-pentanol oxidation in a JSR at 850 K, 5 atm, ϕ = 0.35 (italic), ϕ = 1.0 (bold) and ϕ = 4.0 (plain).

Flame simulations

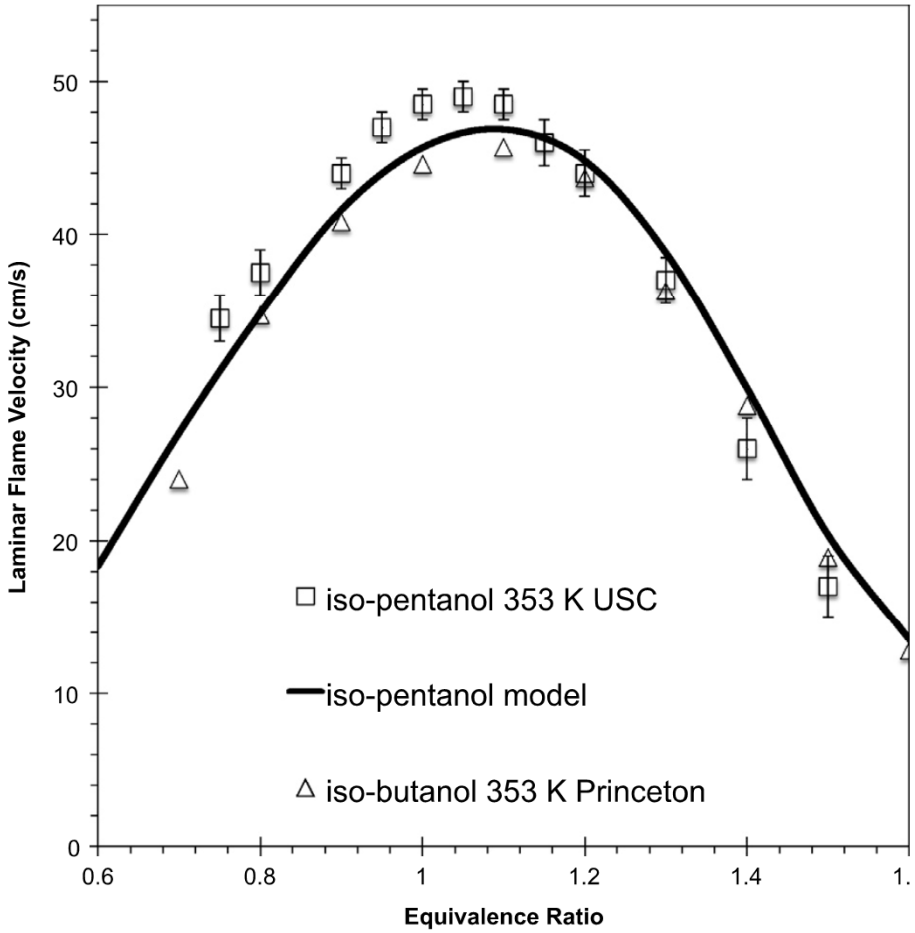

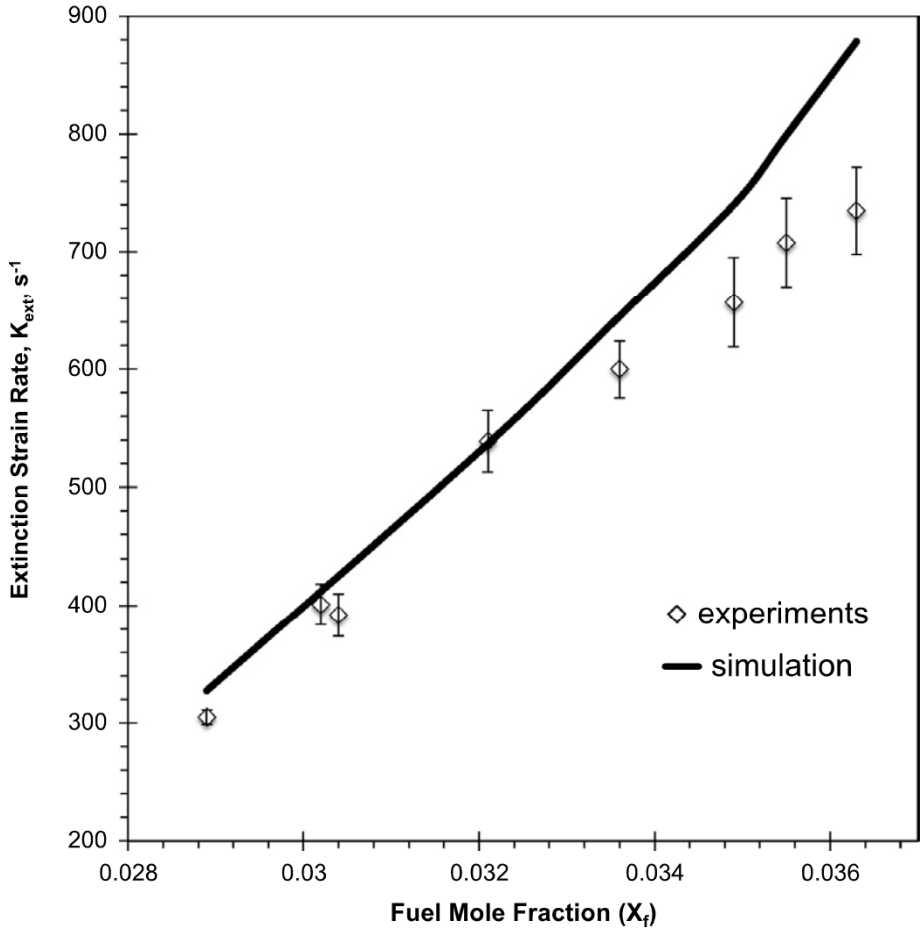

Conclusions

- ST and RCM are complementary
- Understanding the kinetics of fuel oxidation
  - Ignition delay times
  - Speciation data
  - Elementary rate coefficients